
University of Kent

MSc by Research Thesis

2021

# Development of a new CHO Transient Expression Platform for mAb Production; Evaluation of Novel Viral Episome Maintenance Proteins for Transient Gene Expression

Dana Moreno Sanchez

Supervisors:

Mark Smales, Claire Pearce, Chris Sellick, Aisha Krishna

# I Declaration

No part of this thesis has been submitted in support of an application for any degree or qualification of the University of Kent or any other University or institute of learning.

Dana Moreno Sanchez

April 2021

# II Acknowledgments

This project ended up being a much bigger undertaking than I anticipated and wouldn't have been possible without the support of many people. First of all, thank you Mark Smales for the expert advice and feedback. Claire Pearce, I am eternally grateful to you for enabling this project and for trusting me to make it my own. Your leadership and encouragement were invaluable and you will always be an inspiration. I'm also indebted to Chris Sellick and Aisha Krishna for stepping up when needed. Aisha, I'm so grateful to you for taking to the world of expression so quickly and reviewing (and improving) all my writing.

My deepest gratitude also goes to Kymab, which gave me this opportunity, and all the wonderful, kind people who work there. You are too numerous to credit individually, but thanks in particular to Paul Kellam and Anne Palser for helping me with my first unexpected steps in virology. Your expertise (and contacts for sourcing the materials) were invaluable. Lucy Gardner, I appreciate both your CLD expertise and your endless support and encouragement as a friend.

To my team, all the wonderful members of the CET, past and present, thank you for making my workdays amazing, both with the science talk, the support, and being amazing people I am lucky to have worked with. Jemima Paterson, I don't have enough words to thank you for everything you did. Thank you for your science expertise, for your red pen, for your lab skills (I would not entrust my cells to anyone else) and for being a wonderful friend listening to my endless woes and giving me much needed coffee breaks.

Finally, Peter Thomas, thank you for being by my side for all the ups and downs. From bottomless cups of coffee, letting me pick your brain for some good science, and helping me wrestle with R, I couldn't have asked for more from you. I was incredibly lucky to have your support, love and patience during this last year.

# III Abstract

Chinese hamster ovary (CHO) cells are the production system of choice for the expression of monoclonal antibodies (mAbs) and other biotherapeutics. Transient gene expression (TGE) platforms allow the rapid supply of high-quality pre-clinical material and are therefore the expression method of choice for early phase drug development over stable expression methods, which are time and resource intensive. To ensure consistent protein characteristics from discovery to development, it is desirable to express early material in cells closely related to those used during stable cell line development (CLD) and manufacturing. Therefore, adaptation of CLD CHO cell lines that are used for stable expression for early stage TGE is important in the drug discovery and manufacturing pipeline. TGE is characterised by the presence of an extra-chromosomal plasmid which is not integrated into the genome and therefore is lost over time. To establish latency, Epstein Barr virus (EBV) uses the Epstein Barr nuclear antigen 1 (EBNA-1) protein to retain its genome as an episome within a host cell, and has been widely adapted for use in TGE systems leading to improved plasmid retention and increased transient protein yields. EBV however does not naturally infect rodents, demonstrating human tropism, and therefore CHO cell TGE systems that rely on EBNA-1 are unable to achieve the episomal replication that EBV can accomplish during natural infection. This project describes the development of a new TGE system suitable for pre-clinical material supply using a CHO cell line. To improve transient protein expression from this host, the use of two alternative episome maintenance proteins (EMPs) was evaluated: latency associated nuclear antigen (LANA) derived from both KSHV and MHV68. The work describes the successful development of a new CHO cell TGE system through a holistic approach focusing on vector optimisation, bioprocess engineering and cell engineering, achieving comparable titres to other well established TGE systems. Moreover, the results from this work open up promising new areas of research to further increase transient expression yields from CHO and other mammalian cell expression systems.

# IV Contents

# V List of Figures

# VI List of tables

# VII Abbreviations

| | |
|---|---|
| ADCC | Antibody dependant cellular cytotoxicity |
| Akt | protein kinase B |
| BL | Burkitt's Lymphoma |
| CaPi | Calcium phosphate |
| CBD | Chromosome binding domain |
| CDC | Complement dependent cytotoxicity |
| CHO | Chinese hamster ovary |
| CLD | Cell line development |
| CR | Central repeat |
| DBD | DNA binding domain |
| DHFR | Dihydrofolate reductase |
| DoE | Design of Experiments |
| DS | Dyad symmetry |
| EBNA-1 | Epstein-Barr nuclear antigen 1 |
| EBS | EBNA-1 binding site |
| EBV | Epstein-Barr Virus |
| EMP | Episome maintenance protein |
| FOG | Fed batch overgrow |
| FR | Family of repeats |
| GFP | Green fluorescent protein |
| GOI | Gene of interest |
| GS | Glutamine synthetase |
| HC | Heavy chain |
| HCP | Host cell proteins |
| HEK | Human embrionic kidney |
| HHV4 | Human γ-herpesvirus 4 (EBV) |
| HLA | Human leukocyte antigen |
| kLANA | KSHV LANA |
| kLBS | KSHV LBS |
| kMRE | KSHV minimal replicator elements |
| KSHV | Kaposi's Sarcoma-Associated herpesvirus |
| LANA | Latency associated nuclear antigen |
| LBS | LANA binding site |
| LC | Light chain |
| LR | Linking region |
| mAbs | Monoclonal antibodies |
| MFI | Median fluorescent intensity |
| MHC | Major histocompatibility complex |
| MHRA | UK Medicines Health Regulatory Authority |
| MHV68 | Murine herpesvirus 68 |
| mLANA | MHV68 LANA |
| mLANA-F | mLANA with a FLAG tag |
| mLBS | MHV68 LBS |
| mMRE | MHV68 minimal replicator elements |

| | |
|---|---|
| MRE | Minimal replicator elements |
| MSX | Methionine sulphoximide |
| MTX | Methotrexate |
| NLS | Nuclear localization signal |
| ORC | Origin of recognition complex |
| ORF | Open reading frame |
| PEI | Polyethylenimine |
| pkTR | plasmid kTR |
| pmTR | plasmid mTR |
| pNoOri | plasmid no oriP |
| pre-RC | Pre-replication complex |
| PTM | Post translational modifications |
| Qp | Cell productivity measured in picrograms/cell/day |
| rDNA | Recombinant DNA |
| RE | Retention element |
| TCN | Total cell number |
| TE | Transfection efficiency |
| TGE | Transient gene expression |
| TR | Terminal repeat |
| VCN | Viable cell number |
| WPRE | Woodchuck post-transcriptional regulatory element |

# 1 Introduction

## 1.1 The Biotherapeutics Market

Biotherapeutics or biologics are an important, fast-growing class of medicines used for a wide range of indications, including cancer, chronic inflammatory diseases, transplantation, infectious diseases and cardiovascular diseases[1]. Biologic drugs are dominated by recombinant proteins, the most prominent of which are monoclonal antibodies (mAbs). Antibodies are proteins produced by B-cells in response to infection or immunisation. They are comprised of two heavy chains (HC) and two light chains (LC) which come together to form a Y-shaped protein with a variable region that binds its target antigen and a constant domain that determines its function and affects localisation within the body. The two HCs are bound to each other and to the LC by disulphide bonds[2,3]. Each antibody typically only binds a single antigen, which means that their biological effects are highly specific. This makes them incredibly desirable to the biopharmaceutical industry and this is reflected in their share of the market. In 2018, 8 of the top 10 selling drugs in the USA by value were biotherapeutics, 6 of which were mAbs. Global sales for mAbs in 2018 were $122 billion and they are expected to reach more than $200 billion in 2024[4,5].

The first approval of a mAb by the FDA was Muromonab-CD3 in 1986 to treat acute transplant rejection[6] and since then the number has been growing rapidly. There are 93 mAbs currently approved in the USA or EU[6]; 24 of these were approved between 1997 and 2013 and a further 12 were approved in 2020 alone[7] demonstrating the ever increasing interest and importance in this class of drugs. The primary indications for mAb-based therapeutics are oncology and autoimmune conditions, however their utility is increasing the variety of indications for which they are being considered[8–11]. This increasing interest and need for reduced development time have been facilitated by numerous technological improvements, including within production methods.

## 1.2 Recombinant Protein Expression Systems

Recombinant proteins can be produced using a variety of expression platforms, including cell-based systems and the more experimental cell free systems[12,13]. Cell based systems can be mammalian or non-mammalian including bacteria, yeast, plant or insect cells. Since mAbs are complex molecules that require specific post translational modifications (PTM) which affect their folding, biological activity, stability and immunogenicity among others[14], mammalian cells are preferred as they can more faithfully carry out all the required 'human-like' PTMs, glycosylation being of particular importance. Glycosylation of a mAb can affect its biological function, such as antibody dependent

cellular cytotoxicity (ADCC) and complement dependent cytotoxicity (CDC)[15], stability, solubility and immunogenicity. Glycosylation is species and cell type specific and therefore administration to a patient of a protein with a non-self glycosylation profile can induce an anti-drug immune response which reduces the efficacy of the molecule by immune mediated clearance[16]. Glycosylation profiles depend on the cell line in which the protein is produced and the ability of Chinese hamster ovary (CHO) cells to produce a human-like glycosylation profile is one of the major reasons as to why CHO cells are so widely used in the biopharmaceutical industry[17,18].

## 1.3 CHO Cells for Recombinant Protein Production

CHO cells were isolated in 1957 by Theodore Puck and were first used in basic research in contrast to their current focus in manufacturing. Their popularity at the time was related to their ease of culture, large chromosome and phenotypic diversity which eventually lead to a wide family of cell lines[19]. Several CHO host cell lines have been derived from the original cell line, the first of them being CHO-K1 in the 1960s. CHO-DXB11 was later derived from CHO-K1 through deletion of the dihydrofolate reductase (DHFR) gene and was used to produce the first approved recombinant protein, tissue plasminogen activator, in 1986[17]. The CHO-S line was also derived from CHO-K1, popular due to its ability to grow in suspension culture[19].

CHO cells have retained their popularity since their first use and represent the main cell line used to express mAbs. CHO cells are the manufacturing cell line of choice for more than 50% of mAbs approved up to 2017 and all of the mAbs approved in 2017[20]. The heavy focus industry places on CHO cells is partially explained by their facility for PTMs as described above, but also by their proven track record of regulatory approvals, being considered a safe choice for manufacturing. It is standard practice for companies to develop their own CHO-derived hosts to fulfil different manufacturing needs, including higher production rates of mAbs, and to provide freedom to operate. CHO cell lines that are in wide use currently are able to grow in suspension in a chemically defined, serum and protein free media[21].

The early goal of protein expression is to produce material of candidate molecules for research and screening, whilst expression at later stages is used for drug development, including clinical trials and finally market supply once approved. Transient expression is typically used for high throughput material supply for early stage research and small preclinical studies, whereas stable expression is typically used for large-scale manufacturing of biotherapeutics for market supply. These systems differ based on the length of time in which the transgene is maintained in the cell and the yield of product that is achievable. A simplified overview of the process for antibody transient and stable expression is shown in Figure 1.

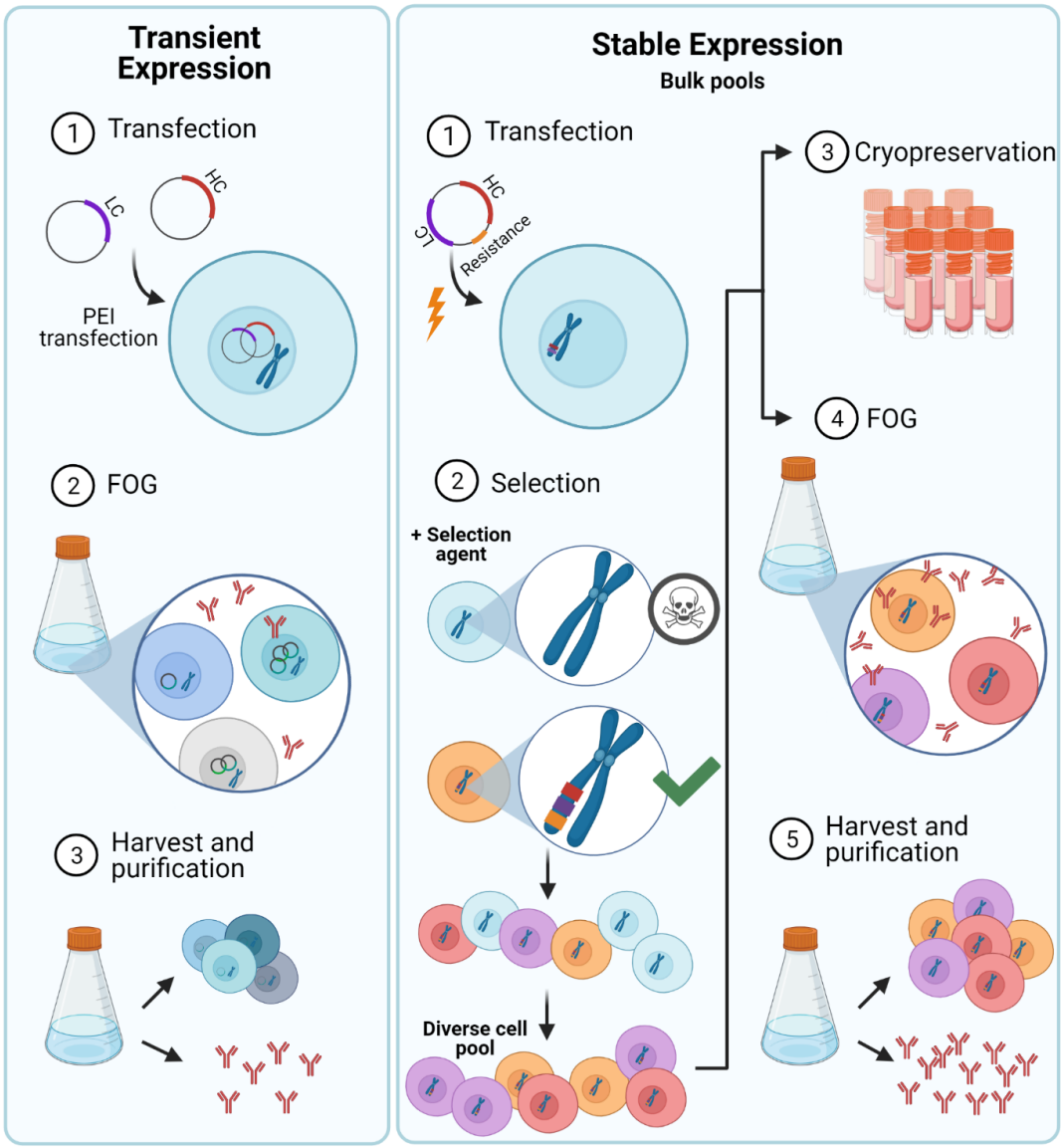


***Figure 1: Comparison of the transient and stable expression of monoclonal antibodies (mAbs).*** *The processes exemplify the standard steps for recombinant protein expression in mammalian cells. Transient expression (left) includes (1) transfection (usually with PEI), (2) fed batch overgrow (FOG) and finally (3) harvest of the supernatant containing the protein of interest. During this process, the plasmid is not integrated into the chromosomes. The transfected cells are represented in different shades of blue to imply variable levels of protein expression. Stable expression (right) shows the steps required to create bulk pools, whereas the creation of single cell derived cell lines would require a longer process including single cell deposition. (1) transfection via electroporation or other methods, plasmid usually contains the necessary genes for mAb expression and an additional resistance or metabolic selection casette (orange). (2) selection is added to the cells, killing the cells which have not integrated the genes of interest (light blue cells). Purple, orange and red cells have integrated the genes and are able to survive. Different colours represent different integration events and different levels of mAb expression, implying a diverse cell pool (bulk pool). (3) creation of cryopreserved cell bank stored in liquid nitrogen (LN) (4) FOG, either from the samples stored in LN or in parallel to this process (5) harvest and purification of the mAbs from the supernatant.*

### 1.3.1 Transient Expression

Transient expression platforms are characterised by the introduction of recombinant DNA (rDNA) which is maintained as extrachromosomal plasmid DNA. Cells begin the protein production process shortly after transfection; however the plasmid DNA is gradually lost over time and through cell divisions and therefore the protein production level decreases quickly. This limits the length of the production process to between 7 and 16 days, usually giving lower titres compared with stable expression methods.

### 1.3.2 Stable Expression

Stable expression is characterised by the integration of the transgene into the host cell genome, ensuring that the gene itself is not lost during cell divisions as is the case in transient transfection, which facilitates long-term high-level expression. It is a more complex system that requires selection to deplete untransfected cells. This requires a selection gene to be delivered alongside the gene of interest (GOI), after which the cells are subjected to selective conditions so that only those that acquired the selection gene are able to survive and grow. The simple versions of this method provide a gene that allows the cells to survive a certain chemical component that is usually toxic for eukaryotic cells, such as geneticin, blasticidin or puromycin, and then this chemical is added to the culture media. An alternative strategy involves auxotrophic selection whereby host cells contain genetic deletions of key genes such as dihydrofolate reductase (DHFR) or glutamine synthetase (GS). When cultured in medium not containing the metabolic substrates (e.g. hypoxanthine and thymidine for DHFR, or glutamine for GS) only cells which have correctly integrated the plasmid containing the DHFR or GS gene into their genome are able to survive and this therefore facilitates selection. The auxotrophy is usually paired with the addition of a chemical component that further inhibits the activity of the enzymes that the genes encode for, methotrexate (MTX) for DHFR and methionine sulphoximide (MSX) for GS. The auxotrophic strategies result in DNA amplification as the cells need to produce high levels of the selection protein which results in an increased copy number of the GOI and increased expression levels, providing an advantage over antibiotic based systems[22,23].

### 1.3.3 Benefits of Stable Expression

Stable cell lines are the cell lines of choice for manufacturing purposes. Decades of research have created cell lines able to produce titres as high as 10 g/L[24]. Manufacturing cell lines are able to maintain these high expression levels over time, whilst maintaining consistency in product quality, making them the choice for manufacturing purposes. Manufacture of the high quantities of mAbs needed for the market usually requires the use of bioreactors in excess of 1000 litres, therefore the cells must be able to maintain protein expression levels and product quality for more than 50 generations as per

regulatory requirements. However, CHO cells demonstrate exceptional phenotypic and genetic heterogeneity even when derived from the same clone[19] and can therefore present issues of protein expression instability even following selection[25]. To fulfil these stringent regulations, clonal populations are produced and screened to generate a cell line that can maintain high yield over generations and the correct product quality[26].

### 1.3.4 TGE Potential

Despite the undeniable benefits of stable cell lines for manufacture of biotherapeutics, the extensive time required for stable cell line development is problematic in cases where rapid generation of material is required. The virus SARS-CoV-2, the causative pathogen of the disease Covid-19, was first discovered in 2019 and quickly became a pandemic throwing the whole world into chaos. This galvanised the scientific community to develop new therapeutics and vaccines against this novel virus, including therapeutic mAbs. A year after the pandemic began, 162 mAbs against covid-19 have been developed, 7 of which have reached clinical trials. Following the decision to progress a mAb into the clinic there is typically a 10-12 month lag before clinical trials are started. To put the scientific effort against Covid-19 into context, the first Covid-19 mAb entered clinical trials in June 2020, just 7 months after the virus was discovered. However, this is still too long in the context of rapid response to a pandemic. As of February 2021, Pfizer, AstraZeneca and Moderna have each produced a vaccine that has been approved for use by the UK Medicines Health Regulatory Authority (MHRA), with a further vaccine by Novavax reporting promising phase 3 clinical trial data. In contrast, no mAbs have yet fully completed phase 3 trials.

Even with the much-reduced timelines for Covid-19 biotherapeutic development, manufacturing was a bottleneck for the fast production of therapeutic mAbs to enable timely clinical trials. The accelerated process observed during the Covid-19 pandemic was achieved mostly by accepting business risks and parallelising processes that are usually run consecutively[27]. The reduced timelines were impressive; however manufacturing and the creation of stable clonal cell lines was still a bottleneck. Therefore, transient expression platforms could be an invaluable tool in rapid response to emerging pathogens and threats, supplying material for toxicology and initial phases of clinical trials[28–30]. Although the main barrier for this is regulatory, this regulatory guidance is widely considered outdated in the field and does not take into consideration other biotherapeutics produced in transient platforms, such as VLPs and adenovirus. Recent studies also show that stable clonal cell lines, favoured for their consistency, can actually demonstrate variability in their transgene copy number and sequence variance, owing to the genetic instability of CHO cells[31,32]. The new sense of urgency brought by the pandemic alongside technical improvements in transient gene expression (TGE) technology and a push for regulatory modernisation could make the use of TGE for human studies a reality.

TGE has improved dramatically in the last 20 years, increasing titre as much as 60-fold and utilising culture volumes of up to 100 L[33–36]. These numbers are encouraging but research is by no means complete. While 3 g/L has been reported from TGE, the variability was high and the results varied widely depending on the mAb sequence, with titres as low as 100 mg/L[35,37,38]. Many published works on TGE quote expression levels in the region of 100s of mg/L, although it is important to note that commercial entities with breakthrough discoveries may prefer not to publish these in order to maintain a competitive advantage[37,39]. An increase in titre would reduce the associated costs by reducing the required culture volume and number of cells per transfection, the latter of which would reduce the presence of contaminating host cell proteins (HCP) which are problematic for downstream processes such as purification. Achieving higher titres could also reduce the duration of the expression and therefore facilitate faster material supply and provide sufficient material for more indepth characterisation studies, pre-clinical and even clinical studies. Although TGE using up to 100 L culture volumes has been undertaken, TGE at such a large volume can be problematic and expensive due to process variability during transfection and the large amount of DNA required. These difficulties can be addressed by achieving improved plasmid retention within the cells during culture, facilitating lower volume transfection and is the subject of this thesis. Overall, improving current TGE technologies and processes would allow faster production of higher quantity and quality material at a lower cost, resulting in shorter timelines for research and early stages of development. An improvement in titre and the ability to achieve higher culture volumes would also mean that TGE becomes a potential option to quickly produce material for the early stages of clinical trials.

## 1.4 Cell Expression System Optimisation

The overall production process of biopharmaceuticals using mammalian cells consists of several steps that are performed in concert to achieve optimal results. Over decades of research, each step has been carefully considered and efforts have been dedicated to their optimisation, individually or alongside other factors. These factors can be grouped into different categories including vector optimisation, bioprocess engineering and cell engineering. Each improvement can rarely occur in isolation and therefore a holistic approach to enhancing TGE is required.

### 1.4.1 Vector Optimisation

Vector improvements focus on optimising the rDNA sequence. It can focus on the GOI, for example using codon optimisation for the cell type or adding an artificial intron to encourage mRNA splicing. Other elements of the vector can be changed, for example incorporating a strong promoter, adding gene insulators or using woodchuck post-transcriptional regulatory element (WPRE) [26,40] to increase

DNA transcription to produce RNA. Modification of the GOI to remove amino acid residues positively associated with protein aggregation can also be carried out[41].

### 1.4.2 Bioprocess Engineering

Bioprocess engineering includes adjusting transfection and other process strategies. Transfection is the process of introducing the vector DNA into the cells and several techniques have been developed depending on the expression type (stable or transient) and cell line. Transfection methods can be categorised into biological (such as viruses), chemical, or physical, with chemical methods being the most popular for TGE. In the context of chemical transfections, initially the main reagent used was calcium phosphate (CaPi)[42], but this has been superseded by the widely used polyethylenimine (PEI)[43]. Other options are available, including cationic lipids such as lipofectamine or FreestyleMax, however the higher price discourages their use for large volume transfection[40,44], where PEI is favoured for this application. PEI is a cationic polymer first used for gene expression in 1995[45]. It is a cost-effective reagent that allows efficient introduction of DNA into a large volume of cells using a simple process. Physical transfections involve disruption of the cell membrane to allow DNA to enter with electroporation being the most popular example. Electroporation works by applying a charge to cells to increase the permeability of the cell membrane, allowing DNA to enter. Electroporation allows a large amount of plasmid DNA to be introduced to cells, and often results in high transfection efficiency, however it is usually reserved for small scale transfection as it has traditionally not been scalable. Flow electroporation is a new iteration of this technology (MaxCyte, Gaithersburg, MDS) which allows the transfection of a large volume of cells. The main drawback of this method however is the need for medium replacement to provide a specific buffer and to concentrate the cells, which complicates the protocol and increases the cost in comparison to chemical transfections[46].

Process strategies include improving culture conditions and media design. Obtaining a high-density culture is a common objective in stable platforms, however transiently transfected cells show a decrease in protein production over time and division as the plasmid is lost. One of the strategies to avoid this is to decrease cell division after transfection. Temperature shift induces a mild hypothermic state (30-33°C) which arrests the cell cycle in G1, reduces the metabolic rate and cell division and subsequently increases titre several fold[47,48]. It is also possible to include chemical additives to arrest cell growth or increase productivity. Histone deacetylases, such as valproic acid (VPA) or sodium butyrate promote histone hyperacetylation and result in higher DNA transcription[40,49], while it has also been reported that cell growth arrest can be achieved with the addition of nucleotides[50]. Feed strategies to replenish nutrients are routinely used to keep the viability high and maintain cultures for a longer period of time[51,52]. Improved transfection procedures for high-density transfection have allowed an increased concentration of cells in the culture without the associated plasmid loss during

cell division[37,39]. However, a high density of cells can result in the induction of apoptosis and depletion of nutrients from the culture media and as such feeds and media need to be adjusted accordingly. This demonstrates the necessity for modifying several aspects of the process (i.e. cell engineering and bioprocessing together) to achieve the best possible outcome.

### 1.4.3 Cell Engineering

Cell engineering for TGE refers to the modification of the host cell line, usually aiming to counteract limitations naturally present in cell systems. These techniques can involve modulation or deletion of endogenous genes, or the introduction of foreign genes. The intended result can be broadly divided into 3 categories, namely inhibition of apoptosis, arresting growth and increasing productivity. Inhibiting apoptosis aims to increase culture viability throughout the culture which can increase titres, but importantly also decreases levels of HCP in the final product which simplifies downstream processes. One method to achieve this is the overexpression of the protein kinase B (Akt) which can protect cells from apoptotic effects of VPA. Arresting growth has been seen to increase protein production and modulate PTMs with a myriad of examples of such approaches available in the literature[47]. This approach has been demonstrated in CHO DG44 cells, which were engineered to overexpress acidic fibroblast growth factor (FGF-1), enhancing specific productivity by also overexpressing cell cycle regulatory proteins such as p18, p21 and p27 causing cell growth arrest in phase G1. An important step related to efficient protein production is manipulation of ribosome biosynthesis[53]. X-box binding protein 1 (XBP-1) overexpression can facilitate ribosomal biosynthesis and its exogenous expression has resulted in an up to a 2.5 fold increase in production[54]. Expression can be conditionally modulated by using microRNA or short-interfering RNA to enhance or silence genes, or globally by total deletion of genes such a Breast Cancer 1 (BRCA1)[55] and Activating Transcription factor 6β (ATF6β)[56].

A cell engineering approach specifically geared towards transient expression is the introduction of viral proteins which allow episomal retention and/or episomal replication of the transgene. A natural example of this is the Epstein-Barr Virus (EBV) which maintains its whole genome as an extrachromosomal plasmid inside infected cells. The exact mechanism of this is provided in more detail in section 1.5, however in brief this is achieved by tethering the viral *oriP* sequence to the host chromosome by the action of EBV nuclear antigen 1 (EBNA-1). Cell engineering approaches have produced cell lines, such as CHO-3E7 and HEK293E, that constitutively express EBNA-1 and this allows plasmid maintenance during TGE, providing the vector has been engineered to contain an *oriP* sequence[57,58].

## 1.5 EBV and Other Herpesviruses

### 1.5.1 Epstein-Barr Virus

In 1958 Denis Burkitt observed and described an aggressive type of cancer common in African children, which he named Burkitt's Lymphoma (BL). Burkitt suspected the cancer to be viral in origin due to its unusual geographical distribution[59]. Sharing his findings during a presentation in London piqued the interest of the scientist Anthony Epstein, who, working with Yvonne Barr later became the first to visualise viral particles in samples recovered from BL patients. In 1964 this virus was named the 'Epstein-Barr virus' (EBV)[60]. EBV was discovered to be the agent causing infectious mononucleosis, is present in 90% of the population and although it is asymptomatic in most cases, it has also been further linked to a variety of other malignancies[61,62].

EBV, also called Human γ-herpesvirus 4 (HHV4), is a double stranded DNA virus with a 172 kb genome[63], which is established inside the infected cells as an extrachromosomal plasmid. The viral genome contains approximately 80 protein coding open reading frames (ORF) and more than 30 different non-coding RNAs[64]. The virus primarily infects B lymphocytes through the interaction of its viral envelope glycoprotein gp350 with CD21 present on the B-cell surface[65], and the binding of gp42 to human leukocyte antigen (HLA) class II molecule[66], although it has also been found capable of infecting T lymphocytes or epithelial cells less efficiently via a CD21 independent mechanism[67–69].

The lifecycle of EBV and all herpesviruses is characterised by lytic and latent phases. During the lytic phase host cell machinery is hijacked by the virus to replicate itself which eventually results in cell lysis. This differs to the latent phase of infection, whereby the virus lies dormant within the host, thus establishing a lifelong latent infection[70,71]. Although not conclusively shown, EBV infection likely initiates in the host by lytic infection of epithelial cells before shifting to latent infection of B-cells where it is able to establish life-long persistence by restricting the expression of its viral proteins and non-coding RNA. It is thus highly specialised to evade the immune system. Other herpesviruses such as alpha and beta cause disease in the lytic form, however EBV pathology is associated with the latent phase, including among others Burkitt's Lymphoma and Hodgkin's lymphoma[72]. Different protein expression patterns are classified as different latent infection cycles (0, I, II, III) and linked with different malignancies. EBNA-1 is expressed in all latency cycles except for latency 0, which is reserved for quiescent memory B cells[71]. It is essential for the maintenance of EBV extrachromosomal episomes in latently infected cells, achieved through sequence specific DNA binding to *oriP*[73,74].

#### *1.5.1.1 EBNA-1*

EBNA-1 is the essential protein allowing EBV to maintain its genome as an extrachromosomal episome in infected cells. It carries this out through 3 distinct mechanisms: episome maintenance by tethering it to the host's chromosome, replicating the viral episome once per cell cycle, and episome segregation by faithfully segregating the replicated episome to the daughter cells upon cell division[75,76]. The N-terminal region of EBNA-1 is able to bind to the host cell chromosomes, while the C-terminal region binds the viral episome in a sequence specific manner, by interaction with EBNA-1 binding sequences (EBS) found within *oriP*. The central region of EBNA-1 contains a glycine-glycine-alanine repeat (GGA repeat), which is responsible for immune evasion. The GGA repeat is flanked by two glycine and arginine rich domains (RGG domains) in regions necessary for EBNA-1 binding to chromatin, known as linking regions (LR1 and LR2)[77,78] (Figure 2). RGG domains are able to bind and interact with several cellular proteins (Figure 3), including chromatin associated proteins such as EBNA-1 binding protein (EBP2)[79,80], the chromatin component high-mobility group box 2 (HMGB2)[81], nucleolin[82], and the histone associated protein Regulator of chromosome condensation (RCC1)[83]. They also have AT-hook activity which allows them to directly bind to AT rich regions[78] and are able to interact with G-quadruplex RNA[84]. G-quadruplex interaction is necessary both for EBNA-1 binding to mitotic chromosomes and for the recruitment of the host's origin recognition complex (ORC) to oriP[85,86].

The central GA repeat functions to reduce presentation of viral antigens on class I HLA proteins by stabilizing EBNA-1 and inhibiting its degradation. Translation of EBNA-1's mRNA is also inhibited by this sequence through formation of highly stable secondary structures called G-quadruplexes that induce ribosome dissociation[87]. This further reduces antigen presentation and contributes to the GA repeat's immune evasion functions[88,89].

The N-terminal domain contains the DNA binding domain (DBD) which is responsible for binding oriP and interacting with its recognition sites. The DBD is also responsible for EBNA-1 dimerization. EBNA-1 forms stable homodimers in solution and also when bound to its recognition sites within the *oriP*, which are presented in pairs. Higher conformations have been observed, with crystal structures of the DBD identifying formation of a hexameric ring comprised of trimers of EBNA-1 homodimers[90].

EBNA-1 has been shown to interact and influence cellular gene expression and affect signalling pathways by interacting with other cell proteins[91]. One such example is USP7, with EBNA-1 outcompeting with it for binding to the transcriptional activator p53 and promoting cell survival in response to cellular stress[92]. EBNA-1 has also been shown to affect gene expression[93,94]. Direct binding to certain sequences within the host's genome, which show some similarity to its own EBS within *oriP* have been shown to alter local gene transcription[95]. The mechanisms for EBNA-1 transcriptional

regulation are not completely understood, however they are probably the result of its interaction with both DNA elements and transcription factors as it can either increase or decrease expression[96,97]. These interactions with cellular proteins have also been shown to have an effect on its episomal replication function. A mutation which renders EBNA-1 unable to bind to USP7 also increases EBNA-1 episome replication 4 fold[98], while EBNA-1 interaction with tankyrase negatively affects the same function[99].

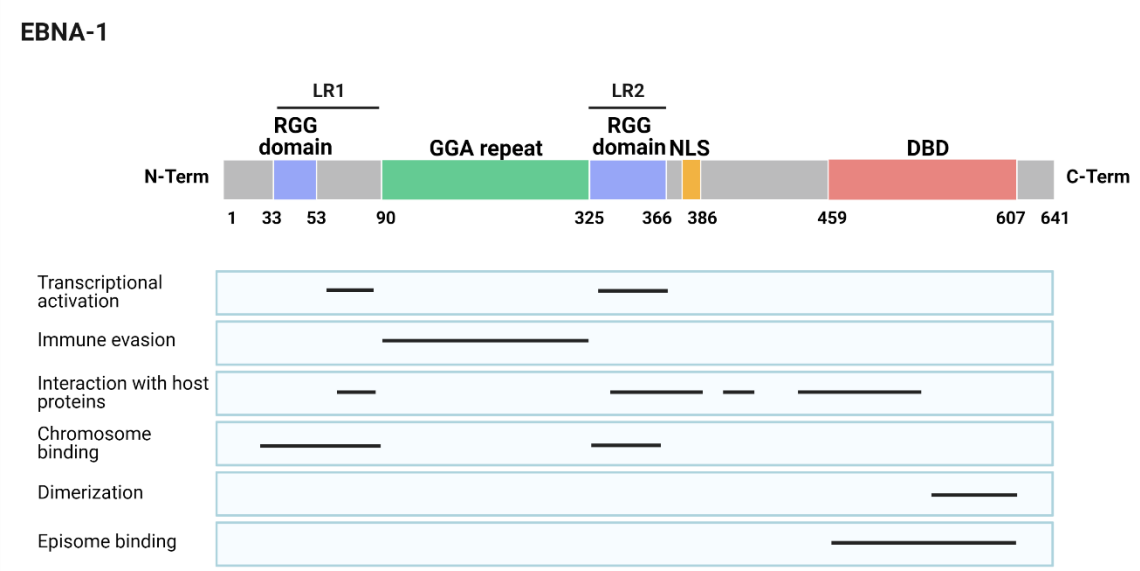


***Figure 2: Schematic representation of EBNA-1.*** *Structure shows the glycine and alanine rich domains (RGG domain, blue box), the glycine-glycine-alanine repeat (GGA repeat, green box), the nuclear localisation site (NLS, yellow box) and the dimerization and DNA binding domain (DBD, red box). Linking regions (LR1 and LR2) are highlighted and include the RGG domains. Black bars in the lower panel show the approximate region responsible for specific functions, defined in the column on the left.*

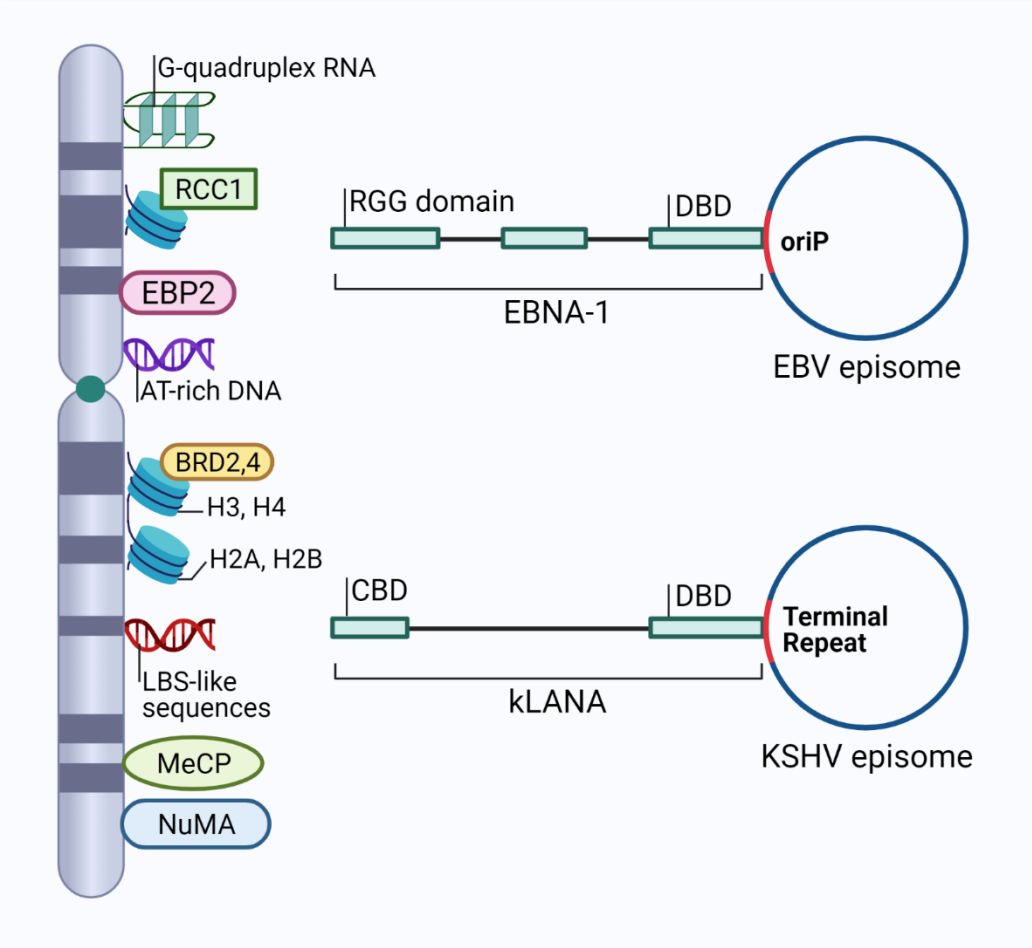


***Figure 3: Representation of EBNA-1 and kLANA episome tethering functions.*** *EBNA-1 RGG domains are able to interact with g-quadruplex RNA, the histone associated protein Regulator of chromosome condensation (RCC1), EBNA 1-binding protein (EBP2), and AT-rich DNA. kLANA chromosome binding domain (CBD) is able to bind the histones H2A and H2B, the histone associated Bromodomain-containing protein 2 and 4 (BRD2,4), LANA binding site (LBS)-like sequences found in the human genome, and methyl CpG binding protein 2 (MeCP2). kLANA's C-terminal region, which contains the DNA binding domain (DBD), is able to bind to the Nuclear mitotic apparatus (NuMA). The DBD of both EBNA-1 and kLANA are able to bind to their recognition sites found in their own origins of replication, oriP for EBV episome and terminal repeat for the KSHV episome. Adapted from Lieberman P. M. (2013).*

#### *1.5.1.2 OriP*

*OriP* is the EBV origin of plasmid replication and is composed of two distinct functional components 1000 bp apart from each other: the family of repeats (FR) and the dyad symmetry (DS)[100]. Both elements contain EBNA-1 recognition sites and are necessary to achieve episome replication and faithful segregation to daughter cells (Figure 4).

The FR element consists of 20 imperfect tandem copies of a 30 bp sequence, each containing an 18 bp EBNA-1 binding site followed by a 12 bp AT-rich element[74,100,101]. The main functions of the FR are stable retention of the viral genome within the nucleus, mitotic segregation and transcriptional

enhancer. EBNA-1 interacts and binds to both the viral episome and the host's chromosomes, linking them and maintaining the viral episome in close proximity to the host's genome. The transcriptional enhancement function of the FR is dependant on EBNA-1 binding[102,103]. The FR elements present in the viral episome are bound through the C-terminal DBD in a sequence specific manner while the N-terminal RGG domains motifs are able to interact with host's chromatin. FR has also been found to direct EBNA-1 to bind to transcriptionally active regions of the chromosome[104] and to stabilise the EBNA-1 bound to the DS site.

The primary function of DS is plasmid replication[105]. DS is approximately 120 bp in length and contains 4 EBS, 2 high affinity and 2 which show lower affinity binding (Figure 4). These sites are arranged in pairs with the distance between the centre of each binding pair equalling exactly 21 bp, this distance being critical for maintenance of its function: the addition of just 5 nucleotides in this gap was found to abrogate function. The 21 bp gap allows 2 molecules of EBNA-1 to organise themselves on the same side of the DNA helix which may explain this stipulation[85,105]. Next to each pair of binding sites are 3 nonamers which bind telomere-repeat binding factors TRF1 and TRF2[106]. The way in which EBNA-1 is able to achieve episomal replication is multifaceted and not fully defined, however it is clear that EBNA-1 is able to recruit the host replication machinery to the DS. The physical mechanism by which EBNA-1 is able to interact with the host proteins needed for replication has not been completely defined, but is related to EBNA-1's ability to interact with G-quadruplex RNA through its RGG-like motifs[86]. The process is initiated when EBNA-1 recruits the host ORC[85] which in turn recruits the additional factors, namely cell division control protein 6 (Cdc6), chromatin licensing and DNA replication factor 1 (Cdt1), and the minichromosome maintenance complexes (MCM)[107], to fully form the pre-replication complex (pre-RC). A summary of the DNA replication process in eukaryotes up to the pre-RC formation is shown in Figure 5. EBNA-1 has also been found to interact with Cdc6 and this may assist its recruitment to the DS[108]. TRF1 and TRF2, which are bound to the nonamers next to the EBNA-1 binding site, also seem to be key contributors to formation of the pre-RC[109]. Other factors have also been found to interact or be part of this process. TRF2 may be necessary to recruit the ORC, while Tankyrase which binds to TRF1 seems to inhibit the function of EBNA-1. The host proteins Timeless and Tipin are related to formation of the replication fork and appear to be involved in episome segregation by forming replication-dependent catenated structures, linking the episomes to the chromosomes[97]. Depletion of Timeless causes loss of the episome and the formation of double stranded breaks, whereas replication forks seem to be stabilised by Timeless[97].

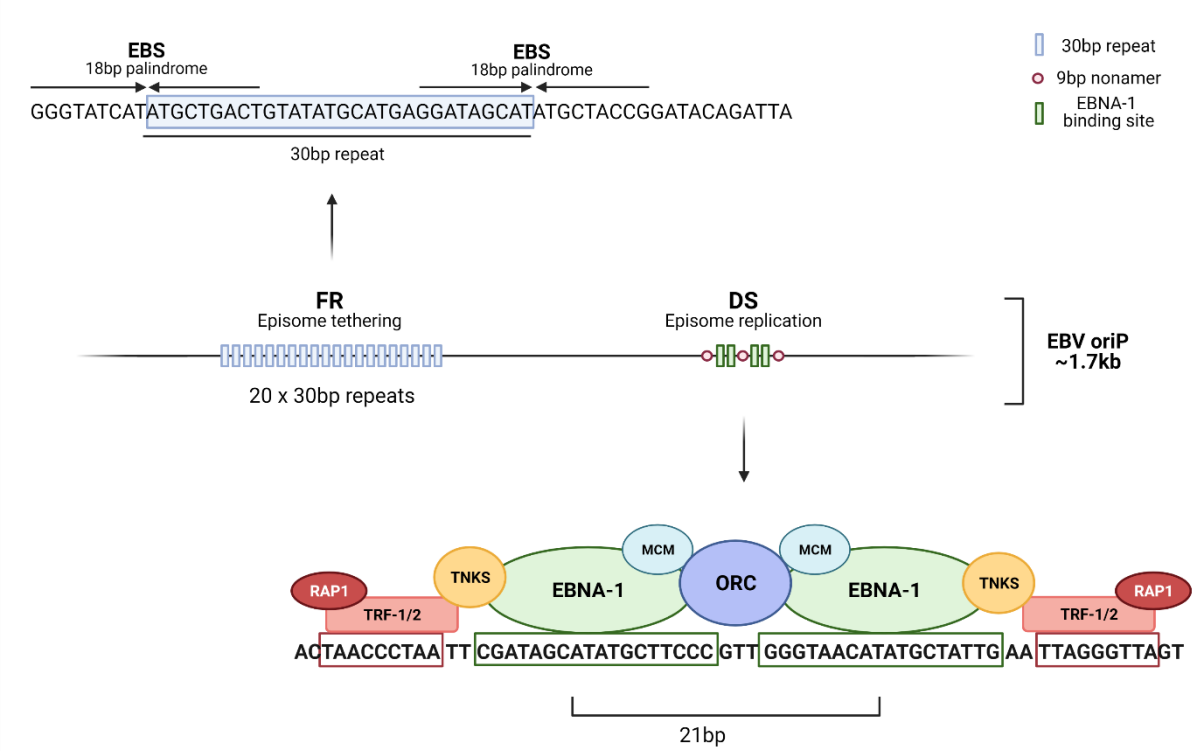


**Figure 4: Schematic of EBV oriP and interacting proteins.** *The origin of replication (oriP) is formed by the family of repeats (FR) and the dyad symmetry (DS), shown in the central panel. Both domains contain EBNA-1 binding sites (EBS) indicated by blue boxes for the FR or green boxes for DS. The FR contains 20 imperfect repeats of a 30 bp sequence; the consensus sequence for the FR repeats is shown in the top panel. The EBS found within the FR are marked by head to head arrows, while a 12 bp AT-rich region is located between each EBS. The DS has 4 EBS (green boxes), sequences for EBS1 and 2 and flanking regions have been enlarged in the lower panel. Each EBS is bound by an EBNA-1 dimer (green). The EBS binding sites are separated by 21 bp and flanked by two 9 bp nonamers with telomere-like sequences (red box) which act as binding sites for TRF1 and TRF2 (light red) which associate with human repressor activity protein 1 (RAP1). EBNA-1 recruits the cellular origin recognition complex (ORC) (blue) which then recruits the minichromosome maintenance complexes (MCM) (light blue), involved in episome replication. The protein tankyrase (TNKS) (orange), which interacts with TRF1, regulates episome replication. Image adapted from Wilson et al. 2018 and Kamranvar, S.A.; Masucci, M.G 2017.*

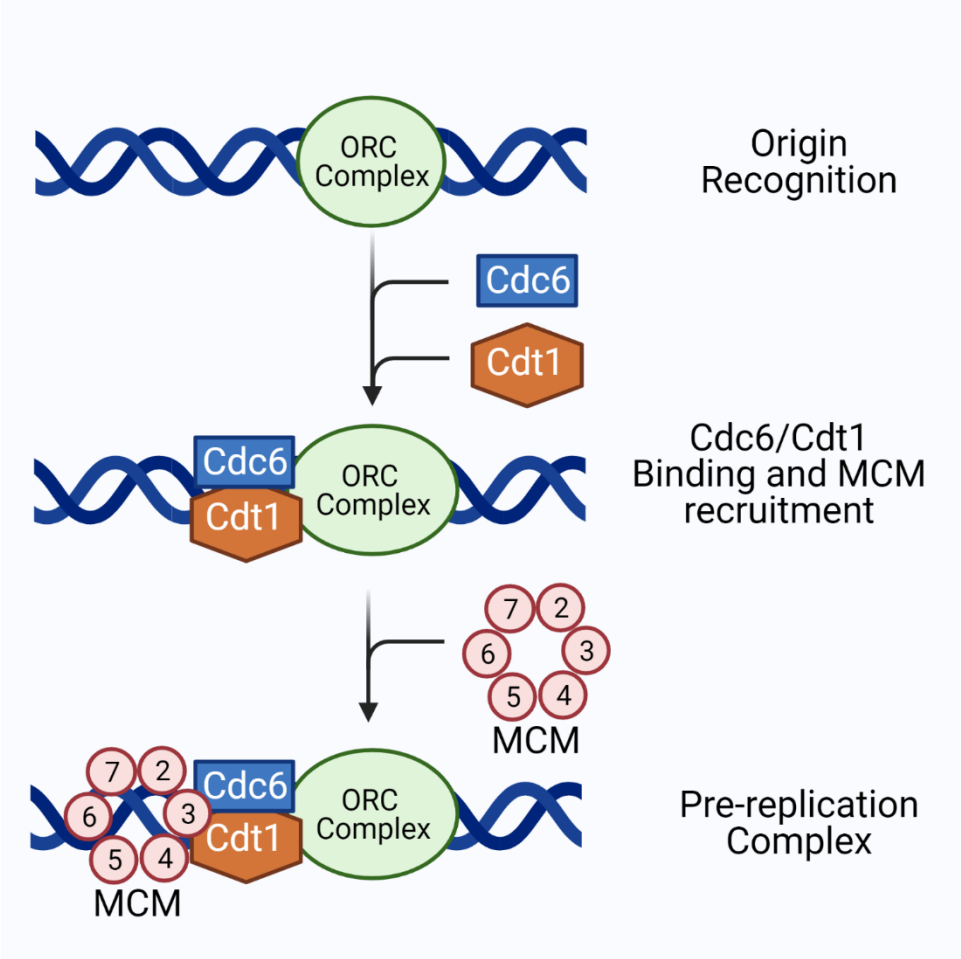


**Figure 5: Pre-replication complex (pre-RC) assembly.** *The pre-RC is assembled step by step during late M to early G1 phase of the cell cycle. In early G1 phase, the origin of recognition complex (ORC) recruits the helicase loaders cell division control protein 6 (Cdc6) and chromatin licensing and DNA replication factor 1 (Cdt1), which promotes the loading of the minichromosome maintenance complexes (MCM), a DNA helicase formed by Mcm2-7 in the form of a hexamer. On transition to S phase, the pre-RC is activated and induces DNA unwinding, this facilitates the loading of additional necessary factors. Cdc6 and Cdt1 are degraded or inactivated during S phase to avoid additional pre-RC formation*[110]*. Image adapted from M. S. Valenzuela 2006.*

## 1.6 Alternative Episome Maintenance Systems

### 1.6.1 EMP in the Context of TGE

The first system in which EBNA-1 was applied for TGE was HEK293[111,112], a human cell line widely used for recombinant protein production. By using EBNA-1, plasmid replication and retention was achieved, allowing a dramatic increase in protein expression. This approach was subsequently translated into CHO cells since they are the preferred manufacturing cell line for biopharmaceuticals. As outlined previously, increasing TGE yield by developing current technologies and strategies translates into faster research and drug development. The first attempt in CHO cells to achieve plasmid retention co-delivered an EBNA-1 expression cassette alongside a plasmid containing *OriP*[57], therefore both GOI and EBNA-1 were expressed transiently. The process was improved when EBNA-1 was stably integrated into the host genome, reliably achieving higher titres. EBNA-1 is pleiotropic and is able to achieve plasmid retention alongside other effects related to increased protein expression, including cytoplasm-to-nuclear transfer and transcriptional enhancement[113].

Although EBNA-1 is able to increase productivity in both HEK293 and CHO cells, EBNA-1 is only able to replicate the plasmid in human cell lines. Several publications investigating plasmid maintenance and replication in a variety of hosts confirm this[67], although it has also been noted that EBNA-1 may achieve low-level plasmid replication in non-CHO rodent cells, these studies are in the minority[114]. EBV displays a narrow tropism and is unable to infect non-human cells, which may explain the species preference of EBNA-1[115].

A strategy to overcome the lack of plasmid replication with this viral system is to combine it with other viral proteins. One study was able to achieve plasmid replication in CHO cells using the Polyomavirus (Py) large T antigen and *pyOri* on the plasmid[57]. Combining this technology with an EBNA-1 *oriP* system and with further bioprocess improvement it was possible to increase protein expression significantly[116]. However, the efficiency of the pyLT/*pyOri* in plasmid replication leaves room for further improvement; the replicated plasmid achieved a maximum level at day 2 post transfection and sharply decreased by day 3, which does not seem compatible with long term maintenance[57].

While an incredibly intricate system, EBV is not unique in its ability to achieve episomal replication of its genome via EMPs, as mechanisms analogous to EBNA-1/*oriP* are demonstrated by all Gammaherpesviruses. EBV's complex and sometimes undefined interaction with the host cell replication machinery may mean that plasmid replication is not possible without extensive humanisation of the CHO cell line. Development of a herpes viral system with natural tropism for rodent cells may present a novel method for improving TGE by achieving plasmid replication.

### 1.6.2 KSHV

Kaposi's Sarcoma-Associated Herpesvirus (KSHV) or human herpesvirus 8 (HHV-8), is a common oncovirus that causes Kaposi sarcoma cancer in HIV-infected patients and has been linked with other malignacies[117–119]. Like EBV, it is a member of the Gammaherpesvirus family, however is grouped in the Rhadinovirus genus[120]. The KSHV viral genome consists of a ~140 kb unique region flanked by multiple ~801 bp terminal repeat (TR) sequences. The unique region contains approximately 90 ORFs, most of which have homology with other herpesviruses[121,122]. Like all herpesviruses, it presents a lytic and latent cycle and maintains the viral genome as an extrachromosomal episome[123].

The episome maintenance protein in KSHV is called latency-associated nuclear antigen (LANA). LANA is present in all Rhadinoviruses and is functionally homologous to EBNA-1, being responsible for episomal retention and replication inside the host cells during latency (Figure 6). KSHV LANA (kLANA) is encoded by ORF73[124] and is a protein consisting of 1162 amino acids[121]. The N-terminus contains the chromatin binding domain (CBD) and the nuclear localization site (NLS) followed by a proline rich region, while the C-terminus contains the DNA binding domain (DBD) and a second NLS[121,125,126]. kLANA has a large internal acidic central repeat (CR) region with immune evasion functions, achieved through self-inhibition of its expression and increased protein stability reducing proteosomal degradation, which leads to a decrease in antigen presentation by the MHCI. In contrast to the GA repeat in EBNA-1, the CR has other functions not related to immune evasion[127]. The CR is mostly comprised by repeats rich in glutamine (Q), glutamate (E), and aspartate (D)[127]. The repeats forming the CR are imperfect and can be further divided in sections. The first CR section contains DED repeats, followed by a longer QED region and a leucine zipper[88,128,129]. While the canonical kLANA sequence has 1162 aa, the size varies greatly among different isolates. The unique regions found in the N-terminal and C-terminal regions are highly conserved, especially the DBD, while the CR region from aa 338 to 797 consists of a variable number of repeats[130].

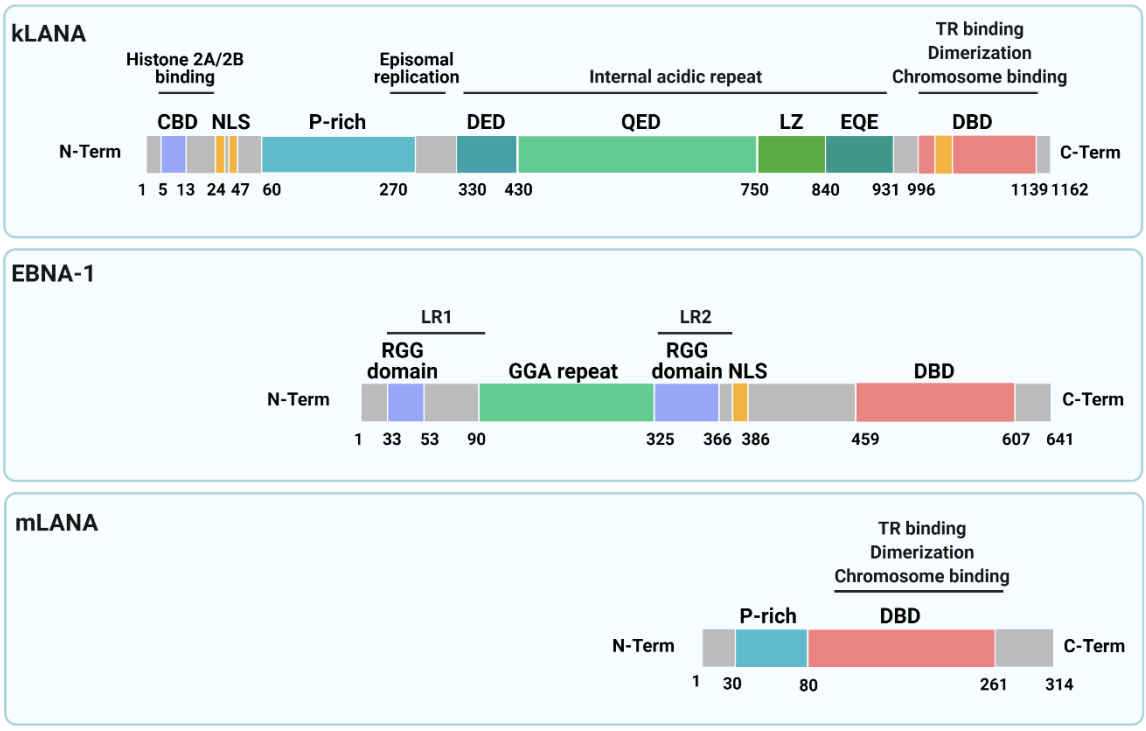


***Figure 6: Schematic diagram of kLANA, EBNA-1 and mLANA structures.****Upper panel shows kLANA structure, lower panel shows mLANA structure. Both contain a proline rich (P-rich) sequence found in the N-terminal domain (N-Term) and a dimerization and DNA binding domain (DBD) with similar functions to EBNA-1's DBD within the C-terminal domain (C-Term). kLANA has an internal acidic repeat comprised of aspartate-glutamate repeats (DED), glutamine-glutamin-aspartate repeats (QED), a leucine zipper (LZ) and a glutamine-glutamate rich region (EQE). Histone binding and episomal replication functional regions are indicated. mLANA does not contain an internal repeat, which partly explains its smaller size. Boxes representing functional domains are not to scale. Refer to figure 2 for the structural details of EBNA-1.*

kLANA is able to tether the viral episome in a similar way to EBNA-1 (Figure 3). The CBD interacts and binds human mitotic chromosomes through its interaction with cellular histones H2A and H2B, LBS-like sequences found in the human genome, methyl CpG binding protein 2 (MeCP2) and members of the bromodomain and extraterminal (BET) protein family BRD2/4 [130–136], while the DBD is able to bind to the kLANA binding sequences (kLBS) in the TR, which fills the same function as EBV's *oriP* sequence. In contrast to EBNA-1's DBD, kLANA's c-terminal region is able to bind chromosomes and the DBD has residual replication activity (25%)[130,137]. The C-terminal region is also responsible for interacting and recruiting the host's ORC to the TR, allowing episomal replication[138]. The basic kLANA structure is a dimer, however it has been observed to form structures composed of tetramers or pentamers of dimers which form a ring or spiral[139].

The TR is formed by non-coding DNA with 85% GC content and is present in a variable number between 35-45 repeats per genome[140]. The TR is the origin of replication for KSHV with analogous function to the EBV *oriP*[131,141,142], although no sequence homology has been found between TR and

*oriP*. Although *oriP* contains two well defined sequences with distinct functions, DS and FR, TR episomal replication and retention functions have not been assigned to different specific sequences. The TR contains kLANA binding sites (kLBS), 20 bp palindromic sequences that interact with the protein through kLANA's DBD. Each kTR contains 3 binding regions, kLBS1 has a high binding affinity and is flanked by kLBS2 and kLBS3, both binding kLANA with lower affinity[126,139]. The space between kLBS1 and kLBS2 is exactly 22 bp centre to centre, which is similar to the EBV DS and its 21 bp spacing[143]. kLBS3 had been previously described as a 32-bp GC-rich region upstream of kLBS1 with an unidentified function but essential for plasmid replication before being identified as another binding site. This was referred to as the "minimal replicator element (MRE)"[144] (Figure 7). A single copy of this MRE has been shown to be sufficient for short-term replication of plasmids *in vitro*[142], however other experiments suggest that at least 2 copies of the TR are necessary to maintain appropriate episome persistence[131] and identify a positive correlation between number of TRs and efficiency of plasmid replication. It has been suggested that possessing at least 2 MRE with a distance of exactly 801 bp between them is the key factor, regardless of the DNA sequence it spans[145]. KSHV uses the host's replication machinery for its own and kLANA has been found to interact with and recruit the ORC, replication factor c (RFC), MCM and other proteins to the TR, akin to EBNA-1[138,146].

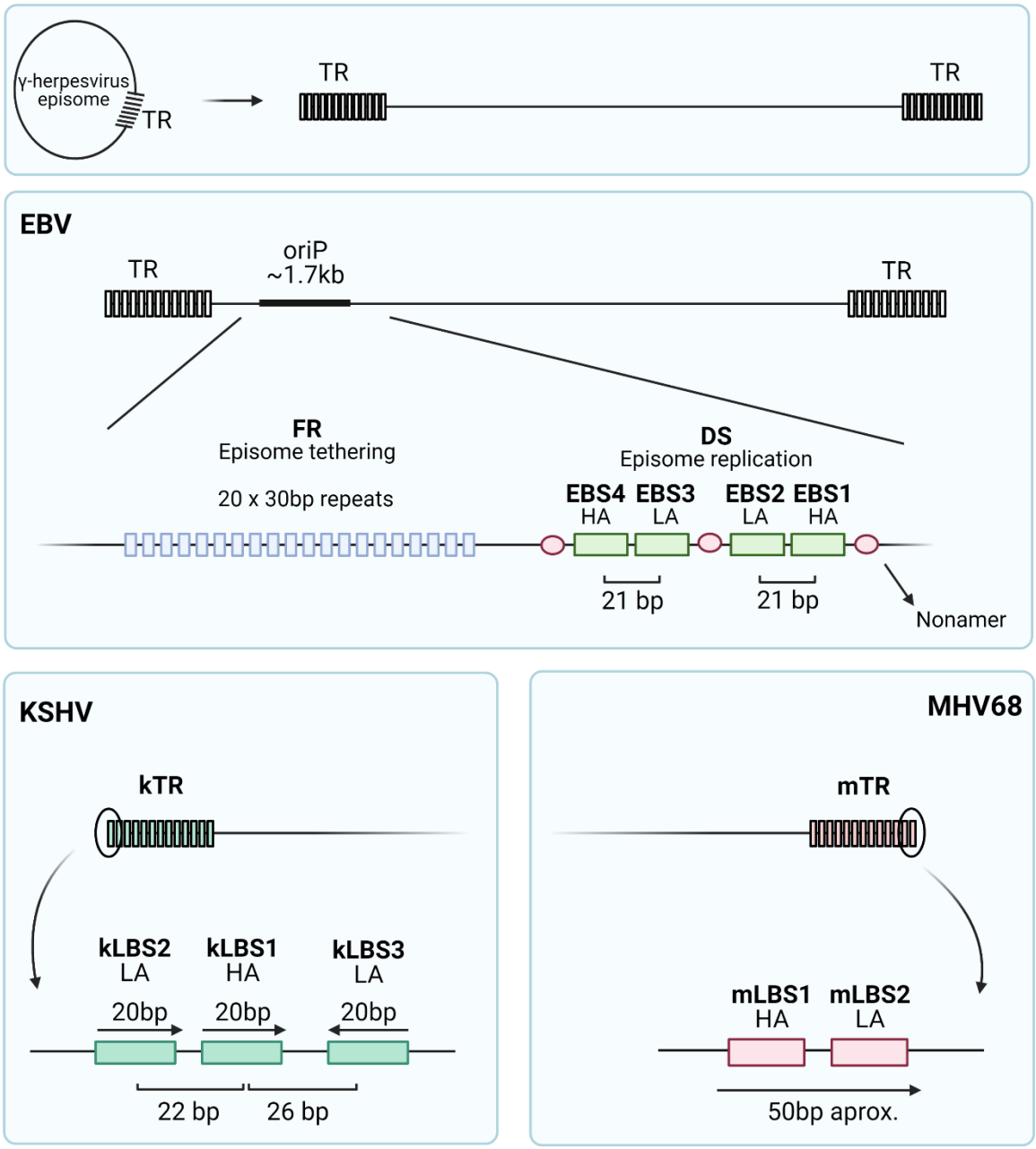


***Figure 7: Schematic representation of the origin of replication for EBV, KSHV and MHV68.*** *Gammaherpesvirus is maintained as an episome, usually represented linearly with the unique region in the centre flanked by terminal repeats (TR). EBNA-1's origin of replication (oriP) is found in the unique region, and is composed of a family of repeats (FR) and a dyad symmetry (DS), responsible for episome tethering and episome replication respectively. DS contains 4 EBNA-1 binding sites (EBS): 2 high affinity (HA) and 2 low affinity (LA) which work in tandem to load EBNA-1. EBS are flanked by 9 bp telomere-like nonamers. KSHV and MHV68 origins of replication are found on their respective terminal repeats (kTR and mTR). Each TR contains several LANA binding sites (LBS and kLBS for kLANA and mLBS for mLANA). kTR has 3 kLBS, a HA kLBS (kLBS1) flanked by 2 LA kLBS (kLBS2 and 3). The distance between kLBS1 and kLBS2 is 22 bp, which is important for its functions and is similar to the 21 bp distance between EBS3 and EBS4, and EBS1 and EBS2. mTR contains 2 mLBS, the specific location of which have not been defined other than they are located within a region of approximately 50 bp.*

### 1.6.3 MHV68

Gammaherpesviruses generally present a highly restricted tropism, usually constrained to a single species[115]. The lack of a robust small animal model for EBV and KSHV presents a barrier to their study, especially to investigate the host response to the virus[147]. Murine gammaherpesvirus 68 (MHV68) is a natural pathogen of rodents. Initially isolated from the bank vole (*Myodes glareolus*) and yellow-necked field mice (*Apodemus flavicollis*), MHV68 readily infects laboratory mice (*Mus musculus*)[148,149]. The close phylogenetic relation to KSHV and EBV has made it possible to use MHV68 as an animal model to study the disease pathogenesis of human herpesvirus[150,151].

The MHV68 episome retention and replication system is more similar to that of KSHV than EBV and is characterised by MHV68 LANA (mLANA) protein and the DNA sequence TR (mTR) found in the viral episome[152]. mLANA is encoded by the ORF73 which is found in the 118 kb unique region of the genome. The viral genome is flanked by a variable amount of copies of the 1213 bp long mTR and each mTR has approximately 78% GC content[153,154].

As expected from a functional analogue to kLANA, mLANA has been found to be directly involved in episome retention and replication[155–157]. mLANA is smaller than most other EMPs consisting of only 314 amino acids in comparison to the 1162 of kLANA[121,153]. The murine mLANA lacks an internal repeat region which partly explains the difference in size, while the C-terminal and N-terminal domain are highly conserved between both proteins, with remarkable structural homology between their DBDs[158]. The N-terminus of mLANA is responsible for interacting with, and binding to, host chromosomal histones H2A/H2B which tethers the viral episome to the nucleus[152]. Similarly to kLANA, the DBD is responsible for forming dimers. LANA dimers can form higher structures: mLANA forms linear oligomers, while kLANA forms ring shaped structures, a difference which may be explained by the different way they bind their respective LBS[159,160]. While kLANA creates a bend in the DNA upon binding the LBS, which has also been observed with EBNA-1 and DS, this has not been demonstrated in mLANA. Even though this could indicate a difference in the way each LANA approaches episomal retention, they can function using the other virus's TR, which actually facilitates an increase in efficiency in the case of combining mLANA and KSHV TR (kTR).

mTR is necessary for mLANA plasmid maintenance and replication. Similarly to LANA, mLANA binds to conserved sequences in mTR, known as mLANA binding sites (mLBS)[161]. Each mLBS contains 2 recognition half sites, requiring mLANA to form dimers to function. In long term plasmid maintenance (90-180 days) the number of mTR present in the plasmid is found to be relevant, with 8 mTRs demonstrating higher efficacy than either 2 or 4[152].

## 1.7 Aims of This Project

This project aimed to investigate the use of the above viral EMPs, kLANA and mLANA, as alternatives to EBNA-1 to improve TGE in a proprietary CHO cell line. A variety of techniques were applied to investigate this. First, kLANA, mLANA and EBNA-1 expression vectors were constructed, providing all the necessary elements for *in vitro* episomal replication. These were then stably or transiently transfected into the host cell line, followed by transfection of a fluorescent reporter or candidate mAb, the expression of which was monitored by flow cytometry, western blotting, qPCR and bio-layer interferometry (Octet) to investigate the impact at both a transcriptional and translational level. Alternative systems to EBNA-1 have received some attention, however to our knowledge no group has successfully managed to use the kLANA or mLANA EMPs to enhance episomal retention in a CHO cell host, therefore this work could be transformative within the field of TGE.

# 2 Materials and Methods

## 2.1 Cells and Media

### 2.1.1 Cell Maintenance

The CHO 1-31 cell line used in this work is derived from CHOK1 cells that had been adapted to serum free, suspension culture conditions. This cell line, and all cell lines derived from it, were cultured in CD-CHO medium (Life Technologies, USA) supplemented with 6 mM L-glutamine (Gibco, USA) and passaged every 3-4 days at a concentration of 0.2-0.3x$10^6$ viable cells/mL using pre-warmed media.

CHO-3E7 cells were used under license from the National Research Council Canada and grown in Freestyle F17 Medium (Invitrogen, USA) supplemented with 10% Kolliphor (Sigma-Aldrich, USA) and 4 mM glutamine. They were passaged every 3-4 days, at 0.15x$10^6$ and 0.1x$10^6$ viable cells/mL respectively.

All mammalian cells were maintained in an incubator set at 36.5°C, 7% $CO_2$ and 70% humidity, unless a temperature shift was performed to 32°C. The flasks used were polycarbonate Erlenmeyer flasks with vented cap E125, E250 and E500 (Corning, USA) containing a maximum of 10% of total flask volume as culture volume and grown in an incubator with a shaking dimeter of 25 mm set at 140 rpm.

### 2.1.2 Small Scale Cell Culture

Smaller volumes of cell culture, between 2 and 3 mL, were grown in 24 deep well plates (24dwps; Axygen, USA) with clamp system and sandwich covers from System Duetz (Enzyscreen, NL). These

were placed in an incubator set at 36.5°C, 7% $CO_2$ and 70% humidity, with a shaking dimeter of 25 mm, set at 250 rpm.

### 2.1.3 Cell Counts

Cell number and culture viability were measured with a Vi-CELL system (Beckman Coulter, USA), Cellometer auto 2000 (Nexcelom, USA) or Guava® easyCyte™, all following the manufacturer's instructions. Cells to be counted with Guava easyCyte were mixed with Guava ViaCount Reagent (Luminex, USA) in a 1:20 or 1:10 dilution depending on the expected cell concentration for a total volume of 200 µL and incubated at room temperature, protected from light, for 5 minutes. Samples were then analysed on a Guava easyCyte using the standard settings included in the software and following the manufacturer's protocol.

### 2.1.4 Cryopreservation of Cells

Stable cell lines were preserved in liquid nitrogen (LN) once recovered from transfection and with a culture viability >95%. Cultures were frozen on day 3 of subculture. Freeze media consisted of 92.5% complete culture medium without selection and 7.5% DMSO (Sigma-Aldrich, USA). An appropriate amount of cell culture to obtain $1.5x10^7$ cells/vial was centrifuged at 200 g for 5 minutes. The cells were then resuspended using cold freeze media, the volume of which was calculated by using the formula: 1.5 mL media x number of vials x 1.1. Cells were gently mixed and 1.5 mL of cells were aliquoted into each 1.8 mL cryovial. The cryovials were promptly transferred to a Mr Frosty (Thermo Scientific, USA) filled with isopropanol as indicated by the manufacturer, which is used to achieve an optimal slow cooling rate, and placed at -80°C for 24 hours after which they were transferred to long term storage in LN.

## 2.2 Generation of Stable Cell Lines

### 2.2.1 Kill Curve to Establish Concentrations of Selection Agent to use for Stable Cell Line Development

To ascertain the appropriate concentration of selection agent for selection of stably transfected cell lines, kill curves were constructed. These were performed by seeding $0.5x10^6$ un-transfected viable cells/mL into 24dwps (culture volume 2 mL) and treating them with escalating concentrations of the selection agent, see "2.2.3 Selection of Stable Cell Pools" for details. The lowest concentration that resulted in complete cell death after 7 days was selected for further use.

### 2.2.2 Transfection to Generate Stable Cell Lines

Electroporation of cells with pcDNA3.1 plasmids were performed using the Gene Pulser Xcell Electroporation Systems (Bio-Rad, USA). Transfection was performed on day 2 or 3 post-subculture. On the day of transfection, $1x10^7$ viable cells per cuvette were centrifuged for 5 minutes at 200 g and resuspended in the appropriate amount of media to give a final concentration of $1.43x10^7$ viable cells/mL. The cells were counted and the volume adjusted as required. A total of 100 µL of DNA at 400 µg/mL was added to each cuvette and mixed with 700 µL of cells, electroporated and immediately transferred to 30 mL of pre-warmed complete media without selection in an E125 flask. Electroporation settings were 300 V, 900 µF and resistance infinity (∞). A total of 3 cuvettes were pooled together in each 30 mL flask, creating bulk pools. 4 hours after transfection, minipools were created from the bulk pool flasks by diluting a sample of the bulk pools to 4000 viable cells/mL and plating 100 µL in each well of a sterile 96 flat bottom well plate (96wp; Corning, USA), resulting in 4000 viable cells/well. The minipool plate was then placed in a static incubator at 36.5°C, 7% $CO_2$ and 70% humidity.

### 2.2.3 Selection of Stable Cell Pools

Cell pools created with pcDNA3.1, which contains the Neomycin resistance cassette, were selected with Geneticin (Thermo Fisher Scientific, USA) at a final concentration of 0.4 mg/mL. 24 hours after transfection the cells were centrifuged for 5 minutes at 200 g and resuspended at a final concentration of $0.5x10^6$ viable cells/mL with fresh, pre-warmed, complete CD-CHO media containing 0.4 mg/mL Geneticin. Cells in flasks were counted and passaged every 3-4 days. During selection, passages were undertaken to maintain cells at concentrations greater than $0.2x10^6$ viable cells/mL. Cell cultures exceeding $0.5x10^6$ viable cells/mL were diluted to $0.2x10^6$ viable cells/mL, whereas cultures with concentrations lower than this were simply diluted 1 in 2 with media. In instances where the cell growth was not sufficient for passage, they were centrifuged at 200 g for 5 minutes and resuspended in fresh media. Minipools in static incubators were put under selection 24 hours post transfection by adding 100 µL of pre-warmed, fresh media containing 0.8 mg/mL Geneticin giving a final concentration of 0.4 mg/mL for each well of the 96wp.

### 2.2.4 Minipool Outgrowth and Adaption to Shaking

After plating the minipools in a 96wp they were placed in a static incubator at 36.5°C, 7% $CO_2$, 70% humidity and monitored every 3-4 days. When the cells reached a confluency of >60% of the well they were transferred to a sterile 24 well flat bottom plate (24wp; Corning, USA) and pre-warmed, complete media containing selection was added to a final volume of 1 mL/well. The now empty wells from the 96wp were refilled with fresh media and returned to the incubator as a backup. The 24wp

was placed in a static incubator and monitored every 3-4 days until the wells reached a confluency of >60%. The cells in the 24wp were resuspended and 900 µL of cell culture transferred to a 24dwp filled with 1 mL of pre-warmed complete media. The 24wp was refilled with 900 µL of fresh media and placed back in the static incubator as a backup.

The 24dwp was placed in a shaking incubator set at 36.5°C, 7% $CO_2$, 70% humidity, 210 rpm (25 mm shaking diameter). After 5 days, 3 mL of fresh media was added and the shaking speed increased to 250 rpm. After 2 days shaking at 250 rpm, the cells in each well were counted and used to inoculate an E125 flask at $0.2x10^6$ cells/mL with a final volume of 15-30 mL depending on cell count. The flasks were returned to the same incubator, but with a decreased shaking speed of 140 rpm. The cells were considered recovered when the culture viability was >95%. The cells in E125 flasks were passaged after 3-4 days to E250 flasks with a total volume of at least 60 mL. Some of this culture volume was subsequently used for cryopreservation (see 2.1.4 Cryopreservation of cells). The cells were then cultured routinely every 3-4 days (see 2.1.1 Cell maintenance).

## 2.3 Transient Expression Studies

### 2.3.1 Transfection for Transient Expression

Various conditions for transient transfection using PEI MAX hydrochloride salt 40k (PEI; Polysciences, USA) were tested with the aim to optimise the transfection process. The values provided in this section correspond to the process that was found to be optimal; all transient transfections were completed using these conditions unless stated otherwise.

PEI was prepared at a concentration of 3 mg/mL in cell culture grade water (Gibco). Cells were passaged 18 hours before transfection in complete media without selection. The DNA was diluted in warm media and mixed. In cases where the genes of interest were for an antibody, the heavy and light chain plasmids were added at a ratio of 1:1. PEI was added directly to the diluted DNA, swirled to mix and incubated for the appropriate amount of time at room temperature. After incubation the mix was swiftly added to the cells, which were then returned to the incubator set at 36.5°C, 7% $CO_2$ and 70% humidity, shaking speed dependant on the volume of the transfection, 250 rpm for plates and 140 rpm for flasks.

***Table 1: Summary of 'optimal' transient transfection conditions determined experimentally for CHO 1-31, including derived cell lines, and CHO-3E7 cell lines.***

| | 1-31 Cell lines | CHO-3E7 |
|---|---|---|
| **Cell Concentration ($10^6$ cells/mL)** | 1 | 2 |
| **DNA Amount (µg/mL)** | 2 | 0.75 |
| **Incubation Time (min)** | 5 | 2.5 |
| **PEI to DNA ratio** | 3 | 5 |

### 2.3.2 Fed Batch Overgrow Cultures

To optimise the transient expression of antibodies and proteins of interest the cells were cultured using a fed batch overgrow (FOG) process for 12 days after transfection. Different conditions were tested, and the following details describe the optimal conditions used for all FOGs unless stated otherwise. The FOG started immediately after transfection and continued for 12 days, with several feeds to avoid nutrient depletion. 24 hours post transfection the cells were counted and supplemented with 0.2% anti-clumping agent (ACA; Invitrogen, USA), 0.25% valproic acid (VPA; Sigma-Aldrich, USA), 4% HyClone Cell Boost 7a Supplement (Cytiva, USA) and 0.4% HyClone Cell Boost 7b Supplement (Cytiva, USA) and placed back in the incubator, where the temperature was changed to 32°C. This temperature was maintained until the end of the FOG. On day 5 post transfection the cells were supplemented with 8% HyClone Cell Boost 7a Supplement and 0.8% HyClone Cell Boost 7b Supplement, and on day 9 with 1% glucose (400 g/L) (Sigma-Aldrich, USA).

## 2.4 Selection of High Expressors using Cyto-Mine® Technology

### 2.4.1 Sample Preparation and Dispensing

1-31 cells were transiently transfected (see "2.3.1 Transfection for Transient Expression") with plasmids containing the heavy and light chain of a monoclonal antibody in human IgG4 format, defined as mAb1. The Cyto-Mine (Sphere Fluidics, UK) sorting took place at 2 different timepoints after transfection, day 2 and day 5. The cells were counted with NucleoCounter NC-3000 (Chemometec, DK) and the appropriate volume to provide 10,000 cells was centrifuged at 300 g for 5 minutes at room temperature. The pellet was resuspended in fresh media and centrifuged again using the above conditions. The cells were then resuspended in encapsulation media which contained 16% (v/v) OptiPrep and 1% (v/v) Pluronic-F68 10% before adding the FRET assay reagents. The final cell concentration was $0.25x10^5$ viable cells/mL. The mix was filtered with a 30 µm cell strainer (Miltenyi Biotec, UK) to remove impurities and 1 mL was loaded into the cartridge and placed in the Cyto-Mine

machine, where the cells were encapsulated. All reagents used for cell capture in picodroplets and FRET assays are proprietary to Sphere Fluidics.

After encapsulation the cells were incubated at 37°C for 30-45 minutes to allow the generation of antibodies inside the picodroplets. The picodroplets were sorted twice, the first sort is less sensitive and used to eliminate empty picodroplets, keeping the selected picodroplets in the cartridge. The second sort before dispensing is used to select the signal range desired from the FRET assay before depositing a single picodroplet in each well. The 384 sterile flat bottom well plates (384wp; Corning, USA) were filled with 50 µL media prior to dispensing and topped up with 50 µL after dispensing the picodroplets. On day 2 a total of 10 plates were filled with picodroplets: 4 corresponding to a mixed population with no selection for a higher signal, and 6 selected for high fluorescence. On day 5 there were a total of five 384wp, 2 mixed and 3 high. Plates were placed in a static incubator, at 37°C, 7% $CO_2$, 70% humidity.

### 2.4.2 Cell Outgrowth

Plates were visually monitored weekly to identify colony growth and recovered wells (defined as wells displaying visible growth within 6 weeks). When wells were deemed recovered, the entire volume was transferred to a 96wp and topped up with 100 µL of fresh media. After the cell lines were transferred to 96wp, the process followed is described in *2.2.4 Minipool outgrowth and adaption to shaking*. Clones taking longer than 6 weeks were deemed unrecoverable and were disposed of.

## 2.5 Molecular Biology

### 2.5.1 DNA Restriction Enzyme Digestion

Plasmid DNA was digested with FastDigest restriction enzymes (ThermoFisher Scientific, UK), following the manufacturer's recommendations. In general, 1 µg of DNA was digested using 1 µL of enzyme in a total volume of at least 10 µL, with the appropriate amount of either FastDigest buffer or FastDigest Green buffer (ThermoFisher Scientific, UK) following the manufacturer's protocol. When performing double digestions, the same ratio was followed (1 µL of each enzyme for each 1 µg of DNA) but the total reaction volume increased to 20 µL. The reactions were incubated in a heat block pre-warmed to 37°C for between 30 minutes and 3 hours.

### 2.5.2 De-phosphorylation with Alkaline Phosphatase (AP)

In cases of difficult ligations where a high amount of background colonies were observed, or when blunt-end restriction enzymes were used, the backbone was dephosphorylated to prevent recircularisation by treating the DNA with FastAP Thermosensitive Alkaline Phosphatase (1 U/µL; ThermoFisher Scientific, UK). 1 µL per 10 µL of reaction was used and reactions were incubated for 10

min at 37°C. The dephosphorylated DNA was purified before ligation (see DNA clean up) or the enzyme was heat inactivated at 75°C for 10 min.

### 2.5.3 DNA Clean up

Digested DNA was purified before downstream applications such as ligations. In cases where the digestion cut small fragments (<15 base pairs (bp)) to be eliminated from the DNA of interest the DNA was purified using Monarch® PCR & DNA Cleanup Kit (New England Biolabs, US) following the manufacturer's directives, except with final elution in molecular biology grade water (Ambion, US). This was necessary when digesting PCR amplified fragments containing restriction enzyme sites in the primers used for the PCR reaction, or in the digestion of small DNA fragments used as adaptors.

When the digestion produced 2 or more bands that needed to be visualized, the digested DNA was run on an agarose gel (see section 2.5.7 – Agarose gel electrophoresis). The relevant agarose bands were cut and the DNA purified with Zymoclean™ Gel DNA Recovery Kit (Zymo Research, US) following the manufacturer's directions.

### 2.5.4 DNA and RNA Quantification

Nucleic acids were quantified with Nanodrop ND-1000 (ThermoFisher Scientific, UK) using the pre-determined settings for DNA, which measures at OD 260 nm to quantify the amount of DNA/RNA (in ng/ul), OD 260:280 nm and OD 260:230 nm to assess their purity. The blank was performed with ultra pure water or TE buffer.

### 2.5.5 DNA Ligation Reaction

Ligation reactions were performed with purified DNA, using T4 DNA Ligase and 10x T4 DNA Ligase Buffer (ThermoFisher Scientific, USA) and following the manufacturer's specifications. 10 ng of vector DNA (backbone) was mixed with the appropriate volume of insert DNA depending on size, 1 µL of T4 DNA Ligase and 1 µL of T4 DNA Ligase Buffer and water to a total volume of 10 µL. The standard molar insert:vector ratio used was 3:1, however in difficult reactions a range including 3:1, 5:1, 10:1 and 20:1 was tried.

$$Insert\ amount\ (ng) = \frac{Insert\ size\ (bp) \times backbone\ amount\ (ng)}{backbone\ size\ (bp)} \times molar\ ratio$$

The reactions were left at room temperature (RT) for a variable amount of time, from 30 min to several hours.

### 2.5.6 PCR Amplification

Polymerase chain reaction (PCR) amplification sequences/genes of interest for cloning purposes was performed with Q5® High-Fidelity 2X Master Mix (New England BioLabs, USA), following the manufacturer's guidelines for both the reaction and thermocycling conditions. The annealing temperature was calculated depending on the primer sequence with the online tool NEB Tm Calculator (https://tmcalculator.neb.com/#!/main). The amplification of difficult, GC rich sequences was performed with KOD Xtreme™ Hot Start DNA Polymerase* kit (Novagen, GE). This includes EBNA-1 full length (EBNA-1F) and kLANA sequences. The entire PCR product was loaded into a 1 or 0.8% agarose gel (see section 2.5.7 - Agarose gel electrophoresis), imaged and the appropriate bands were cut out and purified before proceeding with digestion.

### 2.5.7 Agarose Gel Electrophoresis

Agarose gels ranging from 0.8 to 1.5% (w/v) were prepared with 1x Tris-Acetate-EDTA (TAE) buffer. The agarose powder was mixed with TAE, heated until dissolved and left to cool before adding RedSafe™ Nucleic Acid Staining Solution (Intron Biotechnology, KR) using 5 µL per 100 mL of agarose. The gels were poured into moulds and left at RT or 4°C until set. DNA samples were mixed with Gel Loading Dye, Purple (6X), no SDS (catalogue number: B7025S, New England BioLabs, USA) and loaded on the gel. A ladder, either 1 kb DNA Ladder (New England Biolabs, USA) or GeneRuler 100 bp DNA Ladder (ThermoFisher Scientific, UK) was loaded in a separate well. Ladder choice was dictated by the anticipated size of the DNA loaded. The gels were run with a voltage of 4 V/cm and DNA bands revealed with ultraviolet light using Gel Doc XR+ System (Bio-Rad, USA).

### 2.5.8 Golden Gate Cloning

Golden Gate cloning is a type IIs cloning procedure in which the endonuclease cleaves the target DNA a defined distance outside its recognition site. To increase the efficiency of the process, the backbone vectors contained the ccdB cassette flanked by the *Aar*I sites. The ccdB cassette codes for the protein CcdB, which is toxic to bacteria, and therefore inhibits the growth of any bacteria transformed with the un-modified backbone and facilitates the screening. The cloning was undertaken with GeneArt™ Type IIs Assembly Kit, AarI (Invitrogen, USA). The mix consisted of 3 µL of insert (undigested) at 20 ng/µL, 1 µL of backbone at 75 ng/µL, 1 µL of enzyme and 5 µL of water. The reaction was incubated in a Thermal cycler with cycling conditions of 1 min at 37°C followed by 1 minute at 16°C for 30 cycles, before a final hold at 4°C. 5 µL of this product was used directly to transform competent cells.

### 2.5.9 Transformation of Competent Bacteria with Plasmid DNA

Competent cells used were NEB® 5-alpha Competent *E. coli* (High Efficiency) (New England Biolabs, USA) for most plasmids. For unstable plasmids containing mTR and kTR sequences, One Shot™ Stbl3™

Chemically Competent *E. coli* (Invitrogen, USA) were used and for plasmids containing the camccdb cassette, One Shot™ ccdB Survival™ 2 T1R Competent Cells (Invitrogen, USA) were used.

Cells were removed from storage at -80°C and thawed on ice. Once thawed, 3 µL of ligated DNA was added and incubated for 30 minutes on ice. The cells were heat-shocked in a pre-warmed water bath set at 42°C for 30 or 45 seconds and returned to the ice for 2 or 5 minutes depending on the cell type, following the manufacturer's instructions. Between 500 µL and 900 µL of RT SOC Medium (supplied with the cells) was added to the cells. The vials were incubated at 37°C at 230 rpm for 1 hour. After incubation, 200 µL of cells were spread on a pre-warmed Lysogeny broth (LB) agar plate containing 100 ng/mL ampicillin. The plates were incubated overnight in a static incubator at 37°C.

### 2.5.10 Transient Expression Plasmids

pNoOri: The starting vector used to produce all the PMSC3 variations was pTT5, previously modified to contain the ccdb cassette on the expression site and *Aar*I restriction sites upstream and downstream of the coding sequence which allows for efficient Golden Gate Cloning. pTT5 was digested with *Bgl*II and *Pvu*I which removed the sequence encoding *OriP* and a portion of the sequence encoding the ampicillin resistance cassette. A synthetic DNA string containing the deleted section of the ampicillin resistance sequence and several restriction sites was ordered from GeneArt (ThermoFisher Scientific, USA) and called "deletion string". The string was digested with the *Bgl*II and *Pvu*I, purified and ligated to the previously digested pTT5, creating pNoOri. The ligation product was used to transform One Shot™ ccdB Survival™ 2 T1R Competent Cells as described previously. This vector contained a multiple restriction site (MRS) instead of *oriP*, which was later used to clone mTR and kTR.

pmTR, pkTR: The sequences for *mTR* and *kTR* were obtained from PubMed (GenBank accession number NC_00182 118238-119451 bp for mTR and U75699 for kTR) and synthesized by GenScript (USA). The sequences were cloned into PMSC3 using *Hind*III and *Xba*I and the product used to transform One Shot™ ccdB Survival™ 2 T1R Competent Cells as described.

pOriP-LC, pOriP-HC: These pre-existing plasmids contained expression cassettes for the antibody light chain and heavy chain respectively.

pmTR-HC, pmTR-LC, pmTR-d2EGFP, pkTR-HC, pkTR-LC, p3kTR-d2EGFP, pNoOri-HC, pNoOri-LC, pNoOri-d2EGFP, pOriP-d2EGFP, pOriP-EGFP: The sequence for d2EGFP was obtained from (https://www.addgene.org/browse/sequence_vdb/6372/). The sequence for the monomeric form of EGFP (*mEGFP*) was obtained from PubMed (GenBank accession number LC384836.1). The heavy chain (HC) and the light chain (LC) of mAb1 use human IgG4 PE (huIgG4PE) and IgK constant regions

respectively. The four sequences were ordered from GeneArt with *Aar*I sites added upstream and downstream and a leader sequence and a Kozak consensus sequence upstream of the sequence of interest. They were cloned into the relevant vectors through Golden Gate cloning and the product used to transform the appropriate competent bacteria, as described previously.

### 2.5.11 Stable Expression Plasmids

pcDNA 3.1(+) constructs: The sequences for *mLANA*, *mLANA-FLAG* and *EBNA-1t* were ordered as a CHO codon optimized synthetic construct from GeneArt already cloned in pcDNA3.1(+). The sequence for *mLANA* was obtained from GenBank accession number AAB66457.1, complement of 103925 to 104869 bp. The FLAG sequence (DYKDDDDK, nucleotide sequence: CTTGTCATCGTCGTCCTTGTAATC) was added before the stop codon of *mLANA* to create *mLANA-FLAG* (*mLANA-F*).

The sequence for *kLANA* was obtained with PCR amplification of the plasmid pSG5LANA which was kindly gifted by Prof David J. Blackbourn (University of Surrey). This plasmid contained the entire sequence for *kLANA* (ORF73) and a truncated segment of ORF72. The enzyme KOD Xtreme Hot Start DNA Polymerase was used to avoid mutations and errors. The forward primer was designed to introduce *Hind*III upstream and a Kozak sequence (GCCGCCACC) before the start codon, while the reverse primer added a stop codon at the end of the ORF73 and *Eco*RI downstream of this (FW: GCTAAGCTTCCGCCGCCACCATGGCGCCCCCGGGAA, REV: GCAGGAATTCCGACGGTGGCTTCTAGGGAG).

The sequence for *EBNA-1F* (GenBank accession number M80517.1, 107950 to 109875 bp) was initially obtained as a synthetic construct in pMA backbone. This sequence did not contain the Kozak sequence. To add this, EBNA-1F was PCR amplified with primers containing the region upstream to the start codon and restriction sites *Hind*III and *Eco*RI (FW: GCTAAGCTTCCGCCGCCACCATGTCTGACGAGGGGCAG, REV: GCAGAATTCAAGATGCGCATTTAGG) also using KOD Extreme Hot Start DNA polymerase.

All the constructs for generating stably integrated DNA cell pools were linearized using *Pvu*I and purified before transfection, as below.

### 2.5.12 DNA Linearization and Purification for Electroporation

The DNA used in electroporation, previously linearized with *Pvu*I and phenol-chloroform purified with Phenol:Chloroform:Isoamyl Alcohol 25:24:1 saturated with 10 mM Tris, pH 8.0, 1 mM EDTA (Sigma-Aldrich, USA) was used. The digestion procedure was as described in "DNA restriction enzyme digestion", however the amount of enzyme was calculated as follows:

$$Pvu\text{I}\ required\ (\mu l)\ = \frac{\mu g\ DNA}{Pvu\text{I}\ concentration\ (U/\mu L)}$$

An agarose gel was run after digestion to verify complete linearization before proceeding with the next steps.

A maximum of 750 µL of digested DNA was added to Phase lock gel tubes (Quantabio, USA), using several if necessary, and the same amount of phenol:chloroform:isoamyl added. The tube was closed and mixed by shaking and centrifuged in a bench top centrifuge at >13000 g for 5 min. The upper layer was transferred to a second phase lock gel tube and the addition of 750 µL of phenol:chloroform:isoamyl and centrifugation repeated. The upper layer was transferred to a clean Eppendorf and 1.2 mL of ice cold 100% ethanol and 75 µl 3 M sodium solution added. The tube was mixed by inversion and then centrifuged for 30 minutes at 4°C. The resulting pellet was air dried and resuspended in water, quantified and diluted to 0.4mg/mL.

## 2.6 Protein Extraction and Analysis

### 2.6.1 IgG Quantitation

Antibody expression was quantified using the Octet system and Protein A or Protein G Biosensors tips (PALL FortéBio, USA). Supernatant was isolated by centrifugation at >13000 g in a bench top centrifuge for 5 minutes. This was then diluted 1:3 with 0.01 M HEPES pH 7.4, 0.15 M NaCl, 3 mM EDTA, 0.005% (v/v) Surfactant P20 buffer (HBS-EP) and transferred to polypropylene black 96wp. The tips were soaked in HBS-EP for 10 minutes before starting the experiment and after each sample they were regenerated with phosphoric acid 100 mM and neutralized with HBS-EP. The data was analysed with FortéBio Data analysis 8.2 software using the standard curve equation of 5PL weighted and calculating the binding rate equation on the initial slope.

### 2.6.2 Cell Protein Extraction and Quantitation

A total of 2-6x$10^6$ viable cells/mL were centrifuged at 130x g for 5 minutes, resuspended in 1 mL of Dulbecco's Phosphate-Buffered Saline (DPBS) (Gibco, USA) and centrifuged again as previously. The supernatant was discarded, and the pellet was immediately placed in dry ice before being transferred to a -80°C freezer for storage until required.

Protein was extracted with M-PER™ Mammalian Protein Extraction Reagent (MPER) supplemented with 100 µL Halt™ phosphatase inhibitor cocktail (Thermo Scientific, USA) and 100 µL of 100 mM EDTA. A total of 100 µL/1x$10^6$ cells of supplemented MPER was added to the cell pellet kept on ice. After incubating for 10 minutes the extraction mix was centrifuged at 14000 g for 15 minutes at 4°C. The supernatant was transferred to a fresh microcentrifuge tube and frozen at -80°C if not required for immediate use.

Total extracted cellular protein concentrations were quantified through a Bradford assay. 3 µL of extracted protein was added to 1mL of Quick Start™ Bradford 1x Dye Reagent (Bio-Rad, USA) at room temperature. A standard was generated using the Quick Start Bovine Serum Albumin Standard (Bio-Rad, USA) through serial dilution to give final protein concentrations of 2.0, 1.5, 1.0, 0.75, 0.50, 0.25, 0.13 mg/mL. 10 µL of the standards were added to 1 mL of Bradford Dye Reagent. Samples were mixed and incubated 5 minutes at room temperature before transferring 200 µL to a 96wp and reading the results on a Envision plate reader (PerkinElmer, USA) at a wavelength of 595 nm.

### 2.6.3 SDS-PAGE Analysis

Samples were thawed on ice and 10 µg of total protein was mixed with 5 µL of BOLT LDS Sample Buffer 4X (Invitrogen, USA), 5 µL of 400 nM N-Ethylmaleimide (NEM) (Thermo Scientific, USA) and a variable volume of water to give a total volume of 20 µL. The samples were then mixed thoroughly and loaded onto a precast sodium dodecyl sulphate polyacrylamide gel (SDS-PAGE) Bolt 4-12% Bis-Tris Plus (Invitrogen, USA), assembled in the appropriate gel running apparatus with running buffer made up by diluting 50 mL of NuPAGE™ MES SDS Running Buffer (20X; Invitrogen, USA) to 1 L with distilled water. The SDS-PAGE was run at 200 V for 25 minutes.

### 2.6.4 Western Blot Analysis

For western blotting, SDS-PAGE resolved proteins were transferred from the gel to a nitrocellulose membrane with the iBlot® Dry Blotting System (Life Technologies, USA) following the manufacturer's instructions, running the transfer for 6 minutes. Once the proteins were transferred, to reduce non-specific interactions with the membrane, the membranes were blocked using 5% (w/v) Bovine Serum Albumin, 0.25% Tween20 (Sigma-Aldrich, USA) in DPBS (hereafter called 5% BPST). The membranes were incubated overnight at 4°C with 5% BPST on an orbital platform with gentle agitation. To detect the target protein, the membranes were incubated with the primary antibodies indicated in Table ***2*** at the relevant stages, prior to developing using a horseradish peroxidase (HRP) substrate. In some cases, a secondary antibody that was HRP labelled was used whilst in other cases the primary antibody was directly HRP labelled as outlined in Table ***2***. In between each stage, the membranes were washed using 5% BPST for 15 minutes, changing the buffer every 5 minutes. The HRP substrate used was Pierce™ ECL Western Blotting Substrate (Thermo Scientific, USA) prepared following the manufacturer's instructions. The membrane was covered with the ECL reagent and incubated for 1 minute at room temperature. The excess reagent was drained before transferring the gel to Gel Doc XR+ System for imaging.

***Table 2: Summary of antibodies and conditions used for western blotting.***

| Name | Type | Dilution | Target | Species | Conjugation | Expected MW (of target protein) | Source |
|---|---|---|---|---|---|---|---|
| EBNA-1 0211 | Primary | 1:200 | EBNA-1 | Mouse | None | 56 (full length)<br>35 (truncated) | Santa Cruz Biotechnology |
| Ab4013 Anti-HHV-8 LNA-1 Antibody, clone LN53 | Primary | 1:500 | kLANA | Rat | None | 135 | Abcam |
| Anti-DDDDK tag | Primary | 1:1000 | FLAG tag | Mouse | None | 50 (mLANA) | Abcam |
| Anti-beta Actin antibody [mAbcam 8226] - Loading Control (HRP) | Primary, control | 1:100 | Beta actin | Mouse | None | 42 | Abcam |
| Peroxidase AffiniPure Goat Anti-Mouse IgG (H+L) | Secondary | 1:1000 | Mouse IgG | Goat | HRP | 150 | Jackson Immunoresearch |
| Peroxidase AffiniPure Goat Anti-Rat IgG (H+L) | Secondary | 1:1000 | Rat IgG | Goat | HRP | 150 | Jackson Immunoresearch |

### 2.6.5 Flow Cytometry Analysis

Samples were taken from cells transfected with DNA to result in expression of a fluorescent protein (such as d2EGFP) and from a control expressing mAb1. 50 µL of sample was diluted with 100 µL of DPBS and analysed on a CytoFLEX Flow Cytometer (Beckman Coulter, USA) using the blue laser (488 nm) and the 525/40 BP filter. A total of 10,000 events were collected for analysis using FlowJo version 10 software (BD, USA) (Figure 8).

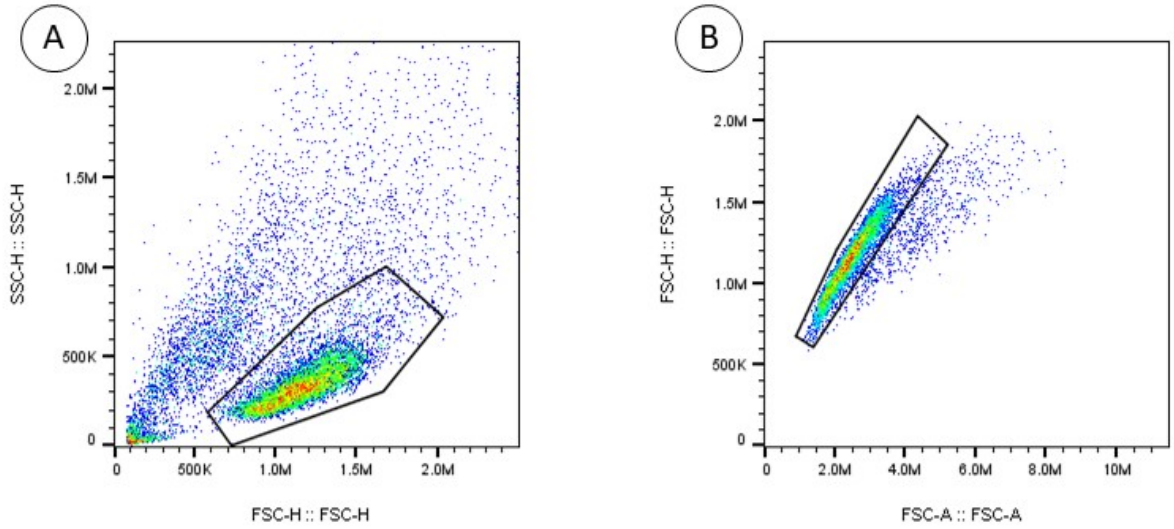


***Figure 8: Representation of a standard gating process for cell samples analysed by flow cytometry using FlowJo software.*** *A) Live cells are identified and gated. B) Cells selected in step A are gated again to select single cells.*

## 2.7 Statistical Analysis and Data Processing

Statistical analysis was performed using R version 3.6.1 (R Core Team, 2019) using the stats package. Graphs were plotted using the ggplot2 R package (Wickham, 2016), flow cytometry data was processed using the flowCore R package (Ellis *et al.,* 2019), and any data frame processing was performed using the tidyverse suite of functions (Wickham H *et al.,* 2019)

## 2.8 Figures

Figures 1 to 7 were created with BioRender.com.

# 3 Results

## 3.1 Process Development

Process engineering includes development of an optimal transfection method as well as the design and evaluation of growth and feed conditions for the fed-batch overgrow (FOG) process, aiming to maximise protein expression. This process can have a dramatic effect on the secreted recombinant protein expression level; however, requires optimisation for each cell line. Nonetheless, a reliable process which gives a high transfection efficiency (TE) and culture viability throughout the FOG is necessary to evaluate and identify increased expression levels following cell engineering efforts. In this work, we divided bioprocess optimization into two parts. The first part evaluated transfection conditions with PEI 40kDa by GFP expression. The second part used 3 expression conditions defined in the preceding experiment, which were evaluated by measuring secreted mAb expression level, culture viability and viable cell number under 2 different FOG conditions.

### 3.1.1. Optimisation of PEI Transfection Conditions with DoE (Design of Experiments) and GFP

PEI based transfection is a generally understood to be a multifactorial event, where the amount of each reagent, cell concentration and the methods to combine them all influence efficacy. Transfection conditions do not translate well between different cell lines, which means that an optimisation step needs to be performed for every cell line. This experiment used a DoE approach to evaluate the effect of cell concentration, DNA quantity and PEI:DNA ratio to achieve optimal transfection conditions for PEI transfection in the 1-31 cell line.

1-31 cells were transiently transfected with pOriP-EGFP following the conditions and order recommended by Design Expert software for the factors of interest summarised in Table 3, minimum and maximum refer to the limit values used in the design of the experiment. Fluorescence was analysed 48 h after transfection using a CytoFLEX flow cytometer to measure the percentage of cells expressing GFP (referred to as transfection efficiency, TE) and the signal intensity of these positive cells, represented as median fluorescence intensity (MFI). TE and MFI were calculated using only the viable cell population. Culture viability was measured at the same time point using a Vi-CELL automated cell counter. These responses are summarised in Table 4, where minimum and maximum indicate the highest and lowest value observed for that response in any sample.

**Table 3: Factors included in the DoE experiment to optimise transfection efficiency for 1-31 cells and their respective design parameters**.

| Factor | Name | Units | Type | Subtype | Minimum | Maximum |
|---|---|---|---|---|---|---|
| **A** | Cell Concentration | $10^6$ cells/mL | Numeric | Continuous | 1 | 4 |
| **B** | DNA amount | µg/mL | Numeric | Continuous | 0.5 | 2 |
| **C** | Incubation time | minutes | Numeric | Continuous | 0.5 | 5 |
| **D** | PEI to DNA ratio | Ratio (w/w) | Numeric | Continuous | 3 | 10 |

**Table 4: Responses being measured to evaluate each transfection condition's performance. GFP positive cells result was analysed including only live cells.**

| Response | Name | Units | Analysis | Minimum | Maximum |
|---|---|---|---|---|---|
| **R1** | GFP positive live cells 48 h | % | Factorial | 1.38 | 99.1 |
| **R2** | MFI 48h | Arbitrary | Factorial | 9051 | 954000 |
| **R3** | Culture viability 48 h | % | Factorial | 8.784474 | 98.6 |

Results were analysed with Design Expert Software using an ANOVA statistical test. The ANOVA test results are summarised in Table 5, only included are those factor interactions with a significant p-value ($p<0.05$). As expected, both the individual factors and their interactions with each other were found to have statistical significance after performing the ANOVA test (p-value<0.05). Cell concentration, DNA amount and PEI to DNA ratio were found to be important for all the responses, however incubation time was found to be relevant only for MFI, with a p-value close to 0.05 (p-value=0.0428).

TE results appeared to be strongly dependant on the cell concentration, with lower cell concentrations performing better than higher cell concentrations (*Figure 9*). Using low cell concentrations, $1x10^6$ cells/mL, TEs greater than 99% were achieved, while no condition achieved TE levels higher than 15% for high cell concentration ($4x10^6$ cells/mL). The factors of PEI:DNA ratio and DNA amount also showed clear interactions with each other. A low PEI:DNA ratio performed well with a high amount of DNA (1 µg/mL) while a high PEI:DNA ratio shifts the response and favours the lowest DNA amount, 0.5 µg/mL.

The data for both TE and MFI levels (Figure 10) appeared similar, with the variables affecting both in a similar way. The main factor affecting TE and MFI seemed to be cell concentration. Lower cell concentrations resulted in higher MFIs and percentage of transfected cells, while higher cell concentrations gave low values for both measurements. PEI:DNA ratio and DNA concentration appear to interact with each other: using low PEI:DNA ratio (3:1) and a higher DNA amounts results in high TE and MFI measurements, while strong fluorescence and high TE for the higher PEI:DNA ratio (10:1) requires lower DNA amounts. Incubation time did not have a strong effect on either TE or MFI.

Culture viability was negatively related to both higher DNA concentrations and PEI:DNA ratio (Figure 11). Lower cell concentrations were generally more sensitive to those factors and gave lower culture viabilities than higher cell concentrations under the same conditions. The area corresponding to the lowest culture viability after transfection is that of low cell concentration and high DNA amount. Overall, culture viability was negatively affected by low cell concentrations, high DNA amounts and high PEI:DNA ratio, with this last factor decreasing culture viability from over 80% to less than 40% using 0.5 µg/mL and 2 µg/mL of DNA respectively, with a PEI:DNA ratio of 10:1. Incubation time did not have a significant effect on culture viability.

None of the conditions tested were suitable for high cell concentrations, as both the transfection efficiency and MFI for the flasks with $4x10^6$ cells/mL show the lowest value (Figure 3). As using a higher starting concentration could increase the final protein titre, it would be of interest to find conditions that allow a higher concentration to be used.

Overall, this experiment was able to identify transfection conditions suitable for future transfections, which give a transfection efficiency close to 100% and appropriate culture viability >85% (Table 6), important for transient platforms that rely on being able to start a FOG immediately after transfection.

**Table 5**: **Summary of the ANOVA test results for transfection optimisation.**

| **R1 – TE - GFP Positive live cells (%)** | | **R2 - MFI** | | **R3 – Culture Viability (%)** | |
|---|---|---|---|---|---|
| **Factors** | **p-value** | **Factor** | **p-value** | **Factor** | **p-value** |
| A-Cell concentration | <0.0001 | A-Cell concentration | <0.0001 | A-Cell concentration | <0.0001 |
| B-DNA amount | <0.0001 | B-DNA amount | <0.0001 | B-DNA amount | <0.0001 |
| C-Incubation time | 0.0428 | C-Incubation time | 0.0997 | C-Incubation time | 0.3083 |
| D-PEI to DNA ratio | <0.0001 | D-PEI to DNA ratio | <0.0001 | D-PEI to DNA ratio | <0.0001 |
| AB | 0.0003 | AB | <0.0001 | AB | <0.0001 |
| AD | 0.0001 | AD | <0.0001 | AC | 0.7654 |
| BD | <0.0001 | BD | <0.0001 | AD | <0.0001 |
| CD | 0.0209 | CD | 0.0068 | BD | <0.0001 |
| ABD | <0.0001 | ABD | <0.0001 | ABD | <0.0001 |
| BCD | 0.0103 | | | | |
| ABCD | 0.0139 | | | | |

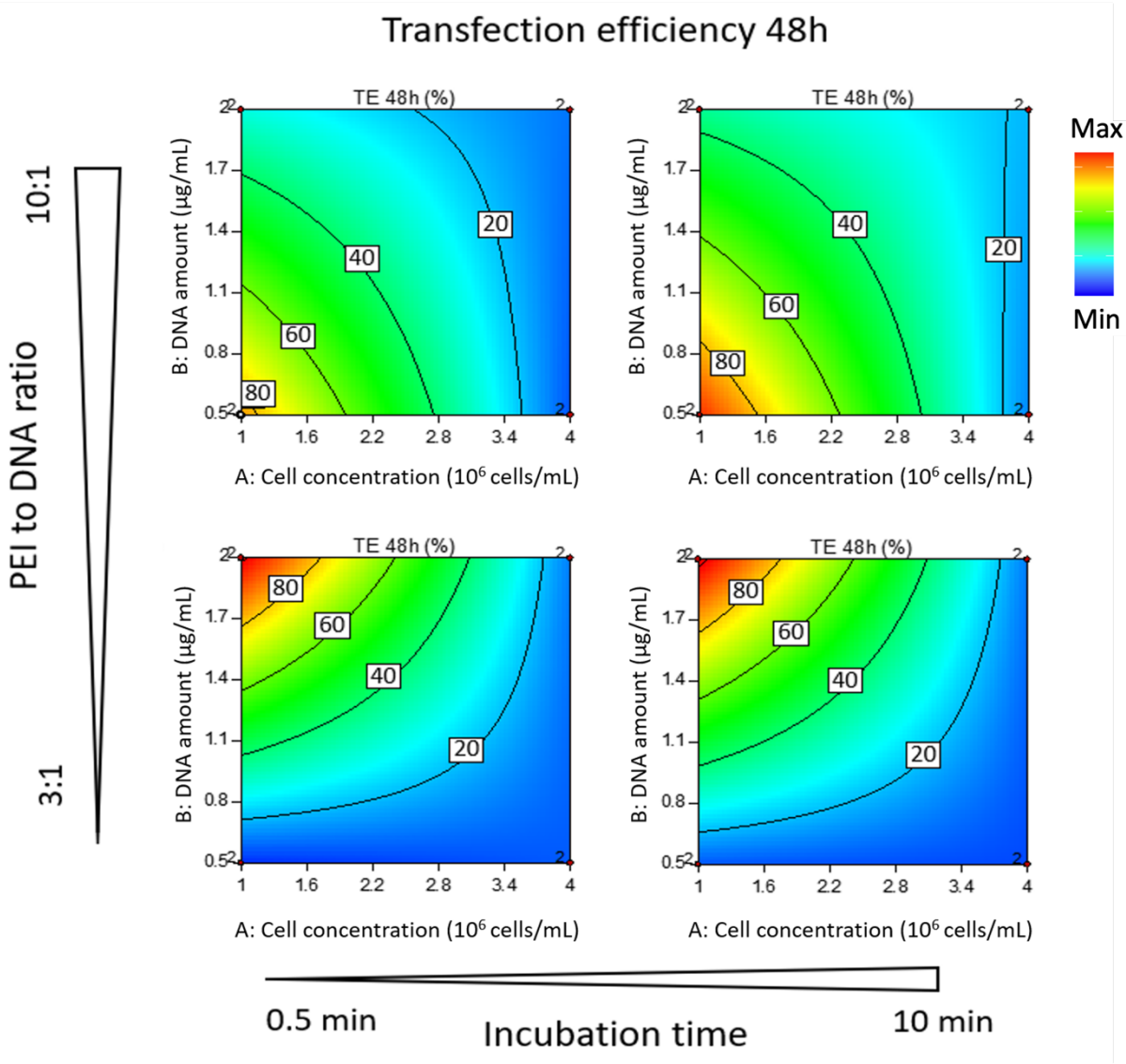


***Figure 9: Transfection efficiency (TE) measured as percentage of live cells expressing measurable GFP signal 48h after transfection.*** *Each 2D contour plot shows TE in percentage, blue corresponds to lower and red higher percentage TE. Cell concentration (x10$^6$ cells/mL) is shown on the x axis of each graph, and DNA amount (µg/mL) on the y axis. The 4 different graphs represent 2 different combinations for the highest and lowest values of the variables PEI to DNA ratio and incubation time. No middle value between those limits (3:1 and 10:1 for PEI to DNA ratio, 0.5 min and 10 min for incubation time) is included in the figure, which represents a snapshot of the whole dataset.*

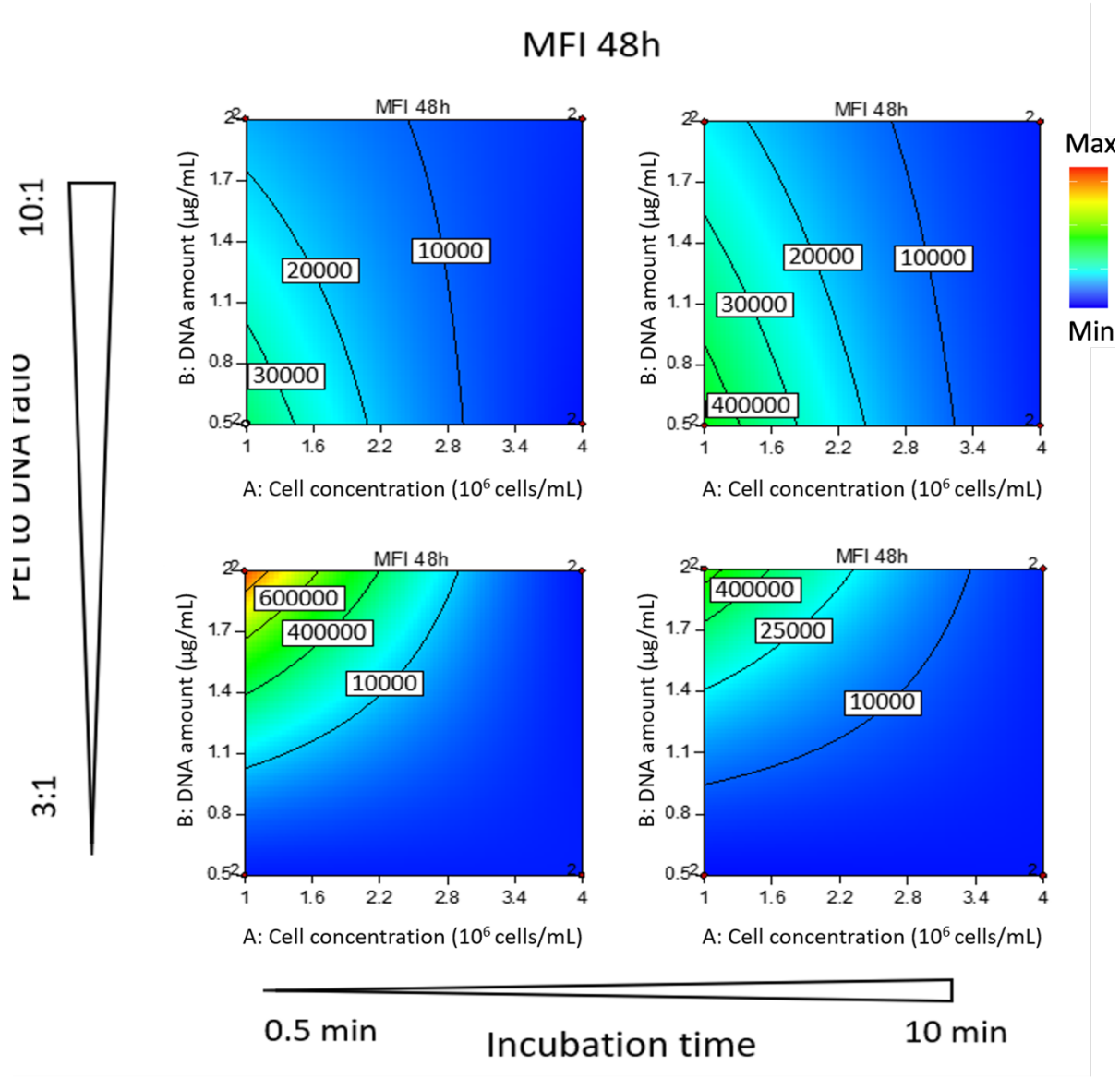


**Figure 10: Median Fluorescence Intensity (MFI) of 1-31 cell line 48 h after transient transfection with PEI.** *Each 2D contour plot shows MFI, blue representing lower and red higher MFI values. MFI was calculated including only live cells positive for GFP expression, excluding negative or dead cells. Cell concentration (x10$^6$ cells/mL) is shown on the x axis of each graph, and DNA amount (µg/mL) on the y axis. The 4 different graphs represent 2 different combinations for the highest and lowest values of the variables PEI to DNA ratio and incubation time. No middle value between those limits (3:1 and 10:1 for PEI to DNA ratio, 0.5 min and 10 min for incubation time) is included in the figure, which represents a snapshot of the whole dataset.*

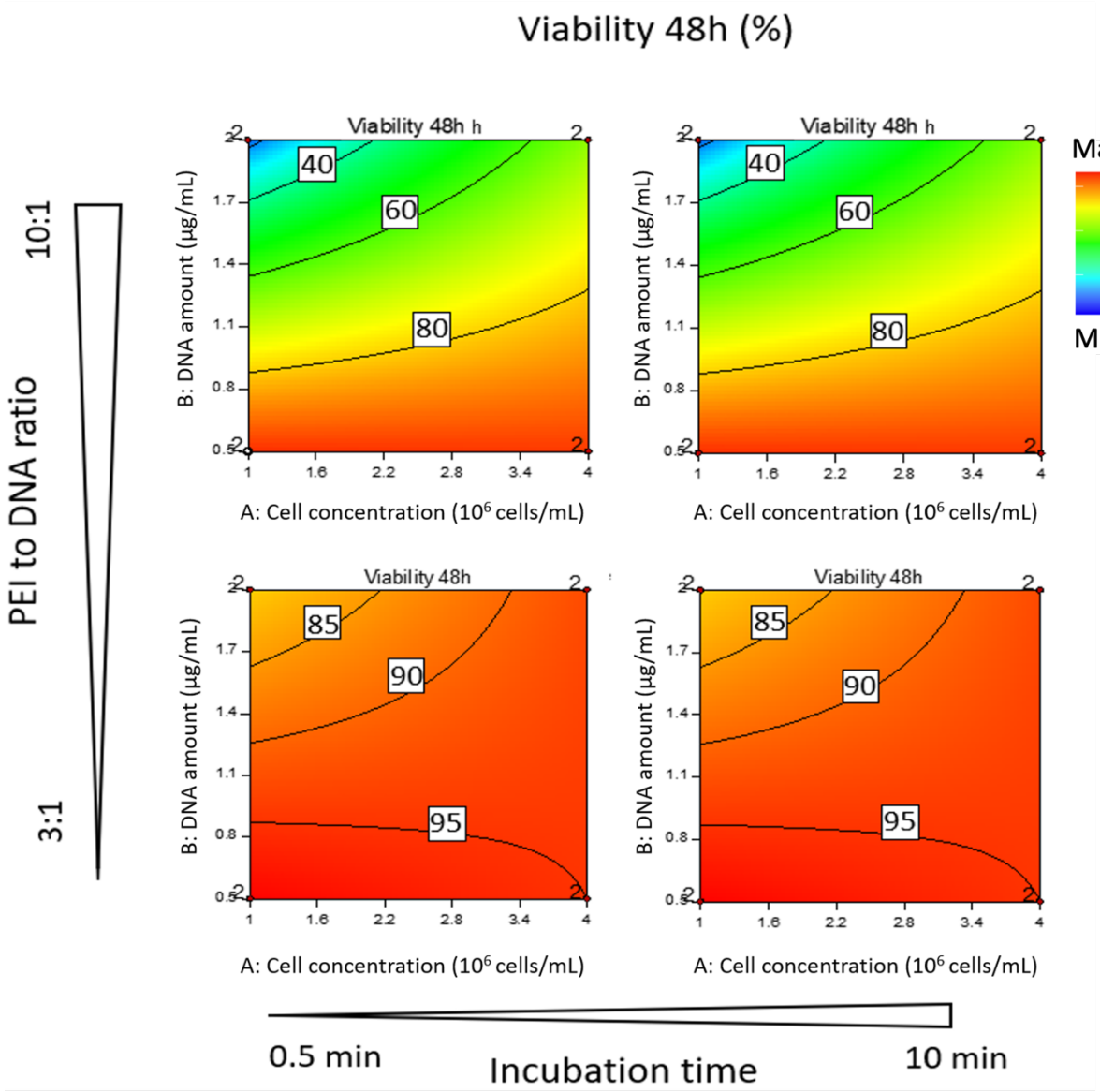


***Figure 11: Culture viability of 1-31 cell cultures 48 h after transient transfection with PEI for transfection process optimisation***. Each 2D contour plot shows culture viability in percentage, blue representing lower and red higher percentage of viable cells. Cell concentration (x$10^6$ cells/mL) is shown on the x axis of each graph, and DNA amount (µg/mL) on the y axis. The 4 different graphs represent 2 different combinations for the highest and lowest values of the variables PEI to DNA ratio and incubation time. No middle value between those limits (3:1 and 10:1 for PEI to DNA ratio, 0.5 min and 10 min for incubation time) is included in the figure, which represents a snapshot of the whole dataset.

### 3.1.2. Determination of Optimal FOG Conditions after Transfection

Expression of a fluorescent protein such as GFP is an easy way to calculate how many cells have been successfully transfected, as it is possible to analyse each cell individually using flow cytometry. However, measuring the overall TE in the cell culture and MFI on each single cell may not correlate with the overall performance of the culture in a fed batch overgrow (FOG). The optimisation of the transfection process is an essential first step, however transfection efficiency results are not enough to predict their behaviour in a FOG process. During a FOG there are more variables affecting the final mAb amount than in the previous experiment, including, but not limited to, culture viability during the cell culture and growth profile. These factors were not measured in the flow cytometry experiments, and productivity over the whole FOG may not correspond to that found by measuring MFI 48 h after transfection with GFP. Therefore, next it was decided to select not just the "best" condition found in the previous section but the best transfection conditions for $2x10^6$ cells/mL and for $1x10^6$ cells/mL, called transfection condition A and B respectively (Table 6). These conditions were selected using the GFP data obtained in the previous section. Best conditions were considered as achieving the highest MFI while maintaining high culture viability (>75%) and TE (>75%). Previously-used laboratory transfection conditions were included as a control, called transfection condition C. Cells were transfected at 30 mL scale with pOriP-HC and pOriP-LC, which encode a huIgG4PE mAb heavy and light chain respectively.

In this experiment 2 different FOG conditions were evaluated: FOG Process 1 that included a temperature shift on day 1, and FOG process 2 where flasks were maintained at 36.5°C until harvest. Feed A and Feed B correspond to HyClone cell boost 7a and 7b supplement as described previously. Details including volumes added are not disclosed. Both processes are summarised in Figure 12.

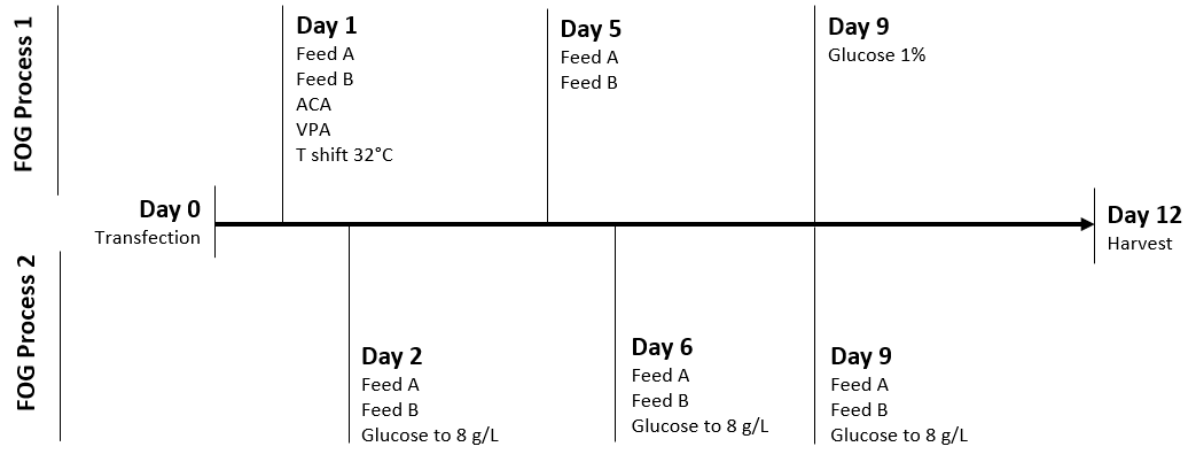


***Figure 12**: **Schematic representation of the feeding regime for FOG process 1 and 2.** Top panel represents FOG Process 1, while bottom corresponds to FOG process 2. Details including volumes added are not disclosed.*

**Table 6: Transfection conditions used to evaluate FOG performance.**

| | | | | | PEI optimisation results | | |
|---|---|---|---|---|---|---|---|
| **Transfection** | **Cell Conc. (x10$^6$ cells/mL)** | **DNA Amount (µg/mL)** | **Incubation Time (min)** | **PEI to DNA ratio** | **MFI 48 h** | **Transfection Efficiency 48 h (%)** | **Culture Viability 48 h (%)** |
| **A** | 2 | 1.25 | 2.75 | 6.5 | 140168 | 77.13 | 89.92 |
| **B** | 1 | 2 | 5 | 3 | 526500 | 97.85 | 79.52 |
| **C** | 2 | 0.75 | 2.5 | 5 | 225575 | 42.7 | 96.55 |

FOG condition 2 was able to achieve higher cell concentrations at mid FOG, however the viable cell number (VCN) and culture viability decreased after reaching a peak in VCN at day 5 (Figure 13). In comparison to the high VCN in FOG condition 2, for transfection conditions A and B FOG condition 1 achieved a lower VCN which remained constant over the duration of the FOG. The culture viability for FOG 1 was also higher than FOG 2, not decreasing below 50%. The decrease in culture viability observed in FOG 2 appeared to be related to its high VCN, which indicates that the conditions are not suitable to maintain the high cell concentration it achieves and further optimisation would be needed to achieve both a high cell density and a high viability at harvest.

An exception to FOG condition 1 maintaining higher culture viability throughout culture is shown in transfection condition C, which achieved a high maximum VCN and had a low final culture viability in

both FOGs. The “gentler” transfection conditions could explain the ability of cells to grow more after transfection using condition C in comparison to A and B. Transfection condition C also gave lower titre (Figure 14), which correlates with the lower TE seen in the previous GFP experiment. However, condition C had higher MFI than condition A while showing lower overall titre in this experiment, which can be explained by the lower TE. Transfection condition C gave only approximately 50% TE, meaning that overall, only half of the cells were transfected and therefore producing antibody. The MFI was calculated excluding negative cells and would not be affected by a population not expressing GFP. The fact that the TE is lower in condition C could also explain the drop in culture viability in both FOGs; non-expressing cells are able to grow quicker, achieving non-sustainable cell concentrations even when grown under FOG condition 1.

FOG condition 1 resulted in a higher titre for all the transfections alongside a higher specific productivity, measured as Qp, which refers to the amount of mAb produced per cell with the units picograms/cell/day (Figure 14). Prior to the decrease in culture viability at day 5, the mAb titre was very similar for both FOG conditions. Taking into account the higher VCN at the same timepoint for FOG condition 2, cells in FOG condition 2 may be less productive than those in FOG condition 1 even at day 5. The further decrease in culture viability and VCN would explain the final difference in titre. At day 12 the difference in titre between FOG 1 and FOG 2 was significant ($p<0.05$) for both transfection conditions A and B.

Although the GFP results for conditions A and B were different in the previous experiment, with condition B showing a higher TE and MFI, the final titre in the mAb experiment was similar. This makes sense in the context of total protein produced related to the starting cell concentration, with condition A having an initial cell concentration of $2x10^6$ cells/mL in comparison to the $1x10^6$ cells/mL of condition B. Condition B makes cells more productive (higher MFI and TE) but condition A has more cells in the FOG to produce mAb, even if they are less productive. This is also obvious when observing the productivity/Qp of both transfection conditions, where B is higher than A specially in FOG condition1 (Figure 14).

In summary, FOG condition 2 gave issues with culture viability and needs further optimisation. Transfection condition B gave the highest MFI and TE overall, and a comparably high titre to transfection condition A. FOG condition 1 and transfection condition B were selected as the best combination of conditions and were used in all further experiments.

A)

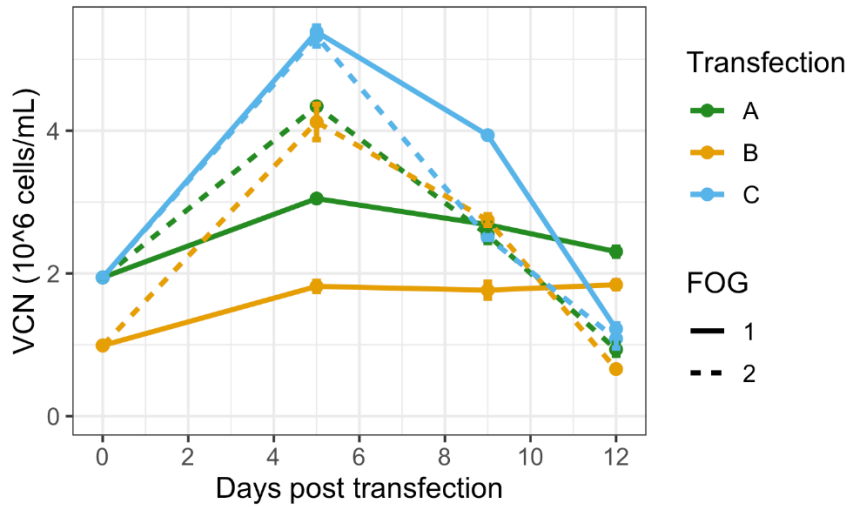


B)

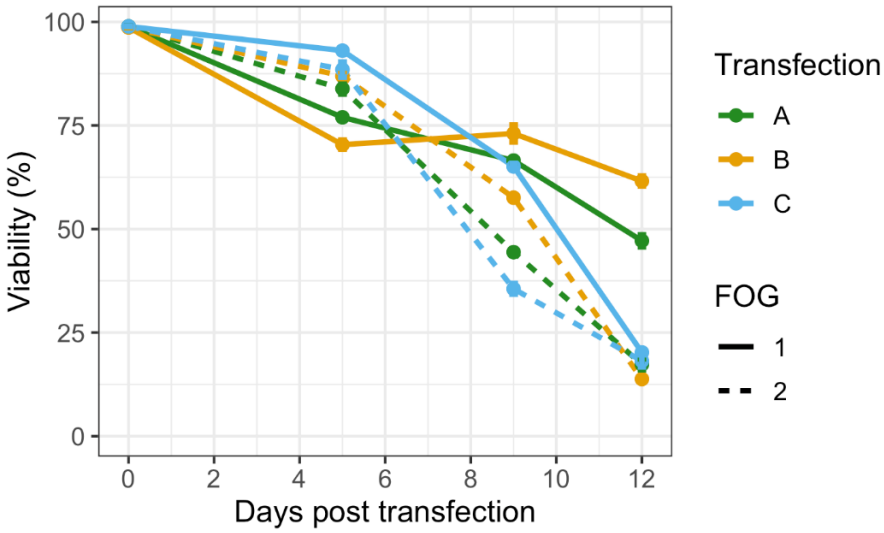


**Figure 13: Viable cell concentration and culture viability of 1-31 cells transiently transfected with several different transfection conditions under FOG conditions 1 or 2.** *A) Viable cell number (VCN) of the cultures, B) Viability of the cultures. Cells were expressing a huIgG4PE mAb in a 12 day FOG. VCN and culture viability were measured with a Vi-CELL automated cell counter. Error bars represent the standard deviation of the mean (n=3).*

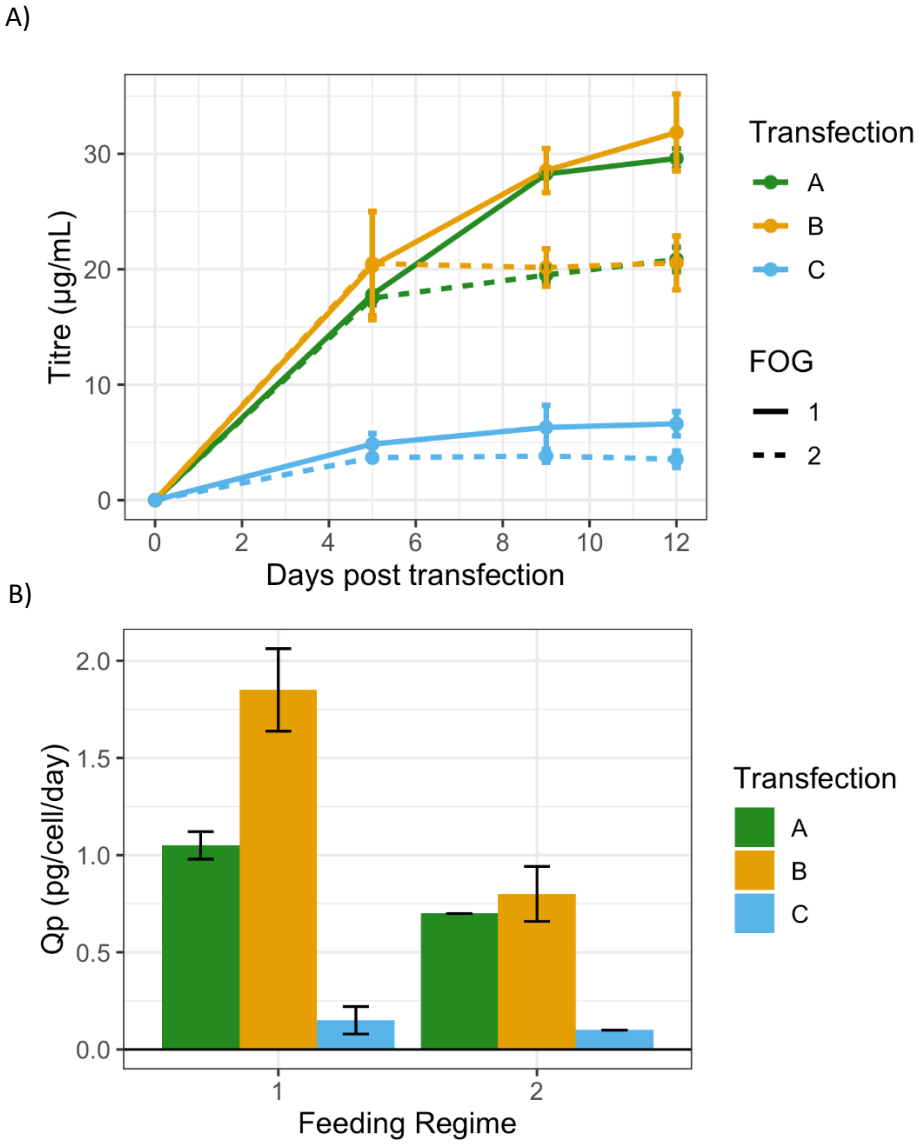


**Figure 14**: **IgG titre and productivity (Qp) for 1-31 cells under different transfection and FOG conditions to determine the optimal conditions for protein expression.** *A) Titre over the course of the 12 day FOG. Titre was obtained by Octet measurement of the supernatant at day 5, 9 and 12. B) Overall productivity of the same sample. Productivity is shown as Qp, which measures pg of mAb produced/cell/day. Error bars represent the standard deviation from the mean (n=3).*

## 3.2 Selection of a Suitable Cell Line for Transient Expression with the Cyto-Mine Instrument

Given the genetic heterogeneity of CHO cells, cell lines derived from a single CHO cell actually represent a heterogenous group of cells with different characteristics, including productivity. Identification of the most productive cells within this mixture is a key starting point for generation of a high producing cell line routinely used for the generation of clonal stable cell lines. We theorised the possibility of selecting a specific cell line naturally more ammenable to transient expression as a first step for the creation of a new host cell line for a new transient platform.

This project used Cyto-Mine single cell analysis to enable the selection of high producing cells after transient transfection. Cyto-Mine technology allows the formation of picodroplets that envelop a single cell, which are then analysed in a similar way to standard flow cytometry. The picodroplets contain FRET assay reagents, with separate antibodies targeting the heavy and light chain of the mAb produced by the cell. FRET only occurs when those detection antibodies (tagged with a red or green fluorophore) bind to the same antibody and are physically close to each other. The red fluorophore is able to capture the electrons released by the green fluorophore and in turn release red signal. In this case, the FRET signal would detect antibodies inside the picodroplet produced by the cell after a period of incubation. Higher FRET correlates with a higher amount of antibody being expressed by the cell and would cause a shift from green fluorescence to red. The cells were sorted depending on their FRET signal and deposited individually in a well. Recovered cell lines were then evaluated for transient expression and results compared to that of the original host cell line, 1-31.

### 3.2.1 Transfection, cell sorting and recovery

1-31 cells were transiently transfected with pOriP-HC and pOriP-LC to express a huIgG4PE mAb. Culture samples for analysis were taken on day 2 and day 5. Samples were processed by adding the FRET reagents and encapsulating the cells in picodroplets ready for analysis and dispensing using the Cyto-Mine. A total of 15x384wp were sorted using Cyto-Mine, each well containing a single picodroplet, selected upon their relative FRET assay level. Of those 15 plates, 10 plates were sorted on day 2 (5 using an animal component free (ACF) set of reagents for the FRET assay and 5 using the standard FRET reagents) and 5 plates on day 5 using only the ACF reagents after observing stronger FRET signals on day 2 from the ACF plates. From the total 5760 sorted cells, only 3 cells eventually recovered and survived the transfer from static plates to shaking flasks (Table 7). The 3 recovered cells had low to medium FRET signal (Table 8) and one of them was found not to be monoclonal through visual analysis of the picodroplet. On the FRET signal graph the 3 recovered cells all show low red shift, with B9 showing the highest shift of the 3, which could be related to the fact that for B9, there was

more than one cell producing antibody in the same picodroplet (Figure 15). For the 3 recovered cell lines vials were cryopreserved in liquid nitrogen storage.

**Table 7: Summary of cell recovery outcome for cells sorted using the Cyto-Mine instrument.**

| | Static | | | Shaking | |
|---|---|---|---|---|---|
| | **384 wp** | **96 wp** | **24 wp** | **24 dwp** | **Flasks** |
| **Cells** | 5760 | 23 | 10 | 6 | 3 |
| **% of total** | 100 | 0.399 | 0.174 | 0.104 | 0.052 |

**Table 8: Cyto-Mine cell lines recovered from 1-31 sorting.**

| Cell line Name | Day sorted | Monoclonal? | Assay signal |
|---|---|---|---|
| **B4** | 5 | Yes | Low |
| **A8** | 2 | Yes | Low |
| **B9** | 5 | No | Medium |

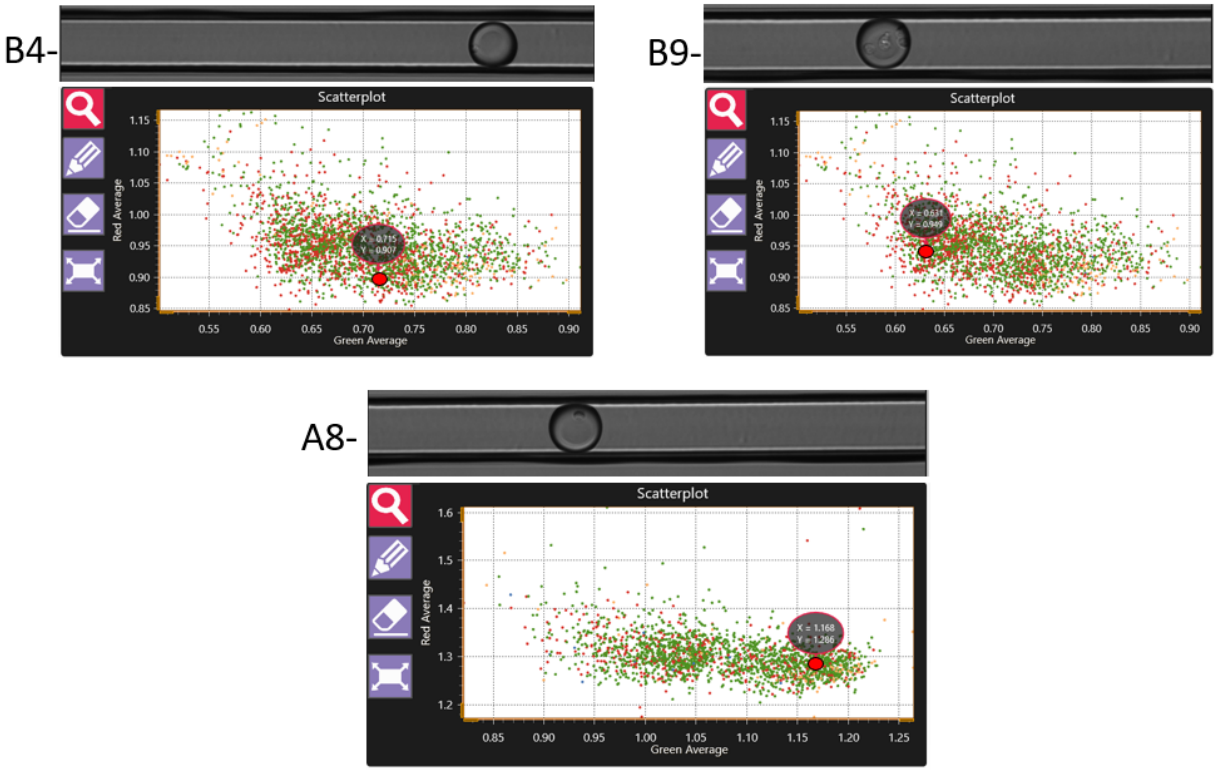


***Figure 15: Results during Cyto-Mine sorting for cell lines B4, A8 and B9.*** *The graph for each cell line includes the FRET assay result and a picture of the picodroplet containing the cell or cells. FRET results are shown with green fluorescence on the x axis and red fluorescence on the y axis, a shift towards red fluorescence alongside a reduction in green fluorescence signifies a higher FRET signal for the picodroplet.*

### 3.2.2 Evaluation of Productivity for Cell Lines Derived from Cyto-Mine Sorting

Once the new cell lines were isolated, their productivity needed to be evaluated to validate the Cyto-Mine selection process and rank their expression levels. In order to do this, Cyto-Mine recovered cell lines B4, A8 and B9, as well as parental cell line 1-31, were transiently transfected with two antibodies, a huIgG4PE and a huIgG1, using the previously described transfection condition B and FOG condition 1.

Both B9 and A8 cell lines showed a higher titre, productivity, culture viability and VCN in comparison to 1-31 for both huIgG1 and huIgG4PE molecules (Figure 16). The increase in titre for both B9 and A8 compared to 1-31 was statistically significant for both of the expressed mAbs, after analysing the day 12 titre using a t-test ($p<0.01$). The Qp for both B9 and A8 were similar, however the higher VCN of A8 results in a final titre higher than B9 (Figure 17).

These data suggest that the Cyto-Mine single cell sorting allowed the selection of cell lines with a phenotype more suited to transient expression, including the ability to maintain higher culture viability during FOG and reach higher VCN, in comparison to the original 1-31 (Figure 16). The increase in titre for B9 and A8 in comparison to 1-31 can be partially explained by the higher VCN and culture viability achieved during the FOG, however the increase in Qp indicates the presence of phenotypic changes causing the increased cell productivity as well as the improved growth profile.

The Cyto-Mine was not predictive of mAb expression for all these 3 cell lines, as A8 was considered a low expressor in the FRET assay used to determine mAb expression. The assay, performed in a single cell inside a picodroplet, could not take into account the variations in cell growth during a FOG. However, as only 3 cell lines recovered (one of them not being monoclonal), it is not possible to make any conclusions on the accuracy of this new technology. Regardless, the ‘new’ host A8 was selected as an alternative to 1-31, with improved protein productivity and a growth profile more suitable for TGE, and taken forward alongside 1-31 for future experiments.

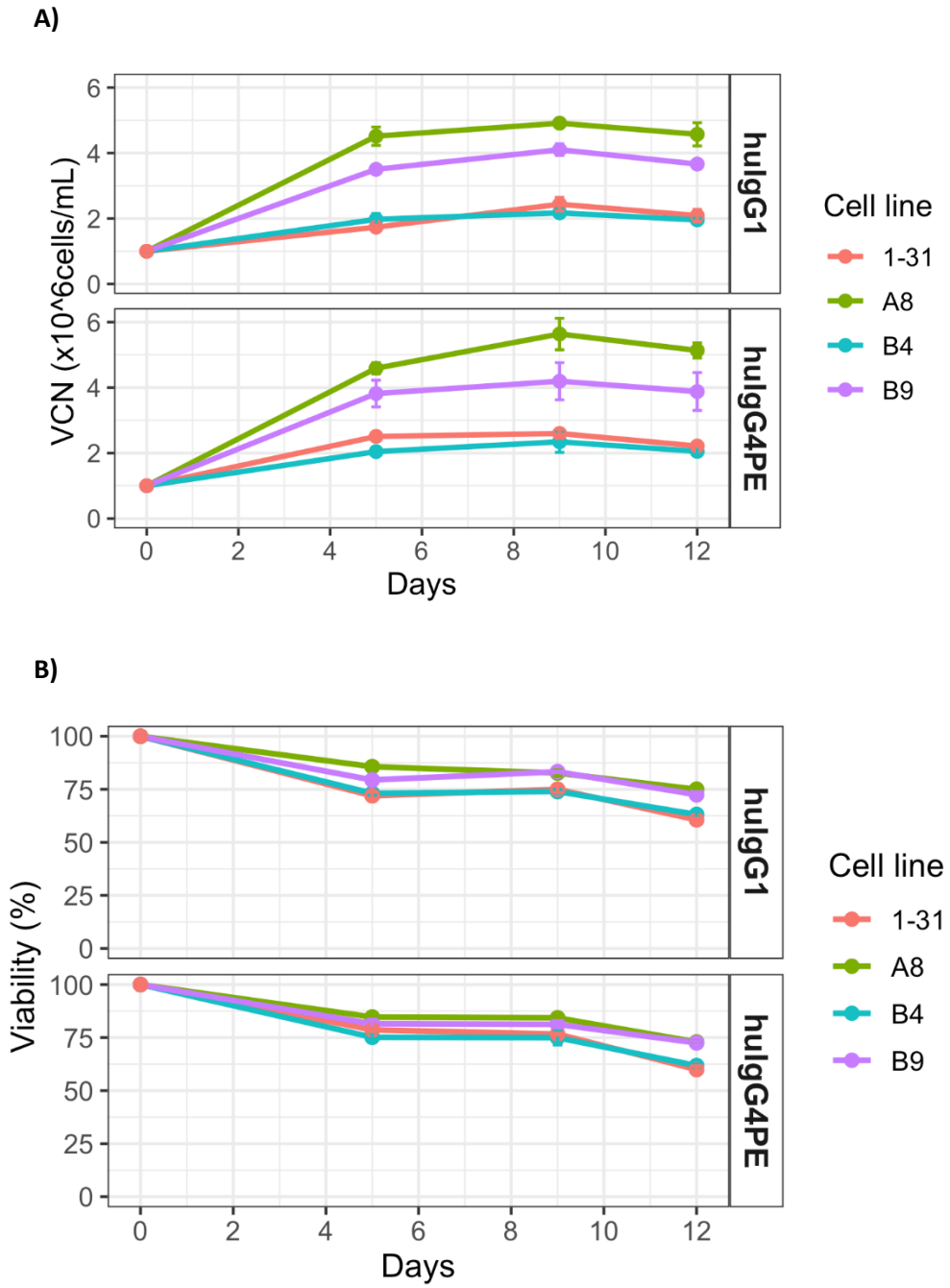


***Figure 16: Viable cell number and culture viability of the transiently transfected 1-31 and Cyto-Mine derived cell lines.*** *A) viable cell number (VCN). B) culture viability of the cell lines expressing a huIgG1 or huIgG4PE mAb in a 12 day FOG. Error bars represent the standard deviation from the mean (n=3).*

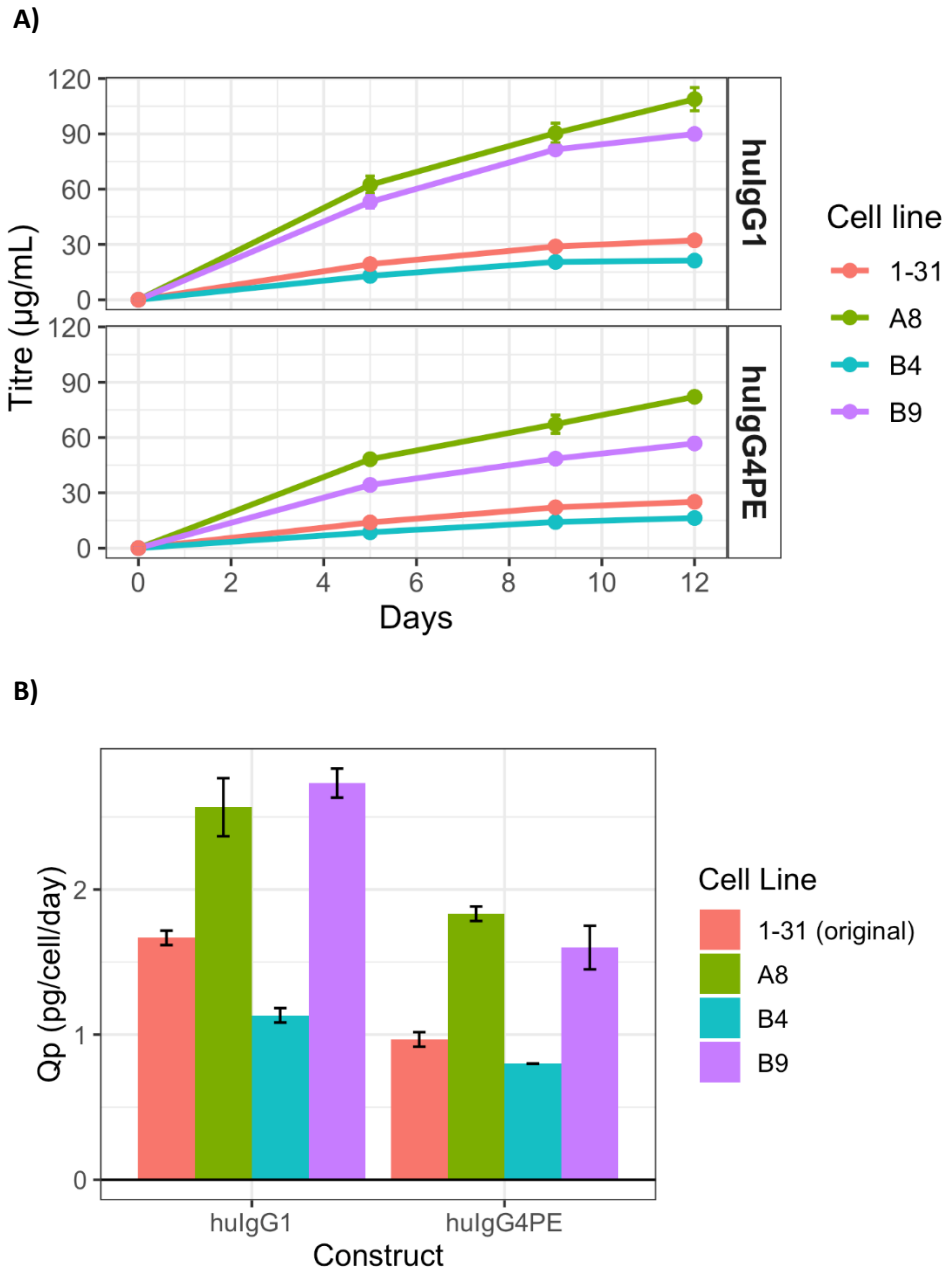


***Figure 17: Transient IgG titre and productivity (Qp) for 1-31 and Cyto-Mine derived cell lines.*** *A) Titre was obtained by Octet measurement of the supernatant at day 7, 9 and 12. B) Productivity is shown as Qp, which measures pg of mAb produced/cell/day. Data corresponds to transient expression of a mAb in either huIgG1 or huIgG4PE format. Error bars represent the standard deviation from the mean (n=3).*

## 3.3 Transient Expression of mLANA

Episome maintenance proteins (EMP) are present in all gammaherpesviruses. They are responsible for maintaining the viral genome as an external episome in the infected cells by tethering the circular viral genome and host chromosome together. They are also responsible for the replication of the episome, which ensures the viral genome is replicated alongside the host chromosomes, by hijacking the host replication machinery.

Epstein Barr Nuclear Antigen 1 (EBNA-1) is the EMP responsible for the episomal maintenance and replication in EBV. The viral episome contains a specific DNA sequence called *oriP*, which interacts with EBNA-1. This EMP has been widely used to adapt cell lines for transient expression by expressing EBNA-1 (transiently or stably) and using plasmid DNA containing the *oriP* sequence. The EBNA-1 *oriP* system has been shown to increase expression yields, however due to EBV's natural tropism for human cells, this system does not allow plasmid replication within CHO cells, and highlights the need for its continued development.

This project therefore investigated the use of alternative EMP systems. One such candidate is MHV68, a gammaherpesvirus which naturally infects rodents. MHV68 contains functionally analogous proteins to EBV, namely the MHV68 Latency Associated Nuclear Antigen (mLANA) and EBV's EBNA-1, and the MHV68's terminal repeat (mTR) and EBV's *oriP*. Kaposi's Sarcoma-Associated Herpesvirus (KSHV), a gammaherpesvirus which is phylogenetically related to MHV68 but infects humans rather than rodents, is also included in this study as a potential alternative. KSHV presents its own equivalents for the elements mentioned (kLANA, kTR and kMRE).

The above EMPs are compared to 2 forms of EBNA-1, EBNA-1 full length (EBNA-1F) and EBNA-1 truncated (EBNA-1t). EBNA-1F represents the wild-type sequence and its translation is naturally repressed by formation of mRNA g-quadruplex structures, which evolved to reduce presentation of viral antigens on host MHC. Since the level of EMP in the cell positively correlates with plasmid maintenance, this is not desirable for an expression system. The EBNA-1t nucleotide sequence contains a deletion in the region of the translation repression sequence and has previously been used for development of CHO cell transient systems.

### 3.3.1 Vector Construction

The first step to evaluate the effect of different EMPs was to confirm that it was possible to express the proteins of interest in the relevant cell line. mLANA and mLANA-F were therefore cloned into the relevant transient expression vector to use for 1-31 and CHO3E7 cell lines.

pTT5 plasmid was modified to create the vectors containing mLANA, mLANA-F and mMRE, which are summarised in Figure 19. mLANA and mLANA-F alongside mMRE were created to be expressed in 1-31, while mLANA and mLANA-F with *oriP* were used in CHO3E7.

pTT5 was digested with *PvuI* and *BglII* to excise EBV *oriP*, and ligated with the also digested "deletion string" to create pNoOri (Figure 20). Digestion of pTT5 with *PvuI* and *BglII* cuts the *oriP* sequence and a portion of the ampicillin resistance cassette. The deletion string is a synthetic DNA sequence containing the deleted part of the ampicillin cassette to restore ampicillin resistance, alongside an upstream multi cloning site that was used to insert the other retention elements of interest. pNoOri plasmid and the commercially synthesised sequence for mMRE, contained within a pUC57 backbone, were digested with *HindIII* and *BglII*. The enzymes cut in the newly created multi cloning site inside the pNoOri to insert the retention element. The digested plasmids were run on a gel, purified and ligated, creating pmMRE (Figure 21 and Figure 22). mLANA and mLANA-F sequences were synthesised commercially with the necessary *AarI* restriction sites upstream and downstream to insert using golden gate cloning. pmMRE and pTT5 were ligated with mLANA and mLANA-F with golden gate cloning, creating pmMRE-mL, pmMRE-mLF, pOriP-mL and pOriP-mLF.

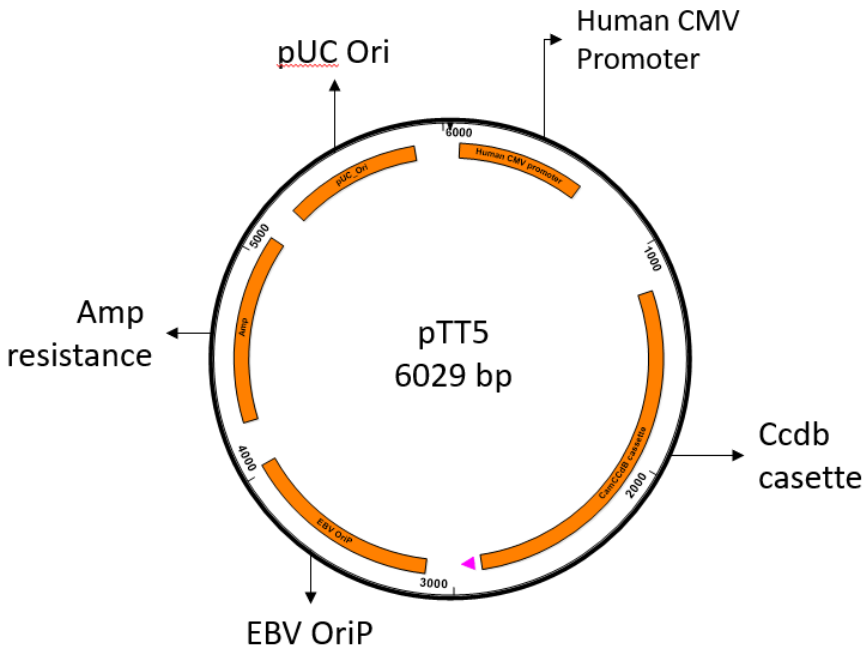


***Figure 18: Vector map of pTT5.*** *Relevant domains are highlighted. Orange colour marks the start and end of the corresponding feature. The small pink triangle corresponds to a poly-A.*

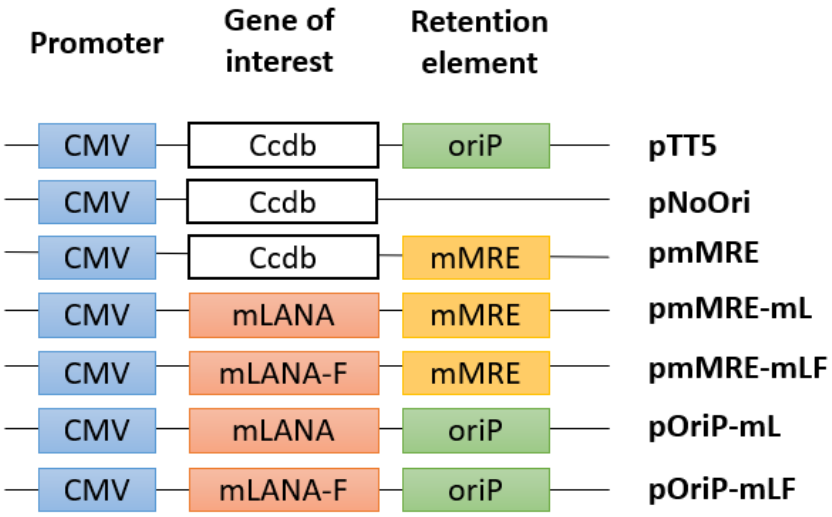


***Figure 19: Summary of plasmids created for transient expression of mLANA.*** *pTT5 was modified to produce the relevant vectors summarised here. pNoOri contains a multi cloning site instead of a retention element. mL = mLANA, mLF = mLANA-FLAG, mMRE = MHV68 minimal replicator element, oriP = EBV ori.*

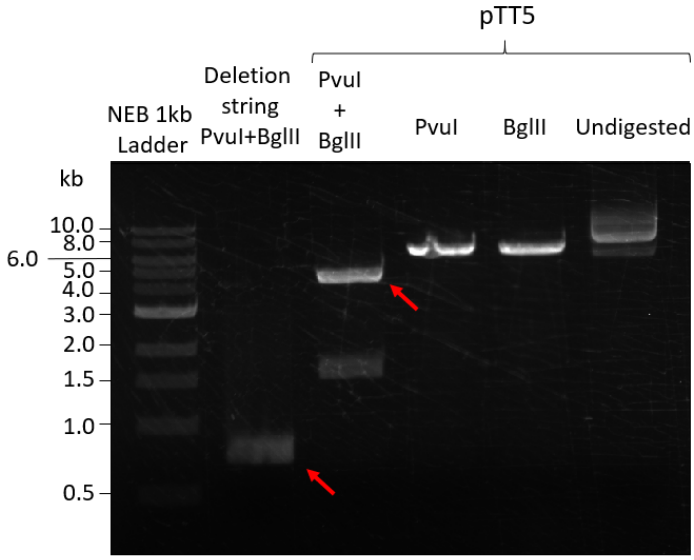


***Figure 20:*** *Agarose* ***gel analysis of the digestion of pTT5 and the "deletion string".*** *DNA was digested and run in a 1% agarose gel at 120 V. Bands marked by the red arrow were cut from the gel, purified and ligated.*

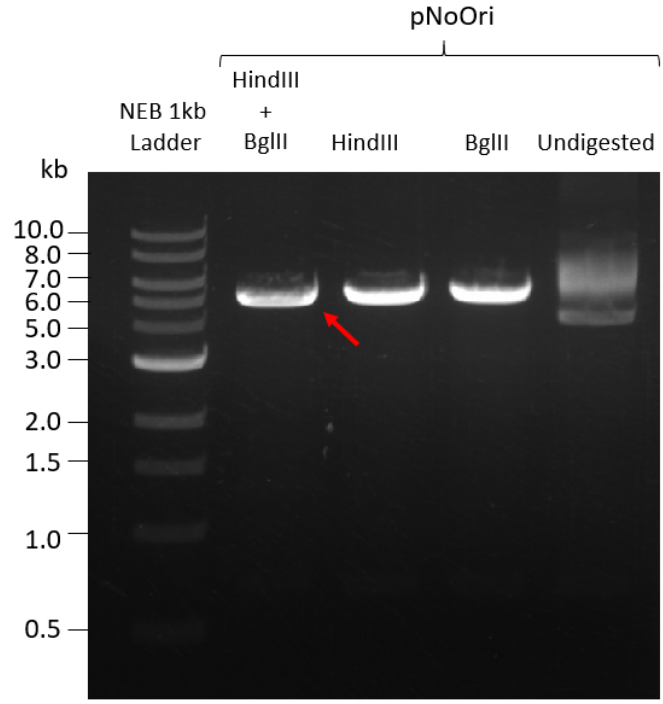


***Figure 21: Agarose gel analysis of the digestion of pNoOri with HindIII and BglII.*** *Plasmids were digested and run on a 1% agarose gel at 120 V. The double digested backbone appears the same size as the single digested backbone as the released fragment is <50 bp. The band highlighted by the red arrow, corresponding to the pNoOri, was cut from the gel and used to create pmMRE.*

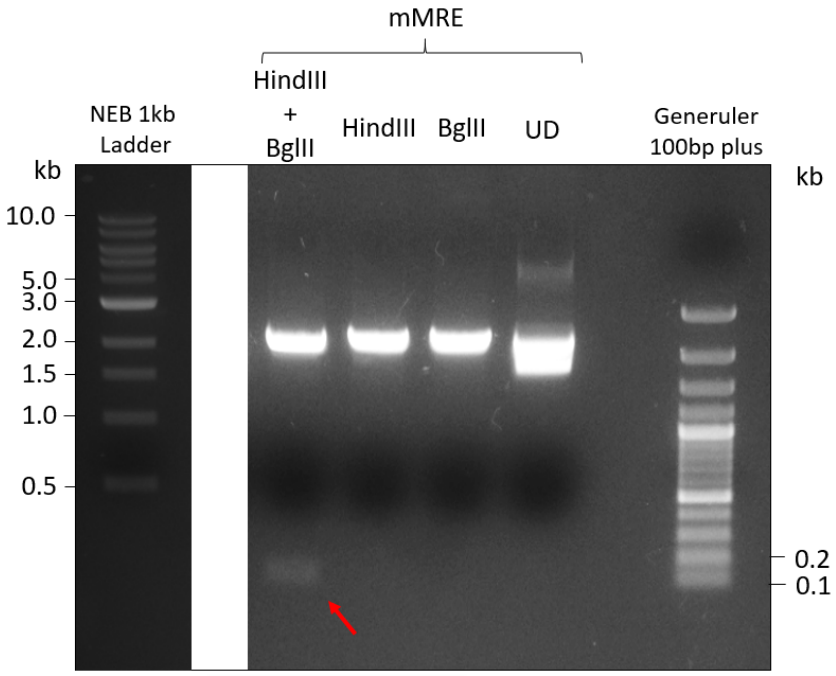


***Figure 22:*** *Agarose gel analysis the* ***digestion of mMRE from the pUC57 cloning vector****. The faint band highlighted by the red arrow was cut from the gel and ligated with the previously digested pNoOri to create pmMRE.*

### 3.3.2 Transfection of ihCHO and Evaluation of mLANA Expression by Western Blot

1-31 cells were transiently transfected with pmMRE-mL or pmMRE-mLF, while CHO3E7 was transiently transfected with pOriP-mL or pOriP-mLF. CHO3E7 were also transfected with pOriP-HC and pOriP-LC to express a mAb as a positive control. Cell samples were then collected on day 9 and frozen immediately on dry ice before storing them at -80°C. Protein was extracted from the cells and a total of 10 ng per well loaded for analysis by western blot, using an HRP conjugated anti-FLAG antibody and an anti β-actin antibody as a loading control. A purified antigen with a FLAG tag was also loaded on the gel as a positive control. No mLANA-FLAG was detected in any of the 1-31 samples (lanes 2-4, Figure 15), while CHO3E7 samples were positive for mLANA-FLAG (lanes 7 & 8, Figure 15) and for the mAb (lane 9, Figure 15), as expected for the CHO3E7 samples. The presence of mLANA in CHO3E7 but not in 1-31 confirmed the protein was/can be expressed, however as CHO3E7 is more productive it's possible that the mLANA-FLAG levels in 1-31 were too low to be detected (Figure 23).

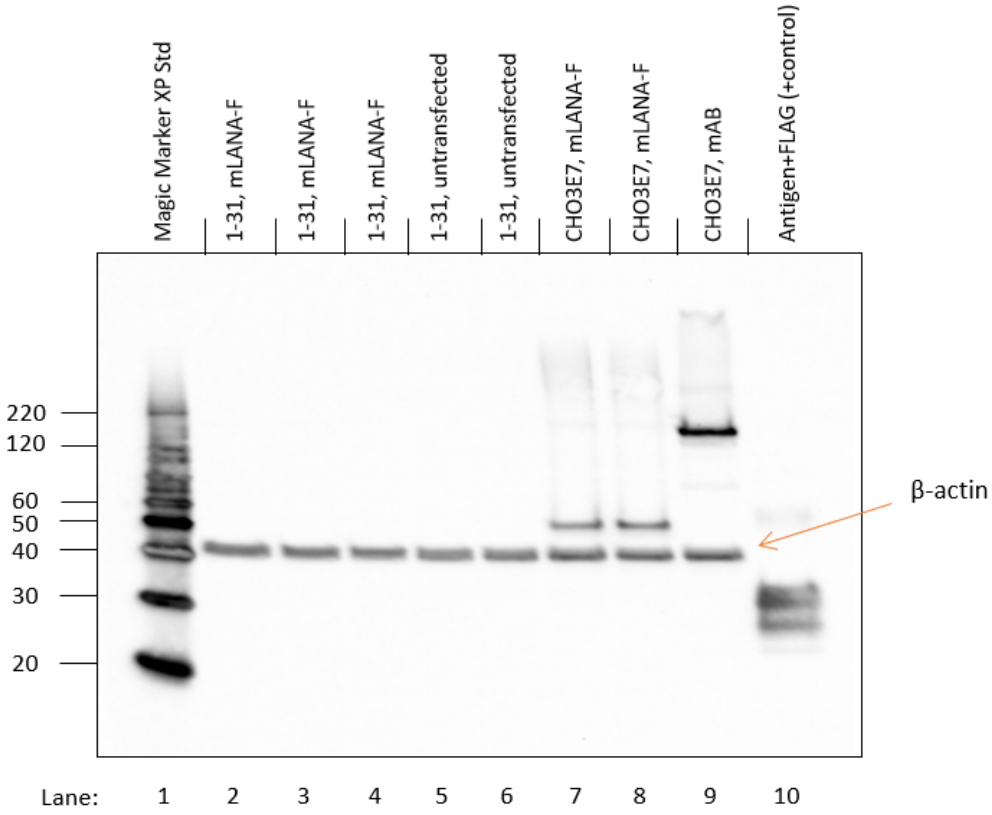


***Figure 23: Western blot analysis of mLANA-FLAG expression in transiently transfected 1-31 and CHO3E7 cells.*** *Anti-FLAG antibody (1:1000) was added to detect the presence of mLANA-F. Anti β-actin (1:1000) antibody was added to detect the housekeeping gene β-actin as a loading control (~40 kDa) and anti-huIgG antibodies (1:1000) were used to detect mAb expression. Lane 2-4: 1-31 cells transfected with pmMRE-mLF. Lane 5 and 6: 1-31 cells, untransfected. Lane 7-8: CHO3E7 cells transfected with pOriP-mLF. Lane 9: CHO3E7 cells transfected with pOriP-HC and pOriP-LC. Lane 10: purified antigen with a FLAG tag as a positive control. 10 ng of total protein was loaded in lanes 2-9, and 0.1 ng of purified protein was loaded in lane 10.*

## 3.4 Stable Expression of EMPs

The previous western blot (Figure 23) showed the expression of mLANA-F was not detectable. Since stable expression is able to achieve higher expression levels compared to transient, the project proceeded regardless as higher stable expression may allow the formation of the appropriate RE/EMP pairs to allow episomal retention and replication. The aim of this section was to first create the necessary vectors containing the EMP sequences and use these for the creation of 1-31 and A8 derived cell lines expressing the EMPs of interest. The end point was the evaluation of mAb expression of these newly created stable pools by using transient vectors modified to contain oriP, mTR or kTR.

### 3.4.1. Vector Construction (pcDNA3.1(+))

#### *3.4.1.1. Vectors for Stable Cell Lines: kLANA, mLANA, mLANA-F, EBNA-1F, EBNA-1t*

Constructs were cloned into pcDNA3.1(+) which contains a neomycin cassette for stable selection, giving the transfected cells geneticin (also called G418) resistance. Derived plasmids maintain the root "pcDNA-" in their names to indicate their backbone. EBNA-1t, mLANA and mLANA-F were ordered as a synthetic gene already cloned into pcDNA3.1(+) and named pcDNA-Eb1t, pcDNA-mL and pcDNA-mLF, respectively. The genes contained a Kozak sequence immediately upstream of the start codon. kLANA gene was obtained in psG5 backbone, while EBNA-1F was obtained in a pMA backbone. Neither of these sequences contained a Kozak sequence or restriction sites compatible with pcDNA3.1(+), therefore it was decided to use PCR to introduce these features. Due to highly repetitive and high GC% sequences, several polymerases failed to amplify the sequence faithfully, introducing errors in the repetitive middle region of the DNA. KOD Xtreme was able to amplify the genes without introducing errors and therefore used in this experiment. The PCR product was run on a gel and the relevant band cut from the gel (Figure 24), digested with *HindIII* and *EcoRI* and ligated with the pcDNA3.1(+) backbone. The backbone was obtained from pcDNA-mL after *HindIII*+*EcoRI* digestion, running the digest in a gel and purifying the appropriate band (Figure 25). Ligation of the digested pcDNA3.1(+) and either kLANA or EBNA-1F produced pcDNA-kL and pcDNA-Eb1F, respectively. Re-circularisation of the *HindIII*+*EcoRI* digested pcDNA3.1(+) backbone created pcDNA-Empty, which did not contain a GOI and was used as a control.

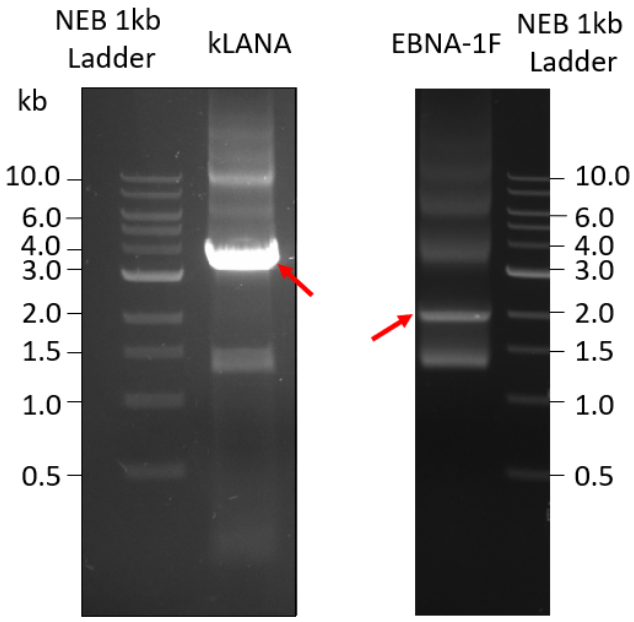


***Figure 24:*** *Agarose gel analysis of the* ***PCR amplification of kLANA and EBNA-1F sequences.*** *Multiple bands show the amplification reaction was not specific, however it was possible to cut the appropriate band (signalled by the red arrow). kLANA expected size was 3.4 kb and the EBNA-1F expected size was 1.9 kb*.

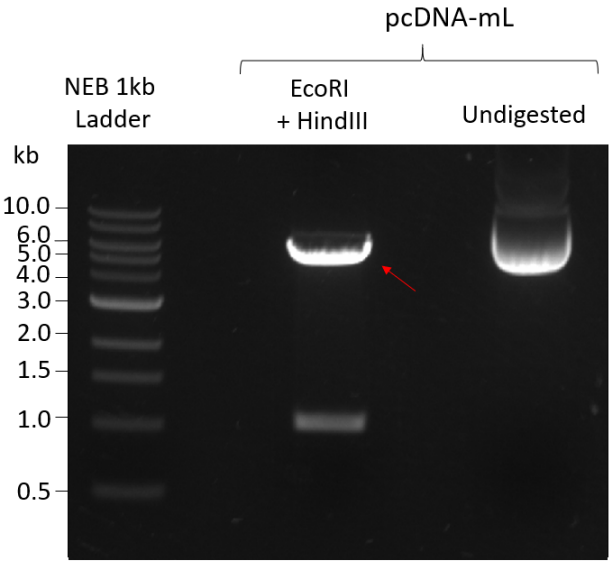


***Figure 25: Agarose gel analysis of the digestion of pcDNA-mL to obtain the pcDNA3.1(+) backbone****. DNA was digested and run in a 1% agarose gel. Band highlighted with the red arrow corresponds to the pcDNA3.1(+) backbone, which was cut from the gel and used in further cloning.*

### *3.4.1.2 Vector for Transient Expression: pTT5 with kTR/mTR/oriP/Empty*

The sequences for kTR and mTR were commercially synthesised and received in a pUC57 backbone. mTR plasmid was cloned in Dam$^-$ bacteria to achieve digestion with *XbaI* after unsuccessfully trying to digest the plasmid received. The plasmids containing mTR and kTR and the backbone pNoOri were digested with *XbaI* and *HindIII*, which cuts upstream and downstream of mTR and kTR and inside the multi cloning site previously added in pNoOri and run on a gel (Figure 26). The bands of 1.2 kb and 0.8 kb, corresponding to the kTR and mTR restriction products respectively, were ligated into the digested pNoOri.

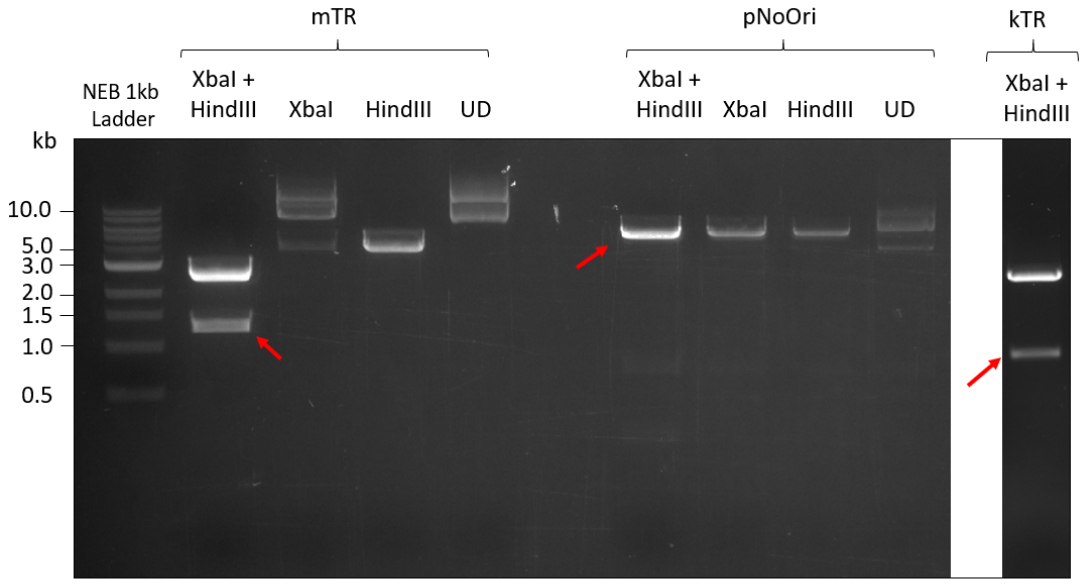


***Figure 26: Agarose gel analysis of mTR, pNoOri and kTR digestion.*** *Digestion of the puc57 backbones releases mTR and kTR segments, of 1.2 kb and 0.8 kb respectively. pNoOri digestion with XbaI and HindIII releases a 145 bp fragment, shown as a faint band in the gel. Red arrows mark the bands that were cut from the gel and purified. UD = Undigested.*

pmTR, pkTR, pNoOri and pTT5 were combined with a synthetic gene coding for the light chain or heavy chain of a huIgG4PE mAb (expressed in previous experiments) or d2EGFP and inserted with golden gate cloning. The sequence for the HC and LC of the huIgG4PE mAb and d2EGFP were synthesised with the appropriate *AarI* enzymes upstream and downstream of the coding sequence to make them compatible with golden gate cloning. The plasmids created are summarised in Figure 27.

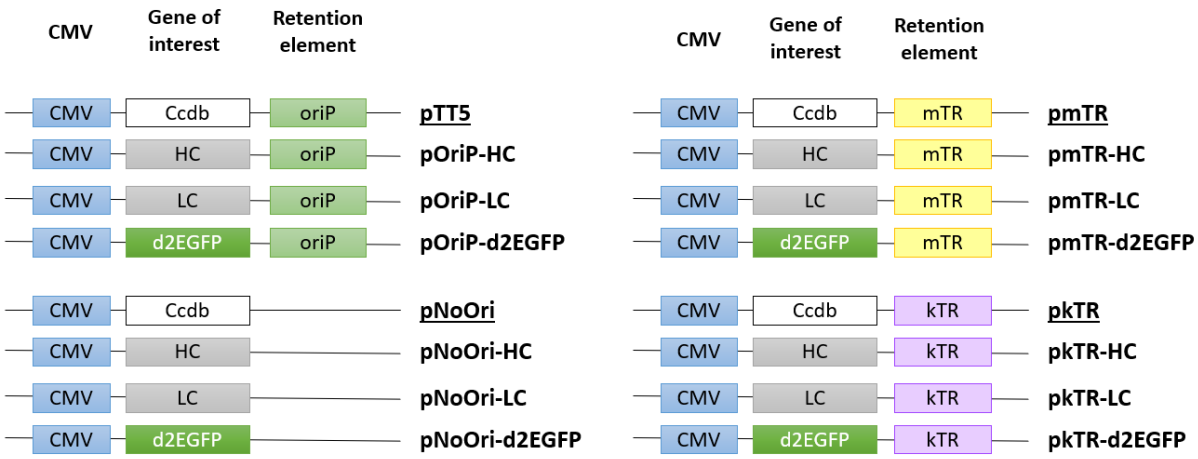


***Figure 27: Schematic diagram of the vectors generated and used for transient expression in cell lines stably expressing EMPs****. Underlines indicate vectors used only for cloning. HC and LC indicate heavy chain and light chain of a huIgG4PE mAb. pOriP-HC and pOriP-LC were not created in this experiment as they were already available. HC = heavy chain, LC = light chain, d2EGFP = short lived GFP, oriP = EBNA-1 ori, mTR = MHV68 terminal repeat, kTR = KSHV terminal repeat.*

### 3.4.2 Geneticin Kill Curve

To generate stable cell lines, it is necessary to determine the effective concentration of the selection agent able to kill cells that do not integrate the plasmid. This parameter is cell dependant and needs to be evaluated for each cell line. With this aim, a geneticin kill curve was performed, which is a dose-response assay where un-transfected cells are exposed to different amounts of geneticin to determine the minimum concentration needed to effectively kill the cells. 1-31 cells were plated in shaking 24dwp at $0.5x10^6$ cells/mL in 2 mL of culture. Geneticin selection was added to the cells in duplicate wells, covering the selection concentration range of 0, 200, 300, 400, 500, 600, 750 and 1200 µg/mL. Culture viability and viable cell number was measured every 3-4 days. Cells were found to be susceptible to geneticin and die when it was added to the media (Figure 28 B). Geneticin was also shown to inhibit cell growth (Figure 28 A). The optimal concentration was selected as the lowest one able to kill all cells within 7 days which in this experiment was 400 µg/mL.

A decrease in culture viability and VCN for cells not under selection was also observed, however this was due to the cells being allowed to reach too-high cell concentrations and was unrelated to the selection.

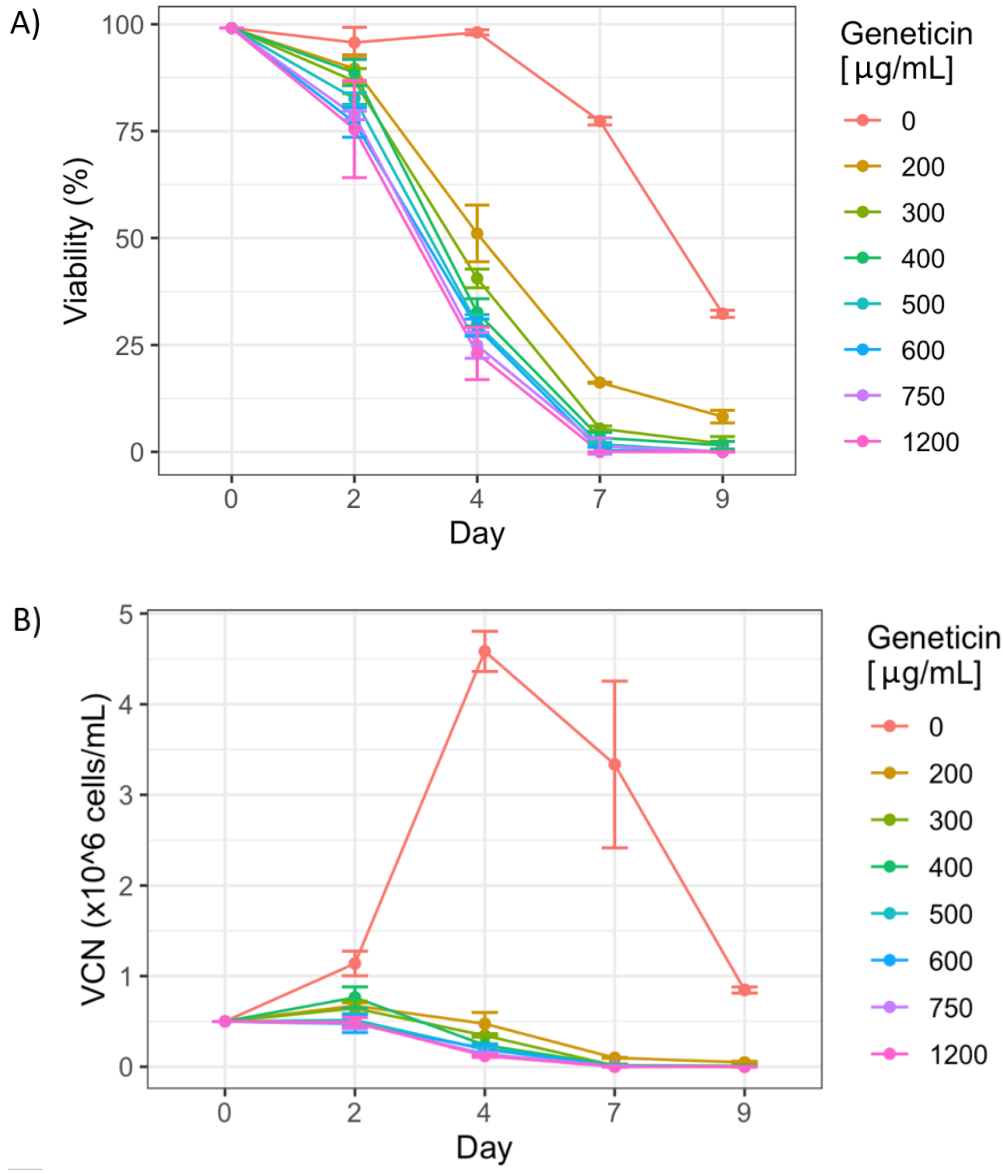


***Figure 28: Geneticin kill curve for 1-31 cells.*** *Results from day 0 to day 4 were measured with a Vi-CELL automated cell counter, while day 7 and 9 data were obtained with Cellometer and combined in the same plot. The change of device was decided after observing Vi-CELL being unreliable in low viability cultures, where debris was counted as dead cells leading to misleading results. A) Culture viability of the cells over 9 days. B) Viable cell number over time.*

### 3.4.3 Cell Line Generation (Transfection, Selection and Recovery)

1-31 and A8 cell lines were used to generate stable cell lines expressing the EMPs with the vectors created in the previous section: pcDNA-Eb1F, pcDNA-Eb1t, pcDNA-kL, pcDNA-mL, pcDNA-mLF and pcDNA-Empty. Cells were electroporated with the plasmid DNA as described previously and placed back in the incubator. Selection was initiated 24 hours after transfection. Cell media was exchanged with fresh media containing 400 μg/mL of geneticin for a final cell concentration of $0.5x10^6$ cells/mL. Cells were monitored every 3-4 days and passaged if the VCN was higher than $0.5x10^6$ cells/mL, if cells failed to grow and stayed at $0.5x10^6$ cells/mL they were passaged with equal amounts of media to a minimum cell concentration of $0.25x10^6$ cells/mL. If the VCN instead was $<0.4x10^6$ cells/mL a media exchange was performed with fresh media containing selection to avoid further cell loss. Both 1-31 and A8 cell lines showed a decrease in culture viability after geneticin addition (Figure 29). Although A8 cell lines started with a lower culture viability after transfection, transfected cells without geneticin quickly recovered to >95% culture viablity (data not shown) while those under selection maintained viability <80% until recovery. Transfected cells recovered differently depending on the cell line, with 1-31 showing a sharper decrease in culture viability in comparison to A8. In general, most A8 cell lines recovered quicker than 1-31, the later reached >90% culture viability on day 22 while A8 achieved this between day 15 and day 19, depending on the EMP being expressed. Untransfected cells were used as a control and died as expected, no data points for untransfected cells were collected after day 19 as no live cells were found in the culture and the flasks were discarded. Cells were considered recovered when culture viability was >90% and doubled at the same rate as the original under no selection. Vials for each cell line were cryopreserved in LN for long term storage after they recovered.

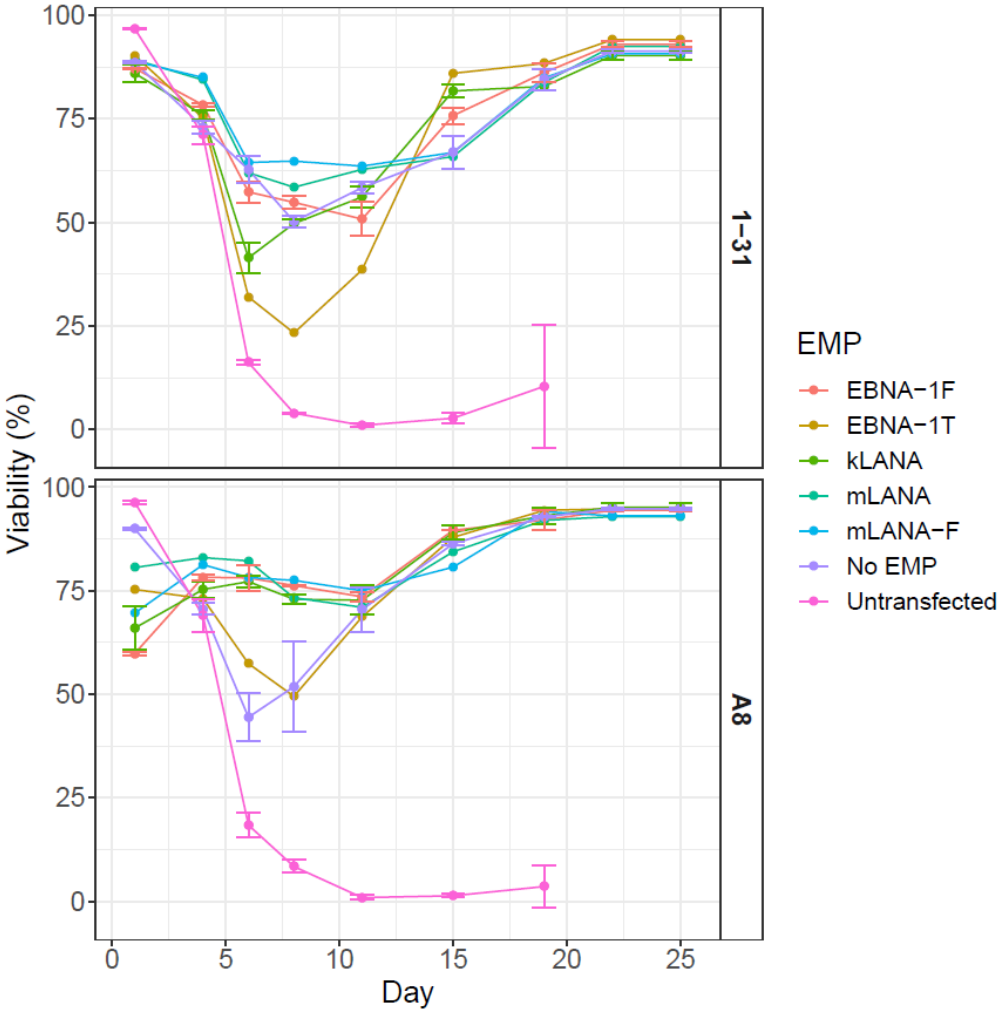


***Figure 29: Recovery of cells after transfection and selection during generation of stable cell lines expressing EMPs created from 1-31 and A8.*** *No EMP = pcDNA-Empty cell lines. Cells were selected with 400 µg/mL of geneticin. Cells were transfected on day 0 and geneticin added on day 1.*

### 3.4.4 Evaluation of GMP Expression in Stable Cell Lines by Western Blot

Samples from the EMP expressing cell lines were collected after the cultures recovered from selection. The objective of the western blot was to evaluate the expression of the EMPs by extracting the total cell protein and analysing it with specific antibodies. No specific antibody for mLANA is commercially available so the aim was to instead detect mLANA-FLAG by targeting the FLAG tag.

Western blot analysis did not detect the presence of EMP for any of the studied cell lines (Figure 22, 23 and 24). Unfortunately, the lack of a positive control for kLANA and EBNA-1F make it impossible to conclude that the protein is not present in the samples. In the case of EBNA-1t and mLANA/mLANA-FLAG however, the positive control included in each western blot showed a positive result, confirming that the detection antibody is able to bind to and recognise the target protein. The lack of a signal for these samples can therefore be attributed to an issue with the protein expression. There are several

potential explanations for this, including a lack of expression of mLANA and EBNA-1 from the cell lines, inadequate folding of the expressed protein or low levels of expression meaning the western blot was not sensitive enough to detect it.

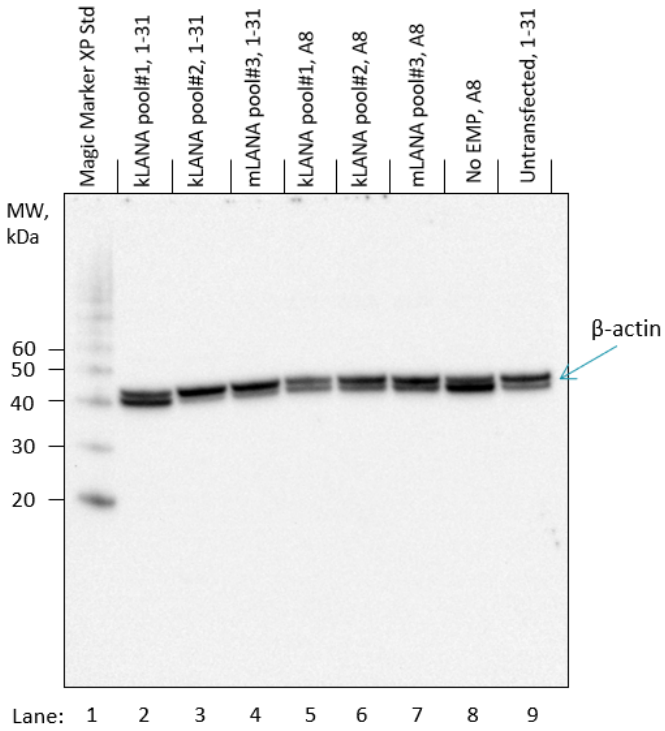


***Figure 30: Expression analysis by western blot of kLANA expression in 1-31 and A8 cell lines after stable transfection and cell line recovery.*** *Anti-kLANA antibody (1:500) was used to detect the presence of kLANA at 220-230 kDa. Anti β-actin (1:1000) antibodies were used to detect the housekeeping gene β-actin as a loading control (~40 kDa). 10 µg of total protein was loaded in each lane.*

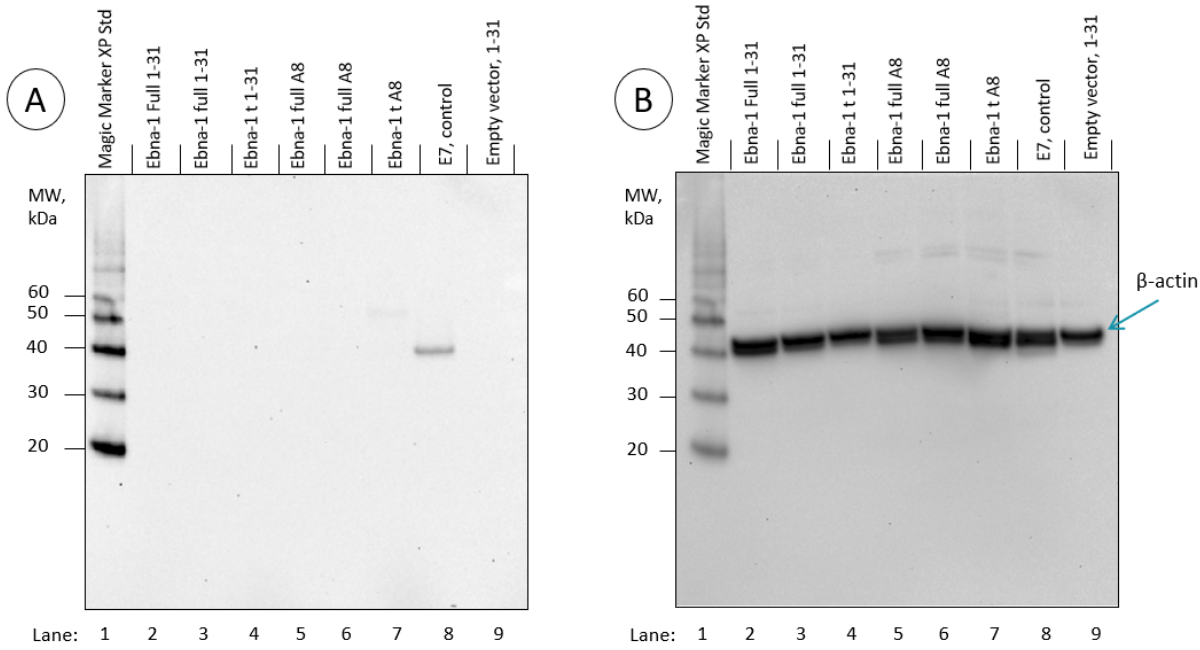


***Figure 31: Expression analysis by western blot of EBNA-1t and EBNA-1F expression in 1-31 and A8 cell lines after stable transfection and cell line recovery****. CHO3E7 samples were loaded in lane 8 as a positive control for EBNA-1t. A) Anti-EBNA-1 antibody (1:500) was added to detect the presence of EBNA-1t and EBNA-1F. B) Represents the same blot as in panel A), after adding anti β-actin antibodies (1:1000) to detect the housekeeping gene β-actin used as loading control (~40 kDa). 10 µg of total protein was loaded in each lane. Expected size for EBNA-1t is 30-40 kDa, EBNA-1F is 56 kDa as a single molecule.*

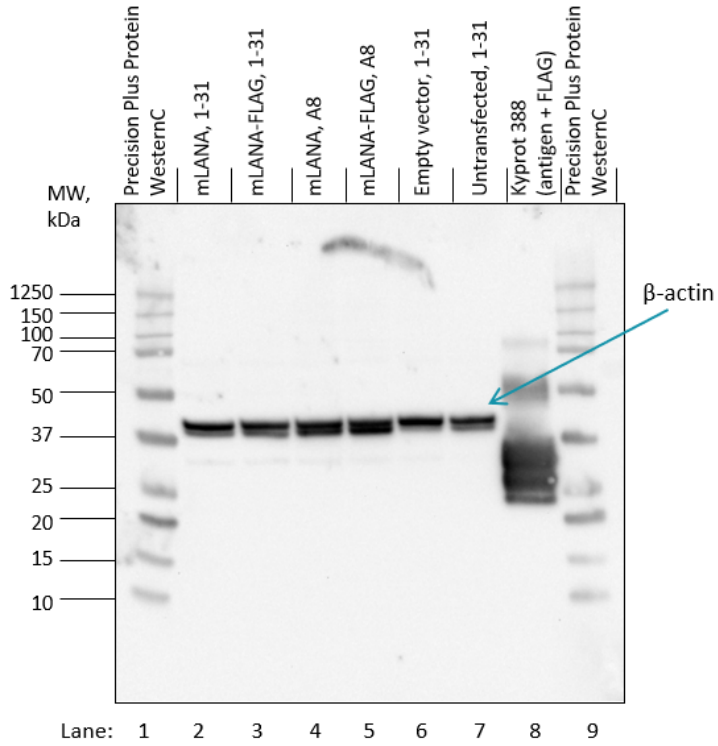


**Figure 32:** ***Expression analysis by western blot of mLANA-FLAG expression in 1-31 and A8 cell lines after stable transfection and cell line recovery****. A) Anti-FLAG antibody (1:1000) was added to detect the presence of mLANA-F. Anti β-actin (1:1000) antibodies were added to detect the housekeeping gene β-actin as a loading control (~40 kDa). Lane 6 contains purified* antigen with a FLAG antibody as a positive control. *10 µg of total protein was loaded in lanes 2-7, and 0.1 ng of purified protein was loaded in lane 8.*

### 3.4.5 Plasmid Retention Evaluation with Short Lived GFP (d2EGFP)

Following the mAb expression evaluation a preliminary analysis (n=1) of plasmid maintenance throughout culture was performed through the indirect method of analysis of a fluorescent protein signal over time. Cell lines expressing EMPs were transfected with plasmids containing the gene for *d2EGFP* and different retention elements (RE) (pNoOri-d2EGFP, pmTR-d2EGFP and pOriP-d2EGFP). The protein d2EGFP is the short lived version of EGFP with a half live of ~2 hours. Cells were transiently transfected with a mix of DNA: 10% of total DNA consisting of the d2EGFP plasmid and the remaining 90% comprising plasmids to express a mAb (pOriP-HC and pOriP-LC (1:1)). For each cell line a negative control transfection was performed with 100% pOriP-HC and pOriP-LC, this control was used to determine the cell autofluorescence. After transient transfection cells were either maintained under FOG conditions to evaluate plasmid maintenance in protein production conditions, or passaged on day 0 and on day 3 to $0.3x10^6$ cells/mL to increase cell growth and evaluate the effect on cell division. Fluorescence was evaluated at day 1, 3 and 5 using flow cytometry analysis on a CytoFLEX instrument. As the cells were analysed before being passaged on day 1, the same data for day 1 was used in the analysis for both passaged and FOG cells.

The flow cytometry data was first gated for live cells, excluding doublets and clumps from the analysis. The measured d2EGFP cell signal was used to create density plots and the threshold for cell autofluorescence was determined using the results from the transfected cells not expressing d2EGFP (control). The area under the curve (AUC) analysis was performed on the density plots to graphically represent the flow cytometry data.

Although the lack of replicates in this experiment does not allow us to draw definitive conclusions, several trends seem to be consistent across all groups. A general decrease in GFP signal over time was observed for all conditions. Cells passaged and actively dividing show a faster decrease of GFP expression than those in a FOG, as expected (Figure 35). For all conditions, at both day 3 and day 5 there was a significant difference in MFI level and TE between passage and FOG conditions ($p<0.01$). The faster decrease seen in actively dividing cells indicates the loss of GFP signal is probably related to plasmid loss occurring upon cell division.

Cells under FOG conditions show peak MFI levels and the highest percentage of positive cells at day 3, followed by a decrease on day 5 (Figure 33, B and C). This could be due to the 32°C temperature shift on day 1, which is linked with increased productivity and results in cell cycle arrest, and thus dilution of the plasmid does not occur as a result of cell division. It could also be related to recovery after the transfection event; as PEI can be cytotoxic, cells may need time to recover from transfection, reaching their peak expression a few days after the event. On actively passaged cells, this peak on day

3 was not seen, and both MFI and percentage of positive cells decrease between both day 1 and 3, and day 3 and 5 (Figure 34, B and C), which can be attributed to the loss of plasmid in actively dividing cells. Cells in FOG conditions experience a decrease in cell growth and therefore lower plasmid loss.

The results presented here indicate the presence of a specific interaction of EBNA-1 expressing cell lines with *oriP* plasmids, as these show both a higher MFI and TE. EBNA-1F and CHO3E7 expression with *oriP* in comparison to pNoOri is significantly higher for both day 3 and day 5 ($p<0.001$). The higher expression compared to other EMP cell lines and RE was already present on day 1, which indicates the effect is not solely related to plasmid maintenance (Figure 33 and Figure 34). Observing the decrease in MFI levels at day 1 to day 3 for both EBNA-1 expressing cell lines (CHO3E7 and EBNA-1F) in combination with *oriP* plasmid shows a slower decrease than with No Ori plasmid for both passaged and FOG conditions. The decrease in MFI for those same cell lines from day 3 to day 5, however, appears to be similar to other cell lines without RE or using plasmid without *oriP*. Plasmid retention specific to the EBNA-1/*oriP* interaction could achieve positive effects in the short term but be unable to slow the decrease of GFP signal from day 3 to 5, as more plasmid is lost upon cell divisions. Comparing MFI levels of CHO3E7 with the EBNA-1F cell line for the same conditions, CHO3E7 appeared to have a higher peak on day 3 that decreased slower (Figure 35). This could be related to a more effective EBNA-1/*oriP* interaction, either by CHO3E7 expressing higher concentrations of the viral protein or presenting a more effective variation of EBNA-1, allowing an improved plasmid maintenance and increase of the positive effect of EBNA-1 on expression.

mTR showed an increase in expression over pNoOri in all cell lines, for cells under both FOG and passage conditions (Figure 33 and Figure 34). Analysis of mTR in comparison to No Ori shows a significant difference ($p<0.001$). The levels decrease at the same rate as pNoOri, indicating the increased expression is most likely not related to plasmid maintenance (Figure 35).

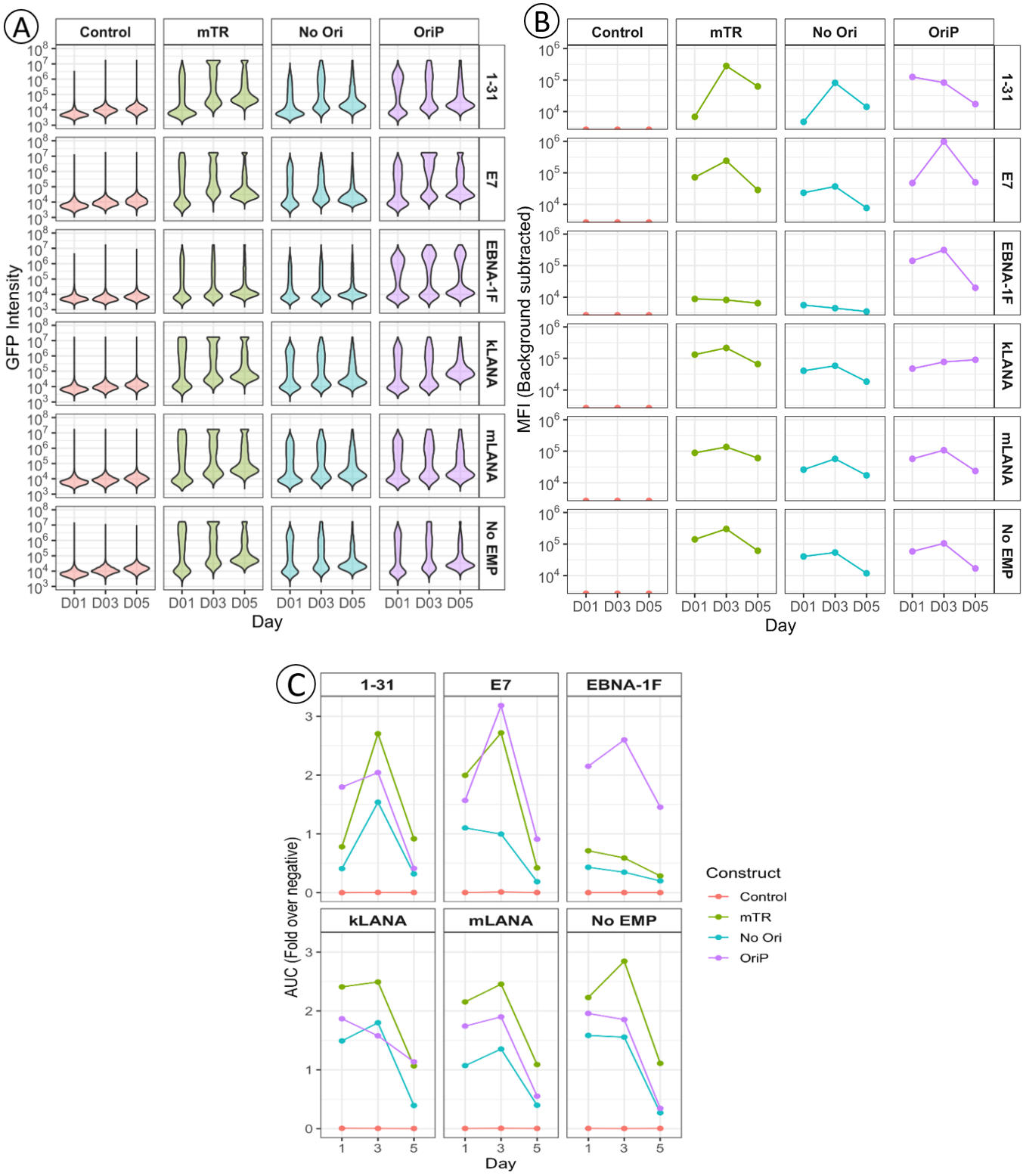


***Figure 33: d2EGFP transient expression levels for different EMP/RE combinations with cells under FOG conditions.*** *Fluorescence was measured with CytoFLEX at day 1, 3 and 5. Population was gated on live, single cells before analysing the data. A) Violin plots showing the distribution of GFP intensity values for all samples. B) MFI was calculated for the total samples and the MFI of the respective control (transfected cells not expressing GFP) subtracted. C) Area under the curve (AUC) from density plots, representing percentage of positives. Datapoints represent AUC of the positive population divided by the AUC of the negative population and indicates proportion of GFP positive cells. n=1*

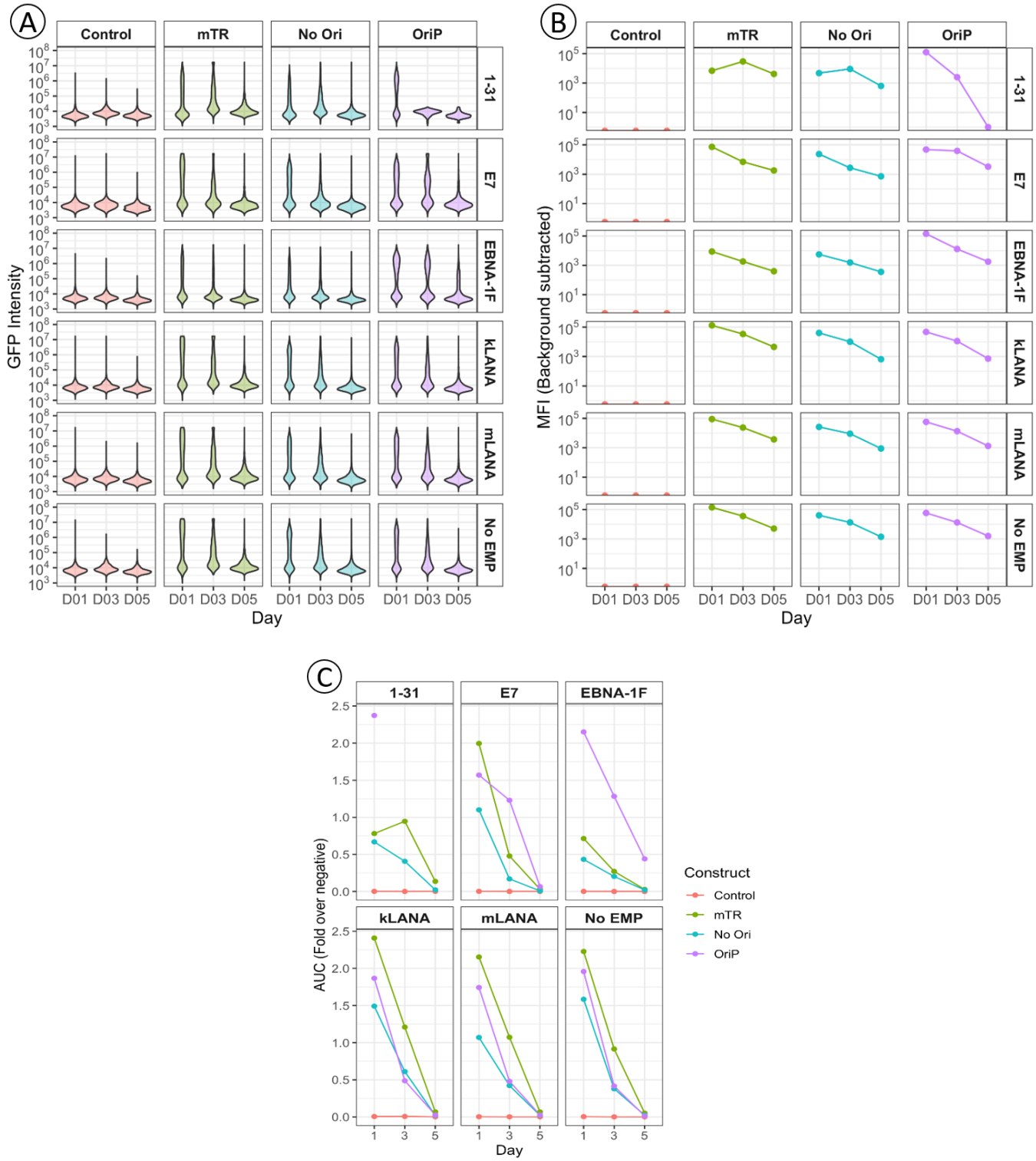


***Figure 34: d2EGFP transient expression levels for different EMP/RE combinations with cells in routine passage conditions.*** *Fluorescence was measured with CytoFLEX at day 1, 3 and 5. Cells were passaged at day 1 and 3 to standard concentrations. Population was gated on live, single cells before analysing the data. A) Violin plots showing the distribution of GFP intensity values for all samples. B) MFI was calculated for the total samples and the MFI of the respective control (transfected cells not expressing GFP) subtracted. C) Area under the curve (AUC) from density plots, representing percentage of positives. Points represent AUC of the positive population divided by the AUC of the negative population and indicates proportion of GFP positive cells. n=1*

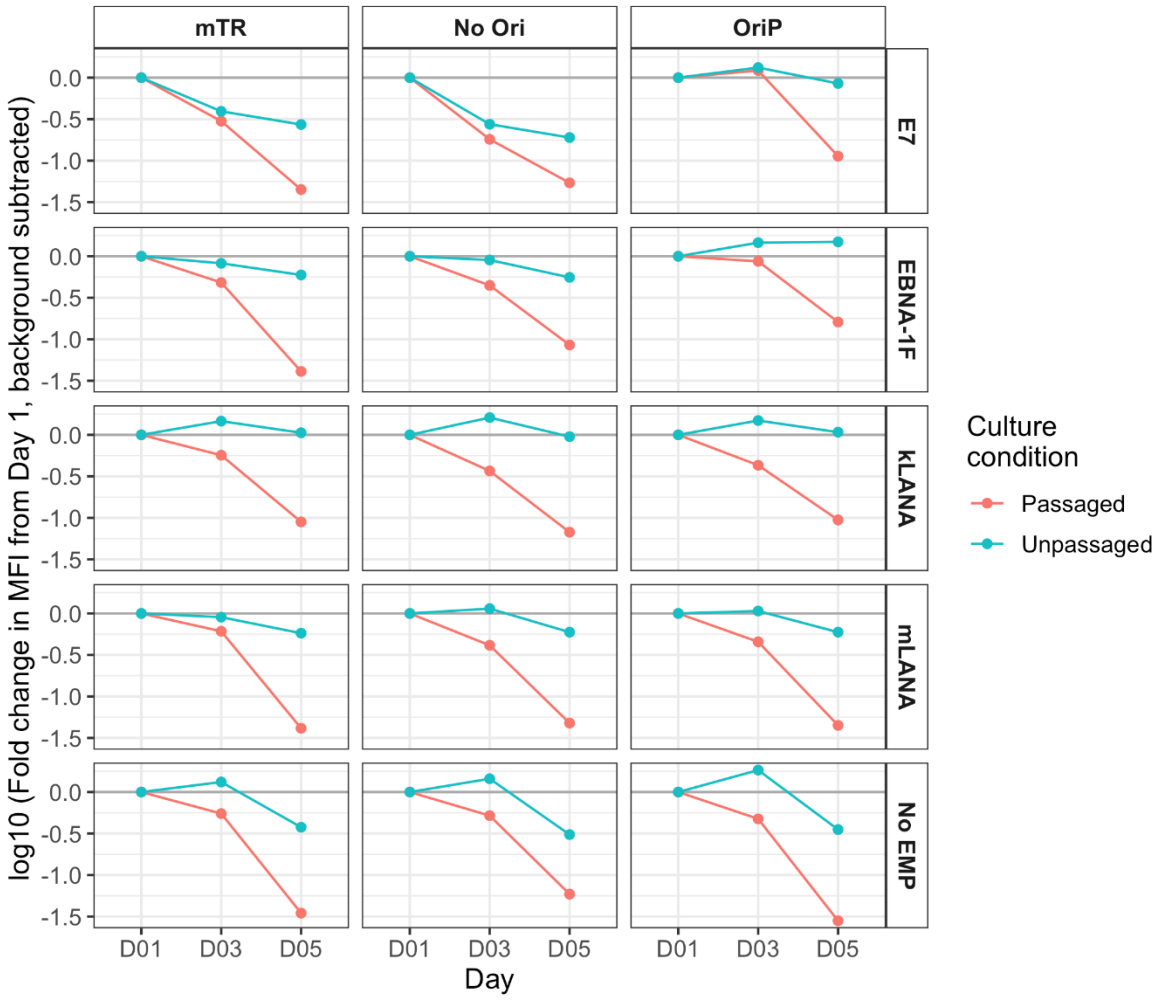


***Figure 35: Comparison of d2EGFP expression over time of cells under FOG conditions and cells in routine passage conditions.*** *MFI fold change from different days compared to that of day 1 for the same conditions. Fold change of non-GFP expressing cells (transfected, expressing mAb) was used as a control and subtracted. Data presented after log transformation, line at y=0 represents no change over MFI on day 1, positive results indicate an increase and negative results a decrease compared to MFI day 1. E7 = CHO3E7. Control = Cells transfected with pOriP-HC and pOriP-LC, GFP negative. Passaged = Cells passaged on day 1 and 3. Unpassaged = Cells under normal FOG conditions. n=1*

### 3.4.6 Evaluation of mAb Expression

To evaluate the effect of EMP on mAb expression the cell lines stably expressing EMPs were transiently transfected with plasmids containing different RE: kTR, mTR, No Ori or oriP. A8 and 1-31 cell lines expressing EBNA-1F, EBNA-1t, kLANA, mLANA or no EMP were transfected with the transient expression plasmids pkTR-HC and pkTR-LC, pmTR-HC and pkTR-LC, pNoOri-HC and pNoOri-LC, or pOriP-HC and pOriP-LC. All the plasmids contained the same HC and LC for a mAb in huIgG4PE format. Titre data corresponds to day 12 values measured by Octet.

EBNA-1F expressing cell lines showed an increase in expression only when paired with *oriP* and no effect when paired with kTR or No Ori plasmid, as expected (Figure 36). The difference between EBNA-1F/oriP and EBNA-1F/No Ori was significant ($p<0.001$). EBNA-1t did not increase the expression when paired with *oriP*, instead the EBNA-1t/oriP combination showed a similar titre to EBNA-1t/No Ori ($p>0.05$). Expression with *oriP* plasmid in cell lines not expressing EBNA-1F gave a non-significant difference to using No Ori plasmid ($p>0.05$), which indicates oriP plasmid is only beneficial for cell lines expressing EBNA-1F and the increased expression is therefore related to the EBNA-1F/oriP interaction.

The presence of mTR in the plasmid increased expression in an EMP independent manner, achieving up to 2-fold greater expression than plasmids without a RE, kTR or oriP (excluding EBNA-1F/oriP data) ($p<0.001$) (Figure 37). Plasmid with mTR gave the highest titre of all the other combinations, similar to EBNA-1F/oriP levels (Figure 38). Unexpectedly, the effect of mTR on expression is less noticeable in cell lines expressing mLANA, especially in the A8 derived mLANA cell line. mLANA decreases the expression in mTR vectors compared with other A8 EMP expressing cell lines, however this is not seen in 1-31 derived cell lines, where mLANA/mTR results in the second highest titre (Figure 39). kTR did not increase the titre for any cell line, with a non-significant difference to using the No Ori plasmid ($p=0.09$), this includes the kLANA expressing cell lines for both 1-31 and A8 (Figure 38).

The highest titre was achieved in the A8 derived cell line expressing kLANA and using mTR plasmid (Figure 39), where it increases titre 2-fold in comparison with pNoOri. This could be due to a specific interaction of kLANA with mTR shown and published by other groups. However, mTR does not seem to have such a strong effect on 1-31 kLANA, where the titre was only 1.7-fold higher in comparison to using a No Ori plasmid. This could either mean that the increase in mAb expression is not due to a specific interaction of kLANA/mTR, or that it is specific but the 1-31 derived cell line does not express enough, if at all, kLANA while the A8 cell line does.

All the cell lines derived from A8 achieved higher expression levels than their corresponding cell line derived from 1-31 (Figure 40). The difference in titre was significant, with a p-value $<0.001$, which maintains the differences observed between the two cell lines previously seen in this work.

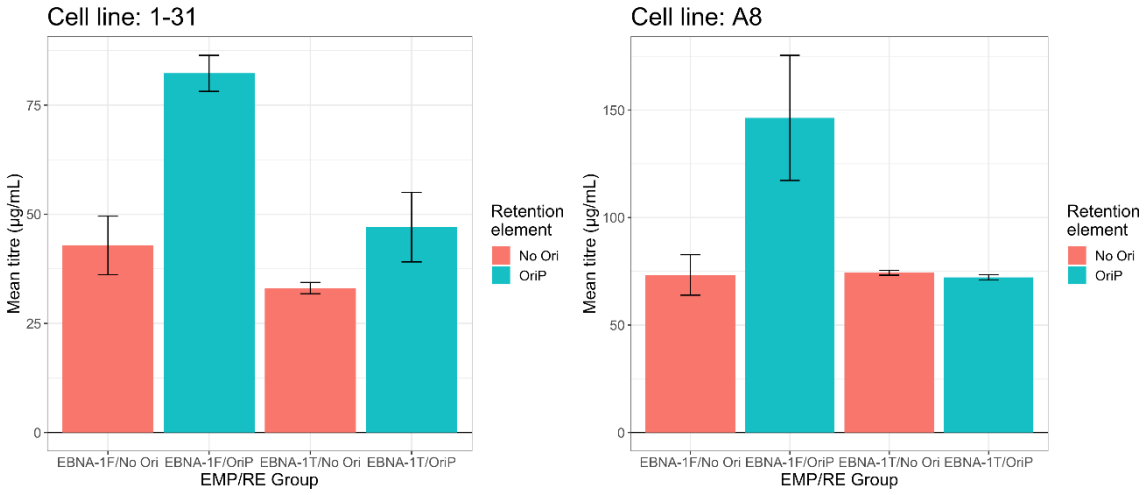


***Figure 36: Transient mAb expression from 1-31 and A8 cell lines expressing EBNA-1 derived proteins with an oriP/No Ori plasmid.*** *The mAb with a huIGg4PE format was quantified by Octet at day 12. EBNA-1F n=4, EBNA-1t n=2.*

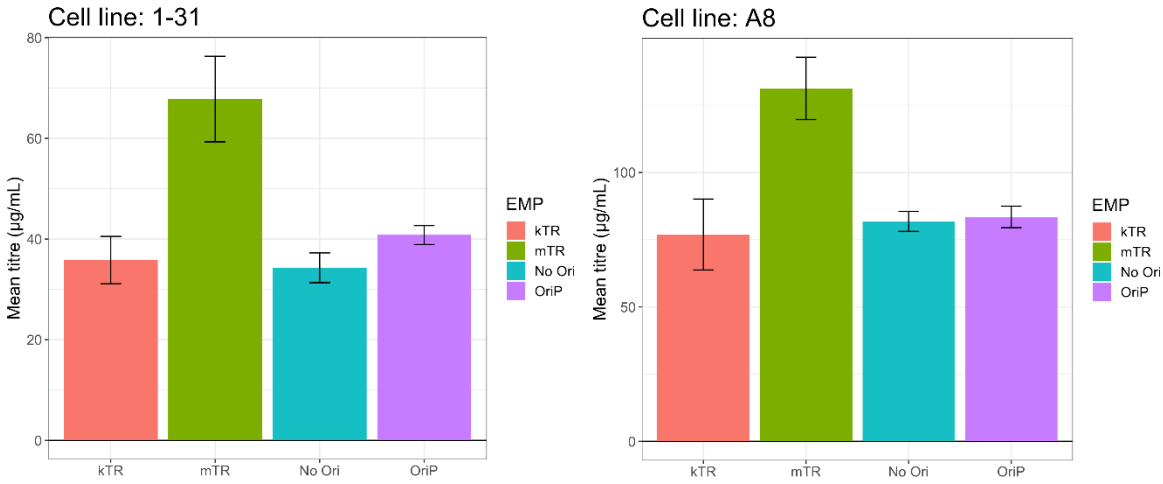


***Figure 37: Comparison of 1-31 and A8 transient mAb expression using different RE plasmids.*** *Results correspond to No EMP cell line. Cell lines were expressing a mAb with a huIGg4PE format, which was quantified by Octet at day 12. Error bars represent the standard deviation from the mean, n=4.*

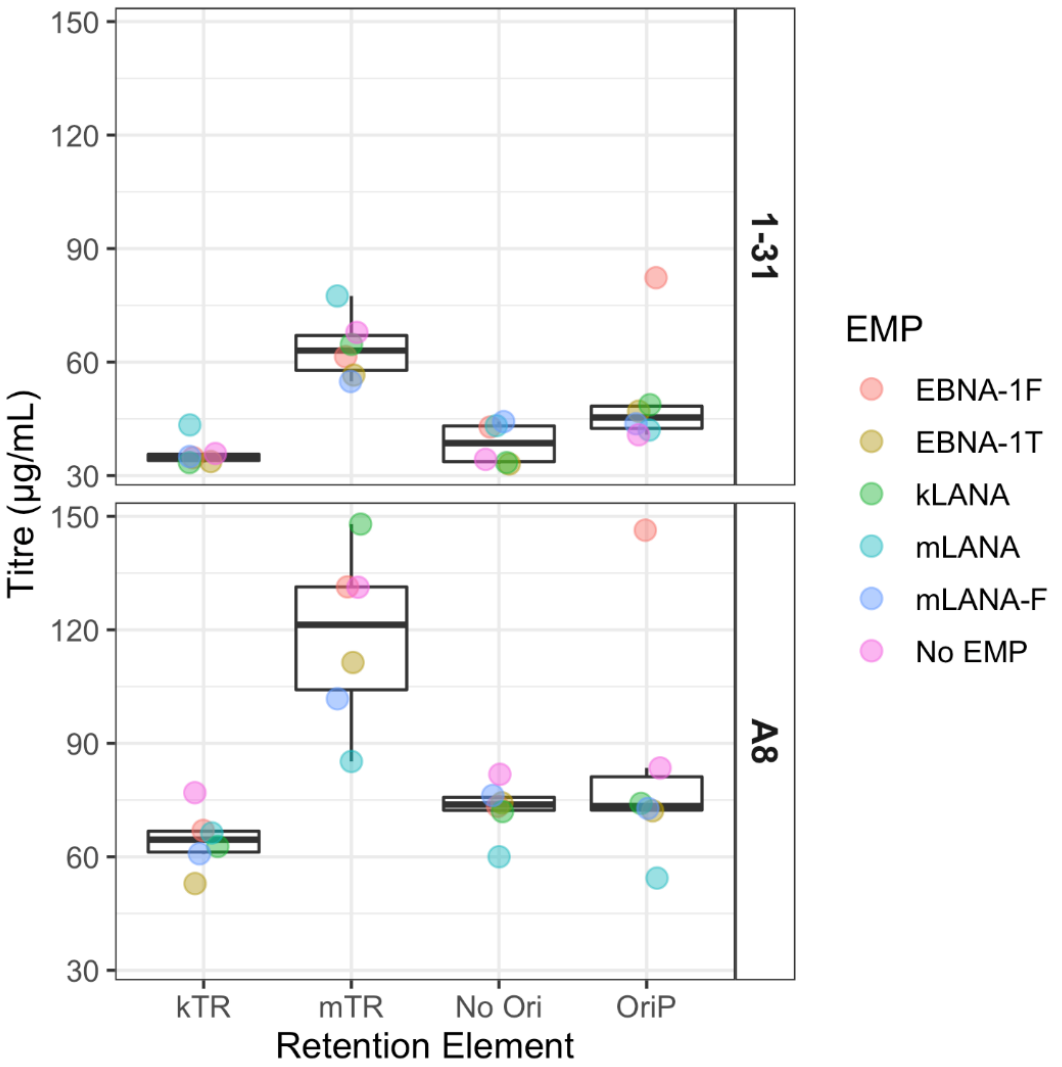


***Figure 38: Box plot summarising results for transient expression of a mAb using RE containing plasmids in EMP stable cell lines.*** *The mAb with a huIGg4PE format was quantified by Octet at day 12. Box size represents data spread, with the line in the centre representing the median value. Point represents the average of the data. n=4 for No EMP, kLANA and EBNA-1F values and n=2 for mLANA, mLANA-F and EBNA-1t.*

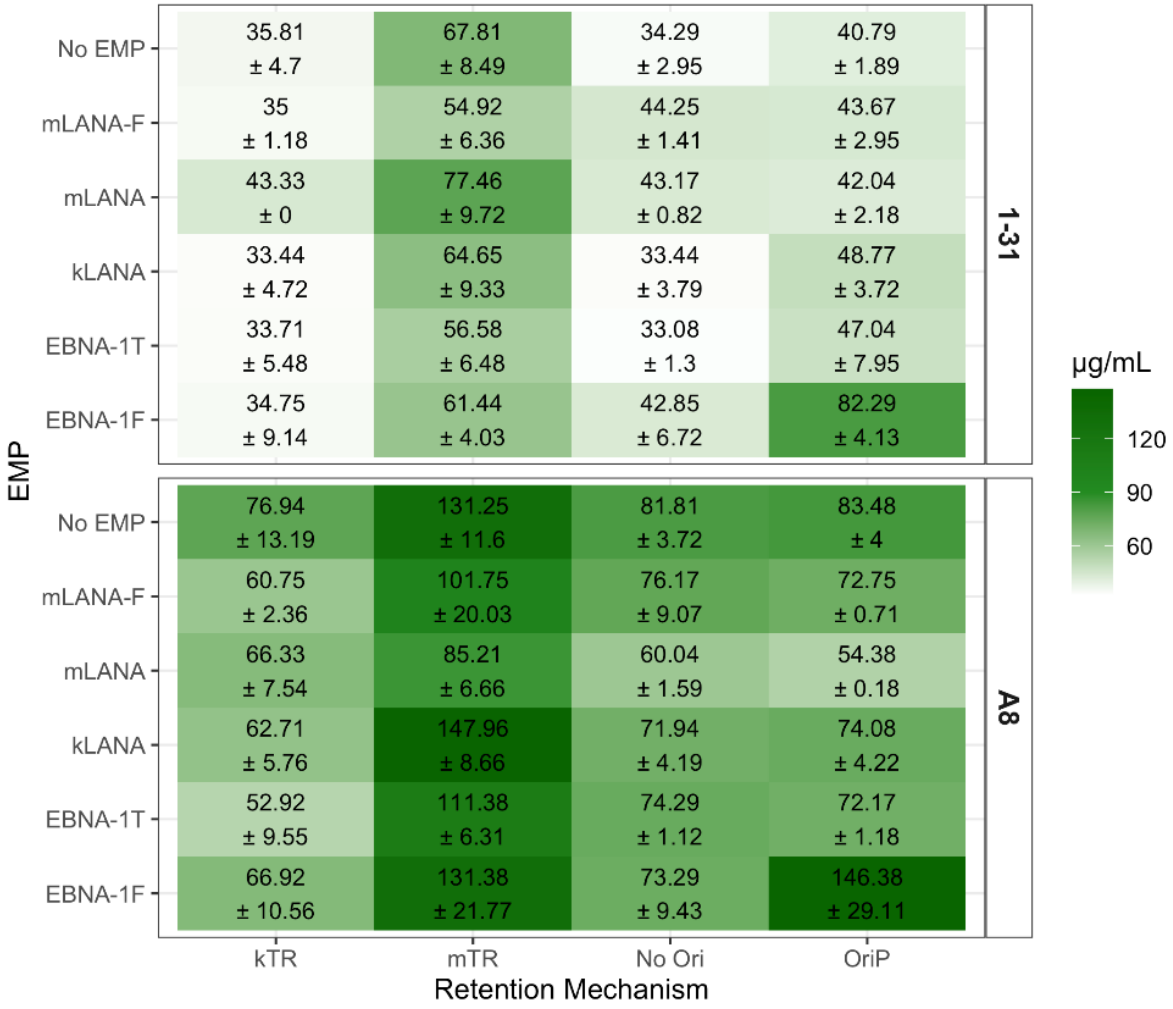


***Figure 39: Results for transient expression of a mAb using RE containing plasmids in EMP stable cell lines.*** *The heat map shows the different expression levels of a huIgG4PE mAb at day 12 for the different cell lines derived from 1-31 or A8 and expressing either no EMP, mLANA-F, mLANA, kLANA, EBNA-1t or EBNA-1F, each one transfected with plasmid containing different retention elements (kTR, mTR, No Ori or oriP) and encoding for the same mAb. Colour intensity reflects IgG expression (µg/mL), with dark green corresponding to the highest results. Average results are used for the heat map, +/- values represent the standard deviation from the mean, n=4 for No EMP, kLANA and EBNA-1F values and n=2 for mLANA, mLANA-F and EBNA-1t.*

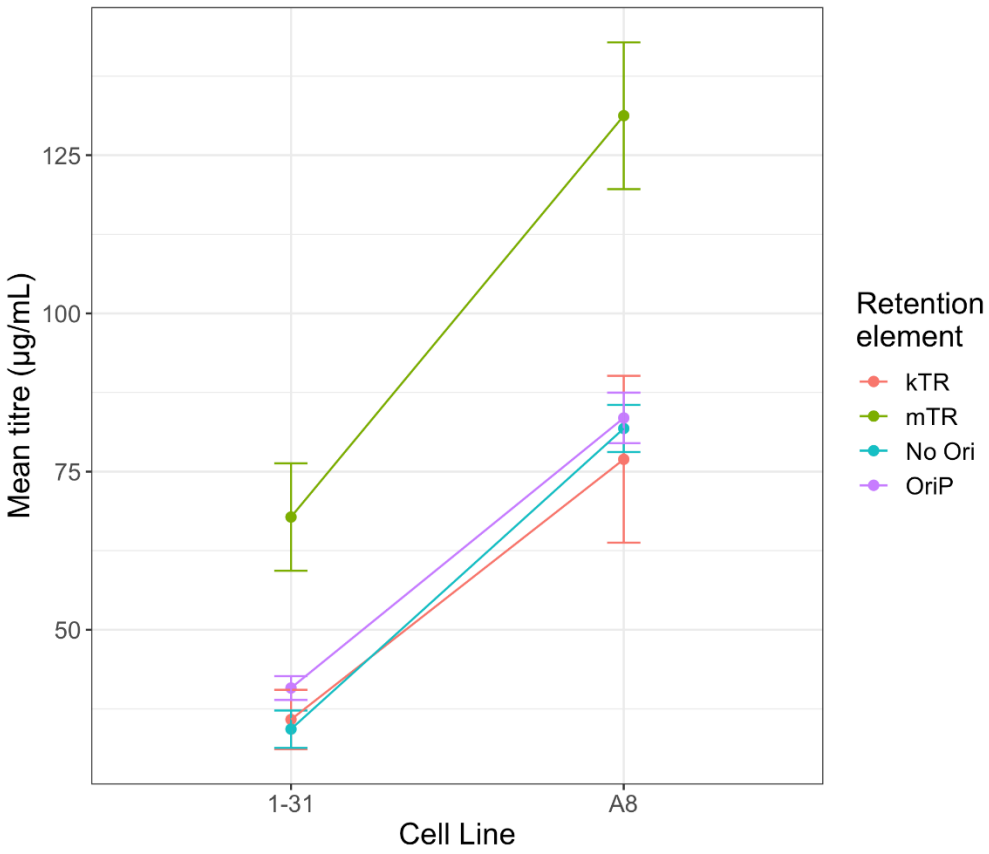


***Figure 40: Dot blot comparing mAb expression of 1-31 and A8 derived cell lines with different retention elements.*** *The mAb with a huIGg4PE format was quantified by Octet at day 12. Data from cell lines expressing different EMPs was averaged in a single data point. Error bars represent the standard deviation from the mean, n=16.*

# 4 Discussion

Transient gene expression (TGE) systems are a widely used alternative to stable platforms for the rapid production of recombinant proteins. They are the foremost choice for the expression of therapeutic proteins for research and pre-clinical supply, and therefore an efficient TGE platform is essential to meet the demands for these proteins. TGE allows the production of up to grams of material in a matter of weeks, with less resource intensive methods that are high-throughput compatible, which allows for the production of a wide panel of proteins to test in the first stages of research[37,40].

Furthermore, even though the need for TGE in research has been widely accepted and is an industry standard practice, recent world circumstances and fears of new viral threats have opened the door to using this rapid process for early clinical trial material supply[28,29]. Indeed, transient expression has been successfully scaled up to 100 L[33]. With both current needs and future potential in mind, the goal for transient expression systems is to improve expression titre of the recombinant protein. Recent research has allowed productivity to increase significantly, with some encouraging reports of up to 2 g/L[35], and the gap between TGE and the impressive 10 g/L reported for stable cell lines shrinking[24]. However, these reports can be inconsistent between the different proteins expressed. Usually across a whole panel of proteins the highest titres (in the g/L range) are only reported with a select few proteins, with lower titres being observed with the rest[35,37].

Chinese hamster ovary (CHO) cells are the favoured cell line for recombinant protein production due to their many advantages (bio-active post-translational modifications (PTM), proven track record for manufacturing)[18] and therefore CHO cell lines have also been the focus for TGE in the last decades[36,40]. The traditional use of HEK cell TGE, although more productive, led to worries about different product quality and protein behaviour related to PTM between HEK produced material for early research and the later stages where stable CHO cell lines are typically used. The use of a single host cell line and an aligned system between stable and transient platforms would in theory allow for consistent product quality from early research through to clinical trials, explaining the current industry's focus on developing CHO TGE systems. To further minimise any possible variation in product quality between CHO cell lines themselves, we have focused on developing a TGE platform using one selected CHO cell line, CHO 1-31, also used for the creation of stable cell lines and manufacturing. With this objective in mind, the project focused on creating the TGE platform from several different angles; development of a process with an optimised PEI based transfection and efficient FOG conditions, selection of a derived cell line more amenable to this process, and finally evaluation of a novel episomal maintenance platform through cell and vector engineering.

Opportunities for bioprocess improvement span the entire TGE process, from transfection of the plasmid DNA to the treatment of cells once transfected to optimise protein expression. Several transfection methods exist, the most widely used for TGE being PEI. The available protocols for PEI transfection vary wildly in regards to the specific time, amounts of different reagents and their proportions, and even the methods of preparation[35,162–165]. The range of options exemplifies the fact that PEI transfection needs to be optimised for individual cell lines. Here key variables were evaluated in the process and determined optimal conditions, achieving more than 90% transfection efficiency measured by GFP expression. This approach considered the DNA amount, cell concentration, PEI to DNA ratio, and incubation time to be the most relevant factors impacting efficiency and recombinant protein expression as determined by GFP, and used a Design of Experiments (DoE) approach supported by Design Expert software to explore the individual variables and their interactions [165]. A limitation to these results is the narrow cell concentration range where the tested conditions were most effective: higher cell concentrations ($4x10^6$ cells/mL) always resulted in <20% TE.

To evaluate the relevance of the transfection conditions in relation to the FOG conditions, we compared the 2 optimal transfection conditions (condition A and B) across 2 cell concentrations to the original, standard transfection condition (condition C) in 2 separate FOG conditions. We observed a 5-fold titre improvement, from ~6 mg/L to ~30 mg/L between the original and the modified transfection conditions (A and B respectively). Interestingly, despite condition B achieving a higher TE and MFI than condition A (Table 6), the 2 conditions gave a similar mAb titre (Figure 14 B). The cause became clear when their productivity (Qp) (Figure 14 A) and total viable cell number (Figure 13 A) were considered. As stated, transfection condition A achieved a sub-optimal transfection compared to B (lower MFI and TE), however since condition A cultures were transfected at a cell concentration of $2x10^6$ cells/mL (double the cell concentration at transfection of condition B), the higher cell number in condition A is likely to have increased the titre compared to the more efficient transfection in condition B. This demonstrates that considering individual variables in isolation can be misleading and enforces the importance of considering all factors and their interactions. Furthermore, assessment of TE using GFP and flow cytometry, although convenient, does not directly translate to mAb expression levels. GFP is a small protein in comparison to mAbs, and cell requirements to produce either are different, as they subject the cells to different stresses and metabolic requirements; GFP is retained intracellularly whilst mAbs are secreted and transit through the secretory pathway of the cell.

Much effort has been dedicated to cell culture media development in an effort to improve titres for both transient and stable expression. In fact, for stable cell lines this is probably one of the greatest contributing factors to the current high titres. Process improvement includes a wide range of options, namely the variety of feeds, their makeup, the time and concentration at which they are added, and

other factors such as including a temperature shift or expression boosting additives, such as valproic acid (VPA). FOG conditions are generally designed with the objective to maximise the amount of recombinant protein produced, but the approaches to achieve this can vary. In stable cell lines an increased titre can be obtained by allowing transfected cultures to reach high cell concentrations (>1x$10^7$ cells/mL)[166]. Unlike stable processes however, transient platforms display a decrease in productivity throughout culture, due to plasmid copy number, which relates to cell productivity, decreasing upon cell divisions. Cells without the target recombinant DNA will tend to grow and proliferate faster than those that express the target recombinant protein and contribute no further to the titre from the culture. For TGE this can be partly overcome by beginning with a higher cell concentration, up to 4x$10^6$ cells/mL at transfection in some reports, which can produce high titres [167]. With the current optimised conditions in mind, attempting to emulate the approach of high concentration at transfection presented two issues: the transfection process gave the best results at low cell concentrations (1x$10^6$ cells/mL) and the feeds and temperature conditions investigated during the FOG were not able to sustain a high cell concentration, as high cell numbers resulted in a significant drop in culture viability after 5 days of culture (Figure 13). FOG condition 2, which gave high cell concentrations but was not able to support these for any period of time, could be further optimised by adding extra feeds and nutrients to support the number of cells and keep the culture viability high until the end of the FOG, or by incorporating a temperature shift that decreases cell growth and gives an increase in cell productivity.

Considering the TE results, it could be possible to explore areas outside of the current limits set in the DoE in an effort to optimise the process for other cell concentrations. The investigations in this study showed incubation time not to be a variable that particularly impacted TE, with p=0.04 for the TE referring to the % of positive cells and p>0.05 in the other responses measured, however exploring longer incubation times may be key to move the effective working area to a higher cell concentration. Protocols recommend up to 30 minutes of incubation time, which means the currently tested range (30 seconds to 10 minutes) only explored less than 50% of the recommended time scale.

CHO cells are genetically unstable which results in variability, even within a clonal cell line. This fact is routinely exploited in stable expression to obtain high titres. After stable transfection, cells are sorted and colonies originating from a single cell screened to find a clone with desirable properties, namely high titre and product quality. The process of gene insertion within the genome leads to variabilities related to the gene copy number and the region of integration, however it has been observed that using the same integration site can still result in different titres[168–170], emphasising the inherent genetic diversity of CHO cells. In this project we identified a clone that was more suitable for transient

expression than the original clone 1-31; the new clone giving in a 3-fold increase in titre without further modifications.

The Cyto-Mine instrument, a novel technology able to sort single cells encapsulated in picodroplets using microfluidics, was used to isolate the new cell line. This technology is combined with a FRET assay able to quantify the mAb produced inside the picodroplet, evaluating the protein expression and secretion of each single cell individually to identify the most productive cells, which can then be selected for recovery. Although Cyto-Mine was used to sort the cells, the low recovery did not allow us to evaluate its effectiveness in determining individual cell expression levels and the potential of the technology to select those cells of interest. The process proved to be stressful to the cells and resulted in <0.05% recovery rate, which meant we were only able to evaluate 3 cell lines, none of which were considered "high" expressors from the FRET assay results. Interestingly however, 2 out of the 3 cell lines ultimately gave higher transient titre than the parental cell line 1-31. This was not only related to an increase in productivity, but also an altered growth profile where the cells grew faster and were able to maintain higher culture viabilities during both FOG and selection in further experiments. The improved growth profile of the newly isolated A8 in comparison to its parental cell line could explain its ability to recover from the sorting, which may have acted as an unexpected selection for more "robust" cells. Similarly to the observation within the TE and FOG optimisation efforts, there are other factors aside from the productivity of a single cell to be considered when trying to optimise the final titre and protein expression of a cell culture. Further optimisation would be required for the Cyto-Mine to be a viable option for selection of new parental cell line, as higher recovery rates closer to 10-30% have been achieved by other groups (personal communication). Enhanced recovery could be achieved by investigating parameters such as different media formulations and additives to aid recovery.

Optimisation of transient transfection and FOG conditions resembles the approach taken to improve stable cell line processes, however transient expression systems contain the additional factor of the rDNA plasmid for transfection. It has been shown that plasmid copy number correlates with transient expression and is lost over time and cell divisions. Plasmid DNA is not faithfully transferred to daughter cells and instead is partially lost during the division event[57,171,172]. The titre improvements in TGE seen in the last 10 years are strongly related to the use of new systems and technologies to improve plasmid retention[35,57,173]. EBNA-1 expression in combination with an *oriP* containing plasmid is a widely used method to increase plasmid retention and improve titre, based on the ability of EBNA-1 to tether the plasmid to the host genome[174]. Linking chromosomes and plasmid allows increased transcription from the plasmid, and avoids the loss of plasmid over cell division, as EBNA-1 facilitates the replication and division of the plasmid to daughter cells. However, this system is not used to its full potential in CHO

cell lines: while plasmid retention is achieved in both CHO and human derived cell lines such as HEK, only in the latter is there plasmid replication[57,67]. A lack of plasmid replication means the total copy number per cell decreases with each cell division even if the existing plasmid is divided effectively minimizing the loss. Findings in this study agree with the lack of episomal replication in CHO cells, as plasmid was lost over time in actively dividing cells (Figure 34).

The EBV genome lacks the information to produce the proteins involved with DNA replication, instead EBNA-1 recruits the hosts own replication machinery to achieve plasmid replication. It has been found to interact with several key factors including the ORC which is essential to start the replication process[85,107]. The requirement for EBNA-1 to recruit and interact with host proteins as reported in the literature may be the cause of the lack of episomal replication in non-human cells. Proteins involved in DNA replication are highly conserved in different species, therefore it is plausible that non-human cell lines contain sufficiently different biosynthetic machinery for EBNA-1 to not recognise them. Therefore, in this study we evaluated the use of alternative episomal maintenance systems from the viruses KSHV and MHV68 with the aim to develop an alternative transient expression mechanism to EBNA-1/oriP, while also studying and comparing these to the performance of EBNA-1/oriP. As MHV68 naturally infects rodents, we theorised that the EBNA-1 homologue mLANA in combination with oriP homologue mTR could achieve plasmid replication alongside plasmid retention by successfully interacting with CHO cell replication machinery proteins.

EBNA-1 has a pleiotropic effect and is able to increase expression not only by achieving plasmid retention but also by increasing plasmid transport to the nucleus and acting as a transcription activator when bound to the FR domain of oriP[113]. This study found EBNA-1/oriP interaction to achieve higher mAb titres than the host cell line (Figure 39). Using EBNA-1 or an *oriP* containing plasmid individually did not increase the final mAb titre, which indicates EBNA-1 needs to interact with *oriP* to increase expression (Figure 38). The heightened expression, when measured as GFP median fluorescence intensity (MFI) with flow cytometry, was observed from day 1 which suggests an increase unrelated to plasmid maintenance over time. Alongside an increase in expression shortly after transfection, which could be explained by EBNA-1 acting as an expression enhancer when combined with *oriP*, GFP expression was maintained at a higher amount over time in comparison to cells without EBNA-1/oriP (Figure 35). The slowed decrease of expression in EBNA-1/oriP, especially under FOG conditions, indicates a functional plasmid maintenance system. The MFI for EBNA-1/oriP cells routinely passaged measured at day 5 post transfection showed a decrease in comparison to the MFI results on day 1 and on day 3; this decrease of expression over time could be explained either by an imperfect plasmid retention system, by the expected lack of plasmid replication, or a combination of both.

EBNA-1t is a truncated version of EBNA-1F, where the repeat DNA found in the centre of the protein is deleted. The internal repeat is responsible for inhibiting EBNA-1 transcription by forming stable tertiary mRNA structures, which relates to the viral strategy to evade the host's immune system. EBNA1-t was expected to maintain the same plasmid retention function of EBNA-1F while achieving higher expression levels, ultimately creating a cell line with an improved plasmid retention function over the EBNA-1F expressing cell lines. Unexpectedly, EBNA-1t did not show an increase in protein expression when compared to the original cell line not expressing an EMP (Figure 36). This absence of function could be due to a reduced effectivity in plasmid retention in comparison to EBNA-1 or to a lack of expression in the cell line. Cells transfected with EBNA-1t had lower culture viabilities under selection, and when using an alternative plasmid with puromycin selection they failed to recover at all (data not shown). This indicates EBNA-1t could be detrimental for 1-31 and A8 cells, which could result in only cells able to silence the integrated gene recovering.

This study did not observe a titre improvement attributable to the interaction between KSHV or MHV68 EMP and their respective RE (kLANA/kTR and mLANA/mTR), interaction which was expected to achieve plasmid retention and/or replication. When observing the loss rate of kTR and mTR containing plasmids this was the same as for those plasmids not containing any RE (Figure 34). However, the lack of detectable EMP expression (Figure 30, Figure 31, Figure 32) by 1-31 represents a severe limitation on drawing firm conclusions. Multiple reports in the available literature have shown the ability of these molecules to achieve plasmid retention and replication *in-vitro*[131,138,142,152,161], which would indicate the observed lack of episomal retention function by kLANA and mLANA observed in this investigation arises from the expression of the EMPs. It is also important to consider that those successful experiments found in the literature were not performed in CHO cells and some effects may be cell line dependent. The use of an indirect method (fluorescence levels of a short lived GFP measured with flow cytometry) to observe plasmid maintenance over time also shows limitations compared to more direct methods, such as Hirst plasmid purification and *DpnI* digestion, as when using an indirect method a low level of plasmid replication could be present but not detected, since it would still be represented by a decrease in d2EGFP signal over time. Furthermore, even though we were correlating d2EGFP with plasmid copy number, cells in FOG conditions could also change their behaviour and become more or less productive when exposed to the stress of a FOG or temperature shift.

Although no EMP/RE specific interaction other than EBNA-1/oriP was shown to provide the expected episomal retention, mTR unexpectedly showed a significant increase in mAb titre for all the cell lines independent from mLANA expression (Figure 38). Levels of protein expression achieved with mTR alone were comparable to those achieved by the well established system EBNA-1F/oriP. This increase

is not related to plasmid retention or replication, shown by the fact that the EMP protein was not necessary to increase the expression, and that the concentration of mTR containing plasmids decayed at the same rate as those without mTR as measured by the percentage of positive d2EGFP expressing cells overtime (Figure 34 C and Figure 35 C). This effect correlates with the ability of mTR to increase the expression of a gene of interest placed in the same plasmid, as reported in the literature[161]. When focusing on the final mAb titre, the mTR enhancement was observed in all cell lines but the mLANA expressing cell line derived from A8 showed the lowest final titre in comparison to the other A8 derived cell lines transfected with the mTR plasmid (Figure 39). The fact that the mLANA expressing cell line derived from A8 appears to be an exception could be surprising, however mLANA has been found to repress mTR related enhancement[161]. This fact is understandable when thought of in the context of MHV68 infecting the host's cell, as a way to evade the immune system: mTR controls expression of mLANA *in vivo* as it contains a promoter for mLANA's open reading frame (ORF). Higher expression of this EMP in the infected cells could lead to the detection of the protein by the host's MHC I, therefore mLANA inhibits its own expression by interacting with mTR; this achieves a controlled reduced level of mLANA expression and evasion from the host immune system [88,175]. This could explain the negative effect of mLANA in mTR related increase in GFP and mAb expression, however the mLANA expressing cell line derived from 1-31 does not present such inhibition. The 1-31 derived mLANA expressing cell line instead showed an increase in expression when transfected with a plasmid containing mTR similar to all other cell lines derived from 1-31. A potential explanation for this difference between both mLANA expressing cell lines, A8 and 1-31 derived, could be a simple lack of mLANA expression in 1-31 and a low level of expression in A8.

We were unable to confirm mLANA expression in both stable cell lines by western blot or qRT-PCR (results not shown), therefore conclusions cannot be drawn from this. However, mLANA repression of mTR is mLANA dose dependent[152], and A8 has been shown to be more productive for mAb expression than 1-31 (Figure 17). This may result in higher EMP expression in A8 cell lines compared to 1-31 cell lines. A higher expression of mLANA could lead to a stronger repression by mLANA of the mTR enhancement, leading to a lower increase in titre by mTR.

The fact that mLANA can inhibit its own expression by interacting with mTR was overlooked at the beginning of this project and could explain the lack of mLANA transient expression in 1-31 while it was successfully expressed in CHO3E7 (Figure 23). The plasmid used in 1-31 contained mLANA in the same vector as the mMRE, a region of the mTR, while the mLANA sequence was cloned in the standard pTT5 with *oriP* for CHO3E7. Although MHV68-MRE has not been linked to reduced expression of a gene situated in the same plasmid, mMRE includes the mLBS found in the mTR[159,161]. Deletion of this binding site from mTR results in a complete abrogation of the mLANA repressive effect on mTR expression

enhancement[161]. The mechanisms by which mLANA inhibits mTR effect on expression have not been defined and the ability of the MHV68-MRE to affect gene expression has not been studied. However, in light of the existing knowledge, it seems reasonable that the MHV68-MRE combined with mLANA may inhibit expression of the gene of interest contained in the same vector, in this case mLANA itself.

Although mTR increased mAb expression in all the cell lines where it was tested, the highest titre was achieved when combined with kLANA (Figure 39). A potential explanation for kLANA/mTR achieving the highest titre from all the combinations in this experiment is that kLANA may be able to bind to mTR and achieve a low degree of episomal maintenance. mLANA and kLANA are similar in structure, though not in amino acid sequence[155,158,159]. They have been shown to be able to interact and function with the other's TR (mLANA/kTR and kLANA/mTR)[176], although the way they interact and shape/conformation of the DNA when bound to the TR is different; kLANA creates a bend in the DNA while mLANA does not[160]. This difference in conformation after binding could explain why the kLANA/mTR interaction did not show inhibition of the mTR expression enhancement.

One of the possible explanations for mLANA inhibition of mTR enhancement is by mLANA interacting with certain host proteins, either by direct interaction or by binding to the mLBS sequences and blocking their interaction with mTR relevant host proteins, or blocking necessary proteins from binding to the DNA. kLANA may simply be unable to bind to the CHO cell genome, since KSHV exclusively infects humans and the proteins implicated in this process may be too different in the 2 species and the required complementary binding sequences may be absent in CHO cells. This concept is based on several hypotheses that would require further assessment. kLANA expression, for example, has not been confirmed. Potentially, kLANA may not be present and the higher titre could be a result of normal cell line to cell line variation. Furthermore, kLANA has shown no effect on titre when kTR plasmid was used. This could be related to plasmid design with kTR, as in some cases it has been observed that 2 kTR are necessary for episomal maintenance, although some effective short-term plasmid replication with only KSHV-MRE has also been shown[138,142,152] or to a simple lack of kLANA expression.

The method by which mTR is able to enhance expression has not been defined in literature, however it seems clear the effect is not related to episomal retention. This leaves the door open to pairing this sequence with *oriP* in the same plasmid to further increase expression achieved in the EBNA-1 cell line.

# 5 Future work

An essential piece of information that would be required to reach further conclusions is the expression level, if any, of the various EMPs of interest. A qRT-PCR method to evaluate this was investigated,

however it was not possible to generate conclusive data in the available time. The next step to continue this work would be to evaluate the presence of mRNA that encode for the proteins of interest. In the case of EMPs, the presence of mRNA does not necessarily correlate with protein expression, as they are known to inhibit their own transcription to avoid the immune system. Further work should thus also focus on confirming protein detection/expression by western blot by evaluating other detection antibodies or increasing the amount of total protein used in case the low amount of EMP was the cause of the lack of signal. Proteomic mass spectrometry approaches could also be used to determine if the proteins were present. Relating to the self-inhibition of EMPs, it would be possible to modify the proteins and delete the regions responsible for self-inhibition, potentially increasing the titre, as achieved with EBNA-1.

It is possible that the EMPs are not being expressed, which could be related to gene silencing in the stable cell lines or that only very low expressing cell lies survive the selection process and the proteins are toxic to CHO cells. It would be interesting to further explore co-transfecting the EMPs transiently and using other methods to generate stable cell lines. The use of GS/MSX selection generally results in higher titres[23], and it would be possible to add insulators to avoid gene silencing [177]. This approach could also be useful even in the creation of EBNA-1F expressing stable cell lines, which was already found to improve transient expression when paired with an *oriP* containing plasmid in this work despite the potential low level of expression. Higher EBNA-1F levels have been shown to correlate with enhanced plasmid retention and increase in transient expression when used for that purpose[173,178]. Generating a cell line with a higher constitutive expression of EBNA-1F using a GS/MSX based selection could lead to improved TGE. It would also be possible to use single cell cloning to identify an EBNA-1 positive high expressing clonal cell line, and another option to increase EBNA-1F is to attempt to avoid the stable mRNA G-quadruplex structures which cause a decrease in transcription. This has previously been achieved by codon optimisation to avoid the specific mRNA patterns without changing the amino acid sequence[87]. This approach could also be attempted with both kLANA and mLANA, as kLANA has an extended region with similar structure and function to EBNA-1's gly-gly-ala repeat, responsible for the self-inhibition[88].

The discovery of the effects of mTR on overall titre was a welcome surprise that needs to be explored further to evaluate its potential and limits. In the short term, it would be interesting to see if the same effect is seen in human cell lines or if it is specific to CHO and rodent cell lines, as that could give some insight into its function. We demonstrated that mTR can increase expression in transient expression and it would therefore be interesting to evaluate if this translates to stable cell lines or if it is only beneficial in extrachromosomal plasmids, which correlates with known biology since MHV68 exists as an extrachromosomal episome in infected cells. More options for further research involve evaluating

if the effect of incorporating more than 1 mTR in the plasmid has an additive effect on expression, whether using truncated versions of mTR would achieve the same effect, and if the location within the plasmid is relevant. The most interesting potential work is to evaluate if mTR can be combined with the EBNA-1/oriP system to further increase the titres achieved in this project.

Although cell and vector engineering are certainly interesting pathways to try and improve a TE platform, there is also room for further bioprocess improvement. The transfection conditions did not achieve good results with high cell concentrations and it would be interesting to try different ratios, incubation times or even PEI addition methods. This could involve the more recently developed direct method, which involves adding DNA and then PEI to the culture in consecutive steps, which has shown interesting results[162,167]. Furthermore, the transfection was optimised for 1-31 however as it has been stated each cell line requires optimisation. Although A8 is closely related to 1-31, it would be necessary to reassess the optimal transfection conditions for A8.

The FOG conditions were not further optimised after the first experiment. A more meticulous study of the culture conditions, including lactate, $O_2$ and glucose level over time would be able to give more insight into the ways to optimise the feeds and feed routine. Viability was seen to decrease rapidly in FOG condition 1, therefore adding a temperature shift prior to this could be a simple method to increase productivity.

# 6 Conclusions

In summary, the results presented here do not rule out that mLANA or kLANA may be potential approaches to improve current TGE platforms. Further research is needed to determine if this is the case and the expression of these molecules needs to be confirmed and assessed, which has proven difficult to achieve in this study. We have been able to show that EBNA-1F/oriP is a valuable modification to increase expression in TGE platforms, however we have also highlighted room for improvement due to the lack of plasmid replication in CHO cells. We believe evaluating alternative viral systems that can naturally maintain episomes in infected host cells represents a useful approach to further improve existing systems that has only been superficially explored until now. The unexpected role of mTR as an expression enhancer demonstrates that after 20 years of research there are still undiscovered, novel ways to improve current platforms.

Overall, we have been able to create a TGE platform from a CHO cell line developed for manufacturing, which is able to transiently express sufficient material for the early stages of research and with the potential for the system to be improved to reach expression levels currently seen in other TGEs. This project has therefore succeeded in its primary aim, namely improving productivity of the 1-31 cell line through development of a novel TGE platform. Several key variables were evaluated including

transfection conditions, FOG conditions, and plasmid retention methods, each factor improving titre several fold. There have been limitations, most notably the inability to accurately assess the expression level of EMPs within the cell lines of interest. Viral proteins present unique challenges to work with in their complex and repetitive sequence, which complicated and delayed key components of this study. However, the evaluation of novel concepts has led to the discovery of mTR as a potential element for vector engineering. Further analysis will be required to completely assess the utility of MHV68 and KSHV viral episome retention systems for TGE platforms, but this study has demonstrated the potential of these system and represents a first step towards exploring novel alternatives based on viral systems.

# 7 Bibliography


(1) (Rob) Aggarwal, S. What's Fueling the Biotech Engine—2012 to 2013. *Nat. Biotechnol.* **2014**, *32* (1), 32–39. https://doi.org/10.1038/nbt.2794.

(2) Zheng, K.; Bantog, C.; Bayer, R. The Impact of Glycosylation on Monoclonal Antibody Conformation and Stability. *mAbs* **2011**, *3* (6), 568–576. https://doi.org/10.4161/mabs.3.6.17922.

(3) Chiu, M. L.; Goulet, D. R.; Teplyakov, A.; Gilliland, G. L. Antibody Structure and Function: The Basis for Engineering Therapeutics. *Antibodies* **2019**, *8* (4). https://doi.org/10.3390/antib8040055.

(4) Dealmakers, B. Moving up with the Monoclonals. *Biopharma Deal.* **2019**. https://doi.org/10.1038/d43747-020-00765-2.

(5) Lu, R.-M.; Hwang, Y.-C.; Liu, I.-J.; Lee, C.-C.; Tsai, H.-Z.; Li, H.-J.; Wu, H.-C. Development of Therapeutic Antibodies for the Treatment of Diseases. *J. Biomed. Sci.* **2020**, *27* (1), 1. https://doi.org/10.1186/s12929-019-0592-z.

(6) Antibody therapeutics approved or in regulatory review in the EU or US https://www.antibodysociety.org/resources/approved-antibodies/ (accessed Jan 28, 2021).

(7) Kaplon, H.; Reichert, J. M. Antibodies to Watch in 2021. *mAbs* **2021**, *13* (1), 1860476. https://doi.org/10.1080/19420862.2020.1860476.

(8) Novak, J. C.; Lovett-Racke, A. E.; Racke, M. K. Monoclonal Antibody Therapies and Neurologic Disorders. *Arch. Neurol.* **2008**, *65* (9). https://doi.org/10.1001/archneur.65.9.1162.

(9) Retinal Physician - New Monoclonal Antibody Treatments in Retina https://www.retinalphysician.com/issues/2017/june-2017/new-monoclonal-antibody-treatments-in-retina (accessed Feb 4, 2021).

(10) Rasetti-Escargueil, C.; Popoff, M. R. Antibodies and Vaccines against Botulinum Toxins: Available Measures and Novel Approaches. *Toxins* **2019**, *11* (9). https://doi.org/10.3390/toxins11090528.

(11) Nair, A. S. Tanezumab: Finally a Monoclonal Antibody for Pain Relief. *Indian J. Palliat. Care* **2018**, *24* (3), 384–385. https://doi.org/10.4103/IJPC.IJPC_208_17.

(12) Palomares, L. A.; Estrada-Moncada, S.; Ramírez, O. T. Production of Recombinant Proteins. In *Recombinant Gene Expression: Reviews and Protocols*; Balbás, P., Lorence, A., Eds.; Methods in Molecular Biology; Humana Press: Totowa, NJ, 2004; pp 15–51. https://doi.org/10.1385/1-59259-774-2:015.

(13) Burgenson, D.; Gurramkonda, C.; Pilli, M.; Ge, X.; Andar, A.; Kostov, Y.; Tolosa, L.; Rao, G. Rapid Recombinant Protein Expression in Cell-Free Extracts from Human Blood. *Sci. Rep.* **2018**, *8* (1). https://doi.org/10.1038/s41598-018-27846-8.

(14) Walsh, G.; Jefferis, R. Post-Translational Modifications in the Context of Therapeutic Proteins. *Nat. Biotechnol.* **2006**, *24* (10), 1241–1252. https://doi.org/10.1038/nbt1252.

(15) Schroeder, H. W.; Cavacini, L. Structure and Function of Immunoglobulins. *J. Allergy Clin. Immunol.* **2010**, *125* (2 0 2), S41–S52. https://doi.org/10.1016/j.jaci.2009.09.046.

(16) Kimball, J. A.; Norman, D. J.; Shield, C. F.; Schroeder, T. J.; Lisi, P.; Garovoy, M.; O'Connell, J. B.; Stuart, F.; McDiarmid, S. V.; Wall, W. The OKT3 Antibody Response Study: A Multicentre Study of Human Anti-Mouse Antibody (HAMA) Production Following OKT3 Use in Solid Organ Transplantation. *Transpl. Immunol.* **1995**, *3* (3), 212–221. https://doi.org/10.1016/0966-3274(95)80027-1.

(17) Butler, M.; Spearman, M. The Choice of Mammalian Cell Host and Possibilities for Glycosylation Engineering. *Curr. Opin. Biotechnol.* **2014**, *30*, 107–112. https://doi.org/10.1016/j.copbio.2014.06.010.

(18) Durocher, Y.; Butler, M. Expression Systems for Therapeutic Glycoprotein Production. *Curr. Opin. Biotechnol.* **2009**, *20* (6), 700–707. https://doi.org/10.1016/j.copbio.2009.10.008.
(19) Wurm, F. M. CHO Quasispecies—Implications for Manufacturing Processes. *Processes* **2013**, *1* (3), 296–311. https://doi.org/10.3390/pr1030296.
(20) Monoclonal Antibodies Approved by the EMA and FDA for Therapeutic Use – ACTIP.
(21) Lewis, N. E.; Liu, X.; Li, Y.; Nagarajan, H.; Yerganian, G.; O'Brien, E.; Bordbar, A.; Roth, A. M.; Rosenbloom, J.; Bian, C.; Xie, M.; Chen, W.; Li, N.; Baycin-Hizal, D.; Latif, H.; Forster, J.; Betenbaugh, M. J.; Famili, I.; Xu, X.; Wang, J.; Palsson, B. O. Genomic Landscapes of Chinese Hamster Ovary Cell Lines as Revealed by the Cricetulus Griseus Draft Genome. *Nat. Biotechnol.* **2013**, *31* (8), 759–767. https://doi.org/10.1038/nbt.2624.
(22) Alt, F.; Kellems, R.; Bertino, J.; Schimke, R. Selective Multiplication of Dihydrofolate Reductase Genes in Methotrexate-Resistant Variants of Cultured Murine Cells. *J. Biol. Chem.* **1978**, *253*, 1357–1370. https://doi.org/10.1016/S0021-9258(17)34875-5.
(23) Jiang, Z.; Huang, Y.; Sharfstein, S. T. Regulation of Recombinant Monoclonal Antibody Production in Chinese Hamster Ovary Cells: A Comparative Study of Gene Copy Number, MRNA Level, and Protein Expression. *Biotechnol. Prog.* **2006**, *22* (1), 313–318. https://doi.org/10.1021/bp0501524.
(24) Huang, Y.-M.; Hu, W.; Rustandi, E.; Chang, K.; Yusuf-Makagiansar, H.; Ryll, T. Maximizing Productivity of CHO Cell-Based Fed-Batch Culture Using Chemically Defined Media Conditions and Typical Manufacturing Equipment. *Biotechnol. Prog.* **2010**, *26* (5), 1400–1410. https://doi.org/10.1002/btpr.436.
(25) Bailey, L. A.; Hatton, D.; Field, R.; Dickson, A. J. Determination of Chinese Hamster Ovary Cell Line Stability and Recombinant Antibody Expression during Long-Term Culture. *Biotechnol. Bioeng.* **2012**, *109* (8), 2093–2103. https://doi.org/10.1002/bit.24485.
(26) Wurm, F. M. Production of Recombinant Protein Therapeutics in Cultivated Mammalian Cells. *Nat. Biotechnol.* **2004**, *22* (11), 1393–1398. https://doi.org/10.1038/nbt1026.
(27) Kelley, B. Developing Therapeutic Monoclonal Antibodies at Pandemic Pace. *Nat. Biotechnol.* **2020**, 1–6. https://doi.org/10.1038/s41587-020-0512-5.
(28) Stuible, M.; van Lier, F.; Croughan, M. S.; Durocher, Y. Beyond Preclinical Research: Production of CHO-Derived Biotherapeutics for Toxicology and Early-Phase Trials by Transient Gene Expression or Stable Pools. *Curr. Opin. Chem. Eng.* **2018**, *22*, 145–151. https://doi.org/10.1016/j.coche.2018.09.010.
(29) Wilkinson, I. The Importance of Transient Antibody Expression in a Pandemic Response. *GEN - Genetic Engineering and Biotechnology News*, 2020.
(30) Liu, C.; Zhou, Q.; Li, Y.; Garner, L. V.; Watkins, S. P.; Carter, L. J.; Smoot, J.; Gregg, A. C.; Daniels, A. D.; Jervey, S.; Albaiu, D. Research and Development on Therapeutic Agents and Vaccines for COVID-19 and Related Human Coronavirus Diseases. *ACS Cent. Sci.* **2020**, *6* (3), 315–331. https://doi.org/10.1021/acscentsci.0c00272.
(31) Cartwright, J. F.; Anderson, K.; Longworth, J.; Lobb, P.; James, D. C. Highly Sensitive Detection of Mutations in CHO Cell Recombinant DNA Using Multi-Parallel Single Molecule Real-Time DNA Sequencing. *Biotechnol. Bioeng.* **2018**, *115* (6), 1485–1498. https://doi.org/10.1002/bit.26561.
(32) Patel, N. A.; Anderson, C. R.; Terkildsen, S. E.; Davis, R. C.; Pack, L. D.; Bhargava, S.; Clarke, H. R. G. Antibody Expression Stability in CHO Clonally-Derived Cell Lines and Their Subclones: Role of Methylation in Phenotypic and Epigenetic Heterogeneity. *Biotechnol. Prog.* **2018**. https://doi.org/10.1002/btpr.2655.
(33) Girard, P.; Derouazi, M.; Baumgartner, G.; Bourgeois, M.; Jordan, M.; Jacko, B.; Wurm, F. M. 100-Liter Transient Transfection. *Cytotechnology* **2002**, *38* (1–3), 15–21. https://doi.org/10.1023/A:1021173124640.

(34) Wulhfard, S.; Baldi, L.; Hacker, D. L.; Wurm, F. Valproic Acid Enhances Recombinant MRNA and Protein Levels in Transiently Transfected Chinese Hamster Ovary Cells. *J. Biotechnol.* **2010**, *148* (2), 128–132. https://doi.org/10.1016/j.jbiotec.2010.05.003.

(35) Daramola, O.; Stevenson, J.; Dean, G.; Hatton, D.; Pettman, G.; Holmes, W.; Field, R. A High-Yielding CHO Transient System: Coexpression of Genes Encoding EBNA-1 and GS Enhances Transient Protein Expression. *Biotechnol. Prog.* **2014**, *30* (1), 132–141. https://doi.org/10.1002/btpr.1809.

(36) Tait, A. S.; Brown, C. J.; Galbraith, D. J.; Hines, M. J.; Hoare, M.; Birch, J. R.; James, D. C. Transient Production of Recombinant Proteins by Chinese Hamster Ovary Cells Using Polyethyleneimine/DNA Complexes in Combination with Microtubule Disrupting Anti-Mitotic Agents. *Biotechnol. Bioeng.* **2004**, *88* (6), 707–721. https://doi.org/10.1002/bit.20265.

(37) Rajendra, Y.; Kiseljak, D.; Baldi, L.; Hacker, D. L.; Wurm, F. M. A Simple High-Yielding Process for Transient Gene Expression in CHO Cells. *J. Biotechnol.* **2011**, *153* (1–2), 22–26. https://doi.org/10.1016/j.jbiotec.2011.03.001.

(38) Zhong, X.; Ma, W.; Meade, C. L.; Tam, A. S.; Llewellyn, E.; Cornell, R.; Cote, K.; Scarcelli, J. J.; Marshall, J. K.; Tzvetkova, B.; Figueroa, B.; DiNino, D.; Sievers, A.; Lee, C.; Guo, J.; Mahan, E.; Francis, C.; Lam, K.; D'Antona, A. M.; Zollner, R.; Zhu, H. L.; Kriz, R.; Somers, W.; Lin, L. Transient CHO Expression Platform for Robust Antibody Production and Its Enhanced N-Glycan Sialylation on Therapeutic Glycoproteins. *Biotechnol. Prog.* **2019**, *35* (1), e2724. https://doi.org/10.1002/btpr.2724.

(39) Stuible, M.; Burlacu, A.; Perret, S.; Brochu, D.; Paul-Roc, B.; Baardsnes, J.; Loignon, M.; Grazzini, E.; Durocher, Y. Optimization of a High-Cell-Density Polyethylenimine Transfection Method for Rapid Protein Production in CHO-EBNA1 Cells. *J. Biotechnol.* **2018**, *281*, 39–47. https://doi.org/10.1016/j.jbiotec.2018.06.307.

(40) Gutiérrez-Granados, S.; Cervera, L.; Kamen, A. A.; Gòdia, F. Advancements in Mammalian Cell Transient Gene Expression (TGE) Technology for Accelerated Production of Biologics. *Crit. Rev. Biotechnol.* **2018**, *38* (6), 918–940. https://doi.org/10.1080/07388551.2017.1419459.

(41) CHO Cell Engineering for Improved Process Performance and Product Quality - Cell Culture Engineering - Wiley Online Library https://onlinelibrary.wiley.com/doi/pdf/10.1002/9783527811410.ch9?saml_referrer (accessed Jan 31, 2021).

(42) Girard, P.; Porte, L.; Berta, T.; Jordan, M.; Wurm, F. M. Calcium Phosphate Transfection Optimization for Serum-Free Suspension Culture. *Cytotechnology* **2001**, *35* (3), 175–180. https://doi.org/10.1023/A:1013101927350.

(43) Pham, P. L.; Kamen, A.; Durocher, Y. Large-Scale Transfection of Mammalian Cells for the Fast Production of Recombinant Protein. *Mol. Biotechnol.* **2006**, *34* (2), 225–237. https://doi.org/10.1385/MB:34:2:225.

(44) Dalby, B.; Cates, S.; Harris, A.; Ohki, E. C.; Tilkins, M. L.; Price, P. J.; Ciccarone, V. C. Advanced Transfection with Lipofectamine 2000 Reagent: Primary Neurons, SiRNA, and High-Throughput Applications. *Methods* **2004**, *33* (2), 95–103. https://doi.org/10.1016/j.ymeth.2003.11.023.

(45) Boussif, O.; Lezoualc'h, F.; Zanta, M. A.; Mergny, M. D.; Scherman, D.; Demeneix, B.; Behr, J. P. A Versatile Vector for Gene and Oligonucleotide Transfer into Cells in Culture and in Vivo: Polyethylenimine. *Proc. Natl. Acad. Sci. U. S. A.* **1995**, *92* (16), 7297–7301.

(46) Steger, K.; Brady, J.; Wang, W.; Duskin, M.; Donato, K.; Peshwa, M. CHO-S Antibody Titers >1 Gram/Liter Using Flow Electroporation-Mediated Transient Gene Expression Followed by Rapid Migration to High-Yield Stable Cell Lines. *J. Biomol. Screen.* **2015**, *20* (4), 545–551. https://doi.org/10.1177/1087057114563494.

(47) Jaeger, V.; Büssow, K.; Schirrmann, T. Transient Recombinant Protein Expression in Mammalian Cells; 2015. https://doi.org/10.1007/978-3-319-10320-4_2.
(48) Wulhfard, S.; Tissot, S.; Bouchet, S.; Cevey, J.; De Jesus, M.; Hacker, D. L.; Wurm, F. M. Mild Hypothermia Improves Transient Gene Expression Yields Several Fold in Chinese Hamster Ovary Cells. *Biotechnol. Prog.* **2008**, *24* (2), 458–465. https://doi.org/10.1021/bp070286c.
(49) Backliwal, G.; Hildinger, M.; Kuettel, I.; Delegrange, F.; Hacker, D. L.; Wurm, F. M. Valproic Acid: A Viable Alternative to Sodium Butyrate for Enhancing Protein Expression in Mammalian Cell Cultures. *Biotechnol. Bioeng.* **2008**, *101* (1), 182–189. https://doi.org/10.1002/bit.21882.
(50) Carvalhal, A. V.; Santos, S. S.; Calado, J.; Haury, M.; Carrondo, M. J. T. Cell Growth Arrest by Nucleotides, Nucleosides and Bases as a Tool for Improved Production of Recombinant Proteins. *Biotechnol. Prog.* **2003**, *19* (1), 69–83. https://doi.org/10.1021/bp0255917.
(51) Sun, X.; Goh, P. E.; Wong, K. T. K.; Mori, T.; Yap, M. G. S. Enhancement of Transient Gene Expression by Fed-Batch Culture of HEK 293 EBNA1 Cells in Suspension. *Biotechnol. Lett.* **2006**, *28* (11), 843–848. https://doi.org/10.1007/s10529-006-9010-1.
(52) Pham, P. L.; Perret, S.; Cass, B.; Carpentier, E.; St-Laurent, G.; Bisson, L.; Kamen, A.; Durocher, Y. Transient Gene Expression in HEK293 Cells: Peptone Addition Posttransfection Improves Recombinant Protein Synthesis. *Biotechnol. Bioeng.* **2005**, *90* (3), 332–344. https://doi.org/10.1002/bit.20428.
(53) Santoro, R.; Lienemann, P.; Fussenegger, M. Epigenetic Engineering of Ribosomal RNA Genes Enhances Protein Production. *PLOS ONE* **2009**, *4* (8), e6653. https://doi.org/10.1371/journal.pone.0006653.
(54) Ku, S. C. Y.; Ng, D. T. W.; Yap, M. G. S.; Chao, S.-H. Effects of Overexpression of X-Box Binding Protein 1 on Recombinant Protein Production in Chinese Hamster Ovary and NS0 Myeloma Cells. *Biotechnol. Bioeng.* **2008**, *99* (1), 155–164. https://doi.org/10.1002/bit.21562.
(55) Matsuyama, R.; Yamano, N.; Kawamura, N.; Omasa, T. Lengthening of High-Yield Production Levels of Monoclonal Antibody-Producing Chinese Hamster Ovary Cells by Downregulation of Breast Cancer 1. *J. Biosci. Bioeng.* **2017**, *123* (3), 382–389. https://doi.org/10.1016/j.jbiosc.2016.09.006.
(56) Pieper, L. A.; Strotbek, M.; Wenger, T.; Olayioye, M. A.; Hausser, A. ATF6β-Based Fine-Tuning of the Unfolded Protein Response Enhances Therapeutic Antibody Productivity of Chinese Hamster Ovary Cells. *Biotechnol. Bioeng.* **2017**, *114* (6), 1310–1318. https://doi.org/10.1002/bit.26263.
(57) Kunaparaju, R.; Liao, M.; Sunstrom, N.-A. Epi-CHO, an Episomal Expression System for Recombinant Protein Production in CHO Cells. *Biotechnol. Bioeng.* **2005**, *91* (6), 670–677. https://doi.org/10.1002/bit.20534.
(58) Ceccarelli, D. F. J.; Frappier, L. Functional Analyses of the EBNA1 Origin DNA Binding Protein of Epstein-Barr Virus. *J. Virol.* **2000**, *74* (11), 4939–4948.
(59) Denis Burkitt and the African lymphoma https://www.ncbi.nlm.nih.gov/pmc/articles/PMC3224008/?report=classic (accessed Feb 1, 2021).
(60) Epstein, M. A.; Achong, B. G.; Barr, Y. M. VIRUS PARTICLES IN CULTURED LYMPHOBLASTS FROM BURKITT'S LYMPHOMA. *The Lancet* **1964**, *283* (7335), 702–703. https://doi.org/10.1016/S0140-6736(64)91524-7.
(61) Raab-Traub, N. EBV-Induced Oncogenesis. In *Human Herpesviruses: Biology, Therapy, and Immunoprophylaxis*; Arvin, A., Campadelli-Fiume, G., Mocarski, E., Moore, P. S., Roizman, B., Whitley, R., Yamanishi, K., Eds.; Cambridge University Press: Cambridge, 2007.
(62) Baumforth, K. R.; Young, L. S.; Flavell, K. J.; Constandinou, C.; Murray, P. G. The Epstein-Barr Virus and Its Association with Human Cancers. *Mol. Pathol.* **1999**, *52* (6), 307–322.
(63) Baer, R.; Bankier, A. T.; Biggin, M. D.; Deininger, P. L.; Farrell, P. J.; Gibson, T. J.; Hatfull, G.; Hudson, G. S.; Satchwell, S. C.; Séguin, C. DNA Sequence and Expression of the B95-8

Epstein-Barr Virus Genome. *Nature* **1984**, *310* (5974), 207–211. https://doi.org/10.1038/310207a0.
(64) Kieff, E. Epstein-Barr Virus and Its Replication. *Fields Virol.* **1996**, 2343–2396.
(65) Nemerow, G. R.; Mold, C.; Schwend, V. K.; Tollefson, V.; Cooper, N. R. Identification of Gp350 as the Viral Glycoprotein Mediating Attachment of Epstein-Barr Virus (EBV) to the EBV/C3d Receptor of B Cells: Sequence Homology of Gp350 and C3 Complement Fragment C3d. *J. Virol.* **1987**, *61* (5), 1416–1420. https://doi.org/10.1128/JVI.61.5.1416-1420.1987.
(66) Alternate replication in B cells and epithelial cells switches tropism of Epstein–Barr virus | Nature Medicine https://www.nature.com/articles/nm0602-594 (accessed Feb 1, 2021).
(67) Jones, K.; Rivera, C.; Sgadari, C.; Franklin, J.; Max, E. E.; Bhatia, K.; Tosato, G. Infection of Human Endothelial Cells with Epstein-Barr Virus. *J. Exp. Med.* **1995**, *182* (5), 1213–1221. https://doi.org/10.1084/jem.182.5.1213.
(68) Skalsky, R. L.; Cullen, B. R. EBV Noncoding RNAs. *Curr. Top. Microbiol. Immunol.* **2015**, *391*, 181–217. https://doi.org/10.1007/978-3-319-22834-1_6.
(69) Shannon-Lowe, C.; Rowe, M. Epstein-Barr Virus Infection of Polarized Epithelial Cells via the Basolateral Surface by Memory B Cell-Mediated Transfer Infection. *PLoS Pathog.* **2011**, *7* (5). https://doi.org/10.1371/journal.ppat.1001338.
(70) Heath, E.; Begue-Pastor, N.; Chaganti, S.; Croom-Carter, D.; Shannon-Lowe, C.; Kube, D.; Feederle, R.; Delecluse, H.-J.; Rickinson, A. B.; Bell, A. I. Epstein-Barr Virus Infection of Naïve B Cells In Vitro Frequently Selects Clones with Mutated Immunoglobulin Genotypes: Implications for Virus Biology. *PLoS Pathog.* **2012**, *8* (5). https://doi.org/10.1371/journal.ppat.1002697.
(71) Babcock, G. J.; Hochberg, D.; Thorley-Lawson, A. D. The Expression Pattern of Epstein-Barr Virus Latent Genes in Vivo Is Dependent upon the Differentiation Stage of the Infected B Cell. *Immunity* **2000**, *13* (4), 497–506. https://doi.org/10.1016/s1074-7613(00)00049-2.
(72) Kenney, S. C. Reactivation and Lytic Replication of EBV. In *Human Herpesviruses: Biology, Therapy, and Immunoprophylaxis*; Arvin, A., Campadelli-Fiume, G., Mocarski, E., Moore, P. S., Roizman, B., Whitley, R., Yamanishi, K., Eds.; Cambridge University Press: Cambridge, 2007.
(73) Lupton, S.; Levine, A. J. Mapping Genetic Elements of Epstein-Barr Virus That Facilitate Extrachromosomal Persistence of Epstein-Barr Virus-Derived Plasmids in Human Cells. *Mol. Cell. Biol.* **1985**, *5* (10), 2533–2542.
(74) Rawlins, D. R.; Milman, G.; Hayward, S. D.; Hayward, G. S. Sequence-Specific DNA Binding of the Epstein-Barr Virus Nuclear Antigen (EBNA-1) to Clustered Sites in the Plasmid Maintenance Region. *Cell* **1985**, *42* (3), 859–868. https://doi.org/10.1016/0092-8674(85)90282-x.
(75) Hussain, M.; Gatherer, D.; Wilson, J. B. Modelling the Structure of Full-Length Epstein–Barr Virus Nuclear Antigen 1. *Virus Genes* **2014**, *49* (3), 358–372. https://doi.org/10.1007/s11262-014-1101-9.
(76) Bochkarev, A.; Bochkareva, E.; Frappier, L.; Edwards, A. M. The 2.2 A Structure of a Permanganate-Sensitive DNA Site Bound by the Epstein-Barr Virus Origin Binding Protein, EBNA1. *J. Mol. Biol.* **1998**, *284* (5), 1273–1278. https://doi.org/10.1006/jmbi.1998.2247.
(77) Mackey, D.; Sugden, B. The Linking Regions of EBNA1 Are Essential for Its Support of Replication and Transcription. *Mol. Cell. Biol.* **1999**, *19* (5), 3349–3359. https://doi.org/10.1128/MCB.19.5.3349.
(78) Sears, J.; Ujihara, M.; Wong, S.; Ott, C.; Middeldorp, J.; Aiyar, A. The Amino Terminus of Epstein-Barr Virus (EBV) Nuclear Antigen 1 Contains AT Hooks That Facilitate the Replication and Partitioning of Latent EBV Genomes by Tethering Them to Cellular Chromosomes. *J. Virol.* **2004**, *78* (21), 11487–11505. https://doi.org/10.1128/JVI.78.21.11487-11505.2004.

(79) Shire, K.; Ceccarelli, D. F. J.; Avolio-Hunter, T. M.; Frappier, L. EBP2, a Human Protein That Interacts with Sequences of the Epstein-Barr Virus Nuclear Antigen 1 Important for Plasmid Maintenance. *J. Virol.* **1999**, *73* (4), 2587–2595.

(80) Kapoor, P.; Lavoie, B. D.; Frappier, L. EBP2 Plays a Key Role in Epstein-Barr Virus Mitotic Segregation and Is Regulated by Aurora Family Kinases. *Mol. Cell. Biol.* **2005**, *25* (12), 4934–4945. https://doi.org/10.1128/MCB.25.12.4934-4945.2005.

(81) Jourdan, N.; Jobart-Malfait, A.; Reis, G. D.; Quignon, F.; Piolot, T.; Klein, C.; Tramier, M.; Coppey-Moisan, M.; Marechal, V. Live-Cell Imaging Reveals Multiple Interactions between Epstein-Barr Virus Nuclear Antigen 1 and Cellular Chromatin during Interphase and Mitosis. *J. Virol.* **2012**, *86* (9), 5314–5329. https://doi.org/10.1128/JVI.06303-11.

(82) Chen, Y.-L.; Liu, C.-D.; Cheng, C.-P.; Zhao, B.; Hsu, H.-J.; Shen, C.-L.; Chiu, S.-J.; Kieff, E.; Peng, C. Nucleolin Is Important for Epstein–Barr Virus Nuclear Antigen 1-Mediated Episome Binding, Maintenance, and Transcription. *Proc. Natl. Acad. Sci.* **2014**, *111* (1), 243–248. https://doi.org/10.1073/pnas.1321800111.

(83) Deschamps, T.; Bazot, Q.; Leske, D. M.; MacLeod, R.; Mompelat, D.; Tafforeau, L.; Lotteau, V.; Maréchal, V.; Baillie, G. S.; Gruffat, H.; Wilson, J. B.; Manet, E. Epstein-Barr Virus Nuclear Antigen 1 Interacts with Regulator of Chromosome Condensation 1 Dynamically throughout the Cell Cycle. *J. Gen. Virol.* **2017**, *98* (2), 251–265. https://doi.org/10.1099/jgv.0.000681.

(84) Norseen, J.; Johnson, F. B.; Lieberman, P. M. Role for G-Quadruplex RNA Binding by Epstein-Barr Virus Nuclear Antigen 1 in DNA Replication and Metaphase Chromosome Attachment. *J. Virol.* **2009**, *83* (20), 10336–10346. https://doi.org/10.1128/JVI.00747-09.

(85) Bashaw, J. M.; Yates, J. L. Replication from OriP of Epstein-Barr Virus Requires Exact Spacing of Two Bound Dimers of EBNA1 Which Bend DNA. *J. Virol.* **2001**, *75* (22), 10603–10611. https://doi.org/10.1128/JVI.75.22.10603-10611.2001.

(86) Norseen, J.; Thomae, A.; Sridharan, V.; Aiyar, A.; Schepers, A.; Lieberman, P. M. RNA-Dependent Recruitment of the Origin Recognition Complex. *EMBO J.* **2008**, *27* (22), 3024–3035. https://doi.org/10.1038/emboj.2008.221.

(87) Murat, P.; Zhong, J.; Lekieffre, L.; Cowieson, N. P.; Clancy, J. L.; Preiss, T.; Balasubramanian, S.; Khanna, R.; Tellam, J. G-Quadruplexes Regulate Epstein-Barr Virus–Encoded Nuclear Antigen 1 MRNA Translation. *Nat. Chem. Biol.* **2014**, *10* (5), 358–364. https://doi.org/10.1038/nchembio.1479.

(88) Blake, N. Immune Evasion by Gammaherpesvirus Genome Maintenance Proteins. *J. Gen. Virol.* **2010**, *91* (4), 829–846. https://doi.org/10.1099/vir.0.018242-0.

(89) Tellam, J.; Smith, C.; Rist, M.; Webb, N.; Cooper, L.; Vuocolo, T.; Connolly, G.; Tscharke, D. C.; Devoy, M. P.; Khanna, R. Regulation of Protein Translation through MRNA Structure Influences MHC Class I Loading and T Cell Recognition. *Proc. Natl. Acad. Sci. U. S. A.* **2008**, *105* (27), 9319–9324. https://doi.org/10.1073/pnas.0801968105.

(90) Deakyne, J. S.; Malecka, K. A.; Messick, T. E.; Lieberman, P. M. Structural and Functional Basis for an EBNA1 Hexameric Ring in Epstein-Barr Virus Episome Maintenance. *J. Virol.* **2017**, *91* (19). https://doi.org/10.1128/JVI.01046-17.

(91) Frappier, L. Contributions of Epstein–Barr Nuclear Antigen 1 (EBNA1) to Cell Immortalization and Survival. *Viruses* **2012**, *4* (9), 1537–1547. https://doi.org/10.3390/v4091537.

(92) Saridakis, V.; Sheng, Y.; Sarkari, F.; Holowaty, M. N.; Shire, K.; Nguyen, T.; Zhang, R. G.; Liao, J.; Lee, W.; Edwards, A. M.; Arrowsmith, C. H.; Frappier, L. Structure of the P53 Binding Domain of HAUSP/USP7 Bound to Epstein-Barr Nuclear Antigen 1 Implications for EBV-Mediated Immortalization. *Mol. Cell* **2005**, *18* (1), 25–36. https://doi.org/10.1016/j.molcel.2005.02.029.

(93) Lu, J.; Murakami, M.; Verma, S. C.; Cai, Q.; Haldar, S.; Kaul, R.; Wasik, M. A.; Middeldorp, J.; Robertson, E. S. Epstein-Barr Virus Nuclear Antigen 1 (EBNA1) Confers Resistance to Apoptosis in EBV Positive B-Lymphoma Cells through Up-Regulation of Survivin. *Virology* **2011**, *410* (1), 64–75. https://doi.org/10.1016/j.virol.2010.10.029.

(94) Kennedy, G.; Komano, J.; Sugden, B. Epstein-Barr Virus Provides a Survival Factor to Burkitt's Lymphomas. *Proc. Natl. Acad. Sci. U. S. A.* **2003**, *100* (24), 14269–14274. https://doi.org/10.1073/pnas.2336099100.

(95) Tempera, I.; De Leo, A.; Kossenkov, A. V.; Cesaroni, M.; Song, H.; Dawany, N.; Showe, L.; Lu, F.; Wikramasinghe, P.; Lieberman, P. M. Identification of MEF2B, EBF1, and IL6R as Direct Gene Targets of Epstein-Barr Virus (EBV) Nuclear Antigen 1 Critical for EBV-Infected B-Lymphocyte Survival. *J. Virol.* **2016**, *90* (1), 345–355. https://doi.org/10.1128/JVI.02318-15.

(96) Coppotelli, G.; Mughal, N.; Callegari, S.; Sompallae, R.; Caja, L.; Luijsterburg, M. S.; Dantuma, N. P.; Moustakas, A.; Masucci, M. G. The Epstein–Barr Virus Nuclear Antigen-1 Reprograms Transcription by Mimicry of High Mobility Group A Proteins. *Nucleic Acids Res.* **2013**, *41* (5), 2950–2962. https://doi.org/10.1093/nar/gkt032.

(97) Dheekollu, J.; Lieberman, P. M. The Replisome Pausing Factor Timeless Is Required for Episomal Maintenance of Latent Epstein-Barr Virus. *J. Virol.* **2011**, *85* (12), 5853–5863. https://doi.org/10.1128/JVI.02425-10.

(98) Holowaty, M. N.; Zeghouf, M.; Wu, H.; Tellam, J.; Athanasopoulos, V.; Greenblatt, J.; Frappier, L. Protein Profiling with Epstein-Barr Nuclear Antigen-1 Reveals an Interaction with the Herpesvirus-Associated Ubiquitin-Specific Protease HAUSP/USP7. *J. Biol. Chem.* **2003**, *278* (32), 29987–29994. https://doi.org/10.1074/jbc.M303977200.

(99) Deng, Z.; Atanasiu, C.; Zhao, K.; Marmorstein, R.; Sbodio, J. I.; Chi, N.-W.; Lieberman, P. M. Inhibition of Epstein-Barr Virus OriP Function by Tankyrase, a Telomere-Associated Poly-ADP Ribose Polymerase That Binds and Modifies EBNA1. *J. Virol.* **2005**, *79* (8), 4640. https://doi.org/10.1128/JVI.79.8.4640-4650.2005.

(100) Reisman, D.; Yates, J.; Sugden, B. A Putative Origin of Replication of Plasmids Derived from Epstein-Barr Virus Is Composed of Two Cis-Acting Components. *Mol. Cell. Biol.* **1985**, *5* (8), 1822–1832.

(101) Shah, W. A.; Ambinder, R. F.; Hayward, G. S.; Hayward, S. D. Binding of EBNA-1 to DNA Creates a Protease-Resistant Domain That Encompasses the DNA Recognition and Dimerization Functions. *J. Virol.* **1992**, *66* (6), 3355–3362.

(102) Gahn, T. A.; Sugden, B. An EBNA-1-Dependent Enhancer Acts from a Distance of 10 Kilobase Pairs to Increase Expression of the Epstein-Barr Virus LMP Gene. *J. Virol.* **1995**, *69* (4), 2633–2636.

(103) Wendelburg, B. J.; Vos, J. M. An Enhanced EBNA1 Variant with Reduced IR3 Domain for Long-Term Episomal Maintenance and Transgene Expression of OriP-Based Plasmids in Human Cells. *Gene Ther.* **1998**, *5* (10), 1389–1399. https://doi.org/10.1038/sj.gt.3300736.

(104) Nanbo, A.; Sugden, A.; Sugden, B. The Coupling of Synthesis and Partitioning of EBV's Plasmid Replicon Is Revealed in Live Cells. *EMBO J.* **2007**, *26* (19), 4252–4262. https://doi.org/10.1038/sj.emboj.7601853.

(105) Harrison, S.; Fisenne, K.; Hearing, J. Sequence Requirements of the Epstein-Barr Virus Latent Origin of DNA Replication. *J. Virol.* **1994**, *68* (3), 1913–1925.

(106) Deng, Z.; Lezina, L.; Chen, C.-J.; Shtivelband, S.; So, W.; Lieberman, P. M. Telomeric Proteins Regulate Episomal Maintenance of Epstein-Barr Virus Origin of Plasmid Replication. *Mol. Cell* **2002**, *9* (3), 493–503. https://doi.org/10.1016/S1097-2765(02)00476-8.

(107) Parker, M. W.; Botchan, M. R.; Berger, J. M. Mechanisms and Regulation of DNA Replication Initiation in Eukaryotes. *Crit. Rev. Biochem. Mol. Biol.* **2017**, *52* (2), 107–144. https://doi.org/10.1080/10409238.2016.1274717.

(108) Moriyama, K.; Yoshizawa-Sugata, N.; Obuse, C.; Tsurimoto, T.; Masai, H. Epstein-Barr Nuclear Antigen 1 (EBNA1)-Dependent Recruitment of Origin Recognition Complex (Orc) on OriP of Epstein-Barr Virus with Purified Proteins. *J. Biol. Chem.* **2012**, *287* (28), 23977–23994. https://doi.org/10.1074/jbc.M112.368456.

(109) Deng, Z.; Atanasiu, C.; Burg, J. S.; Broccoli, D.; Lieberman, P. M. Telomere Repeat Binding Factors TRF1, TRF2, and HRAP1 Modulate Replication of Epstein-Barr Virus OriP. *J. Virol.* **2003**, *77* (22), 11992–12001. https://doi.org/10.1128/JVI.77.22.11992-12001.2003.
(110) Bochman, M. L.; Schwacha, A. The Mcm Complex: Unwinding the Mechanism of a Replicative Helicase. *Microbiol. Mol. Biol. Rev. MMBR* **2009**, *73* (4), 652–683. https://doi.org/10.1128/MMBR.00019-09.
(111) Durocher, Y.; Perret, S.; Thibaudeau, E.; Gaumond, M.-H.; Kamen, A.; Stocco, R.; Abramovitz, M. A Reporter Gene Assay for High-Throughput Screening of G-Protein-Coupled Receptors Stably or Transiently Expressed in HEK293 EBNA Cells Grown in Suspension Culture. *Anal. Biochem.* **2000**, *284* (2), 316–326. https://doi.org/10.1006/abio.2000.4698.
(112) Meissner, P.; Pick, H.; Kulangara, A.; Chatellard, P.; Friedrich, K.; Wurm, F. M. Transient Gene Expression: Recombinant Protein Production with Suspension-Adapted HEK293-EBNA Cells. *Biotechnol. Bioeng.* **2001**, *75* (2), 197–203. https://doi.org/10.1002/bit.1179.
(113) Kishida, T.; Asada, H.; Kubo, K.; Sato, Y. T.; Shin-Ya, M.; Imanishi, J.; Yoshikawa, K.; Mazda, O. Pleiotrophic Functions of Epstein-Barr Virus Nuclear Antigen-1 (EBNA-1) and OriP Differentially Contribute to the Efficiency of Transfection/Expression of Exogenous Gene in Mammalian Cells. *J. Biotechnol.* **2008**, *133* (2), 201–207. https://doi.org/10.1016/j.jbiotec.2007.08.035.
(114) Mizuguchi, H.; Hosono, T.; Hayakawa, T. Long-Term Replication of Epstein-Barr Virus-Derived Episomal Vectors in the Rodent Cells. *FEBS Lett.* **2000**, *472* (2–3), 173–178. https://doi.org/10.1016/S0014-5793(00)01450-2.
(115) McGeoch, D. J.; Rixon, F. J.; Davison, A. J. Topics in Herpesvirus Genomics and Evolution. *Virus Res.* **2006**, *117* (1), 90–104. https://doi.org/10.1016/j.virusres.2006.01.002.
(116) Codamo, J.; Munro, T. P.; Hughes, B. S.; Song, M.; Gray, P. P. Enhanced CHO Cell-Based Transient Gene Expression with the Epi-CHO Expression System. *Mol. Biotechnol.* **2011**, *48* (2), 109–115. https://doi.org/10.1007/s12033-010-9351-9.
(117) Wabinga, H. R.; Mugerwa, J. W.; Parkin, D. M.; Wabwire-Mangen, F. Cancer in Kampala, Uganda, in 1989–91: Changes in Incidence in the Era of Aids. *Int. J. Cancer* **1993**, *54* (1), 26–36. https://doi.org/10.1002/ijc.2910540106.
(118) Chang, Y.; Cesarman, E.; Pessin, M. S.; Lee, F.; Culpepper, J.; Knowles, D. M.; Moore, P. S. Identification of Herpesvirus-like DNA Sequences in AIDS-Associated Kaposi's Sarcoma. *Science* **1994**, *266* (5192), 1865–1869. https://doi.org/10.1126/science.7997879.
(119) Beral, V. Epidemiology of Kaposi's Sarcoma. *Cancer Surv.* **1991**, *10*, 5–22.
(120) Moore, P. S.; Gao, S. J.; Dominguez, G.; Cesarman, E.; Lungu, O.; Knowles, D. M.; Garber, R.; Pellett, P. E.; McGeoch, D. J.; Chang, Y. Primary Characterization of a Herpesvirus Agent Associated with Kaposi's Sarcomae. *J. Virol.* **1996**, *70* (1), 549–558.
(121) Russo, J. J.; Bohenzky, R. A.; Chien, M. C.; Chen, J.; Yan, M.; Maddalena, D.; Parry, J. P.; Peruzzi, D.; Edelman, I. S.; Chang, Y.; Moore, P. S. Nucleotide Sequence of the Kaposi Sarcoma-Associated Herpesvirus (HHV8). *Proc. Natl. Acad. Sci. U. S. A.* **1996**, *93* (25), 14862–14867. https://doi.org/10.1073/pnas.93.25.14862.
(122) Neipel, F.; Albrecht, J. C.; Fleckenstein, B. Cell-Homologous Genes in the Kaposi's Sarcoma-Associated Rhadinovirus Human Herpesvirus 8: Determinants of Its Pathogenicity? *J. Virol.* **1997**, *71* (6), 4187–4192. https://doi.org/10.1128/JVI.71.6.4187-4192.1997.
(123) Boshoff, C.; Chang, Y. Kaposi's Sarcoma–Associated Herpesvirus: A New DNA Tumor Virus. *Annu. Rev. Med.* **2001**, *52* (1), 453–470. https://doi.org/10.1146/annurev.med.52.1.453.
(124) Kellam, P.; Boshoff, C.; Whitby, D.; Matthews, S.; Weiss, R. A.; Talbot, S. J. Identification of a Major Latent Nuclear Antigen, LNA-1, in the Human Herpesvirus 8 Genome. *J. Hum. Virol.* **1997**, *1* (1), 19–29.
(125) Barbera, A. J.; Ballestas, M. E.; Kaye, K. M. The Kaposi's Sarcoma-Associated Herpesvirus Latency-Associated Nuclear Antigen 1 N Terminus Is Essential for Chromosome Association,

DNA Replication, and Episome Persistence. *J. Virol.* **2004**, *78* (1), 294–301. https://doi.org/10.1128/jvi.78.1.294-301.2004.

(126) Garber, A. C.; Hu, J.; Renne, R. Latency-Associated Nuclear Antigen (LANA) Cooperatively Binds to Two Sites within the Terminal Repeat, and Both Sites Contribute to the Ability of LANA to Suppress Transcription and to Facilitate DNA Replication. *J. Biol. Chem.* **2002**, *277* (30), 27401–27411. https://doi.org/10.1074/jbc.M203489200.

(127) Kwun, H. J.; da Silva, S. R.; Qin, H.; Ferris, R. L.; Tan, R.; Chang, Y.; Moore, P. S. The Central Repeat Domain 1 of Kaposi's Sarcoma-Associated Herpesvirus (KSHV) Latency Associated-Nuclear Antigen 1 (LANA1) Prevents Cis MHC Class I Peptide Presentation. *Virology* **2011**, *412* (2), 357–365. https://doi.org/10.1016/j.virol.2011.01.026.

(128) De León Vázquez, E.; Kaye, K. M. The Internal Kaposi's Sarcoma-Associated Herpesvirus LANA Regions Exert a Critical Role on Episome Persistence. *J. Virol.* **2011**, *85* (15), 7622–7633. https://doi.org/10.1128/JVI.00304-11.

(129) Alkharsah, K. R.; Schulz, T. F. A Role for the Internal Repeat of the Kaposi's Sarcoma-Associated Herpesvirus Latent Nuclear Antigen in the Persistence of an Episomal Viral Genome. *J. Virol.* **2012**, *86* (3), 1883–1887. https://doi.org/10.1128/JVI.06029-11.

(130) Piolot, T.; Tramier, M.; Coppey, M.; Nicolas, J.-C.; Marechal, V. Close but Distinct Regions of Human Herpesvirus 8 Latency-Associated Nuclear Antigen 1 Are Responsible for Nuclear Targeting and Binding to Human Mitotic Chromosomes. *J. Virol.* **2001**, *75* (8), 3948–3959. https://doi.org/10.1128/JVI.75.8.3948-3959.2001.

(131) Ballestas, M. E.; Kaye, K. M. Kaposi's Sarcoma-Associated Herpesvirus Latency-Associated Nuclear Antigen 1 Mediates Episome Persistence through Cis-Acting Terminal Repeat (TR) Sequence and Specifically Binds TR DNA. *J. Virol.* **2001**, *75* (7), 3250–3258. https://doi.org/10.1128/JVI.75.7.3250-3258.2001.

(132) Barbera, A. J.; Chodaparambil, J. V.; Kelley-Clarke, B.; Joukov, V.; Walter, J. C.; Luger, K.; Kaye, K. M. The Nucleosomal Surface as a Docking Station for Kaposi's Sarcoma Herpesvirus LANA. *Science* **2006**, *311* (5762), 856–861. https://doi.org/10.1126/science.1120541.

(133) Mercier, A.; Arias, C.; Madrid, A. S.; Holdorf, M. M.; Ganem, D. Site-Specific Association with Host and Viral Chromatin by Kaposi's Sarcoma-Associated Herpesvirus LANA and Its Reversal during Lytic Reactivation. *J. Virol.* **2014**, *88* (12), 6762–6777. https://doi.org/10.1128/JVI.00268-14.

(134) You, J.; Srinivasan, V.; Denis, G. V.; Harrington, W. J.; Ballestas, M. E.; Kaye, K. M.; Howley, P. M. Kaposi's Sarcoma-Associated Herpesvirus Latency-Associated Nuclear Antigen Interacts with Bromodomain Protein Brd4 on Host Mitotic Chromosomes. *J. Virol.* **2006**, *80* (18), 8909–8919. https://doi.org/10.1128/JVI.00502-06.

(135) Viejo-Borbolla, A.; Ottinger, M.; Brüning, E.; Bürger, A.; König, R.; Kati, E.; Sheldon, J. A.; Schulz, T. F. Brd2/RING3 Interacts with a Chromatin-Binding Domain in the Kaposi's Sarcoma-Associated Herpesvirus Latency-Associated Nuclear Antigen 1 (LANA-1) That Is Required for Multiple Functions of LANA-1. *J. Virol.* **2005**, *79* (21), 13618–13629. https://doi.org/10.1128/JVI.79.21.13618-13629.2005.

(136) Matsumura, S.; Persson, L. M.; Wong, L.; Wilson, A. C. The Latency-Associated Nuclear Antigen Interacts with MeCP2 and Nucleosomes through Separate Domains. *J. Virol.* **2010**, *84* (5), 2318–2330. https://doi.org/10.1128/JVI.01097-09.

(137) Krithivas, A.; Fujimuro, M.; Weidner, M.; Young, D. B.; Hayward, S. D. Protein Interactions Targeting the Latency-Associated Nuclear Antigen of Kaposi's Sarcoma-Associated Herpesvirus to Cell Chromosomes. *J. Virol.* **2002**, *76* (22), 11596–11604. https://doi.org/10.1128/JVI.76.22.11596-11604.2002.

(138) Lim, C.; Sohn, H.; Lee, D.; Gwack, Y.; Choe, J. Functional Dissection of Latency-Associated Nuclear Antigen 1 of Kaposi's Sarcoma-Associated Herpesvirus Involved in Latent DNA Replication and Transcription of Terminal Repeats of the Viral Genome. *J. Virol.* **2002**, *76* (20), 10320–10331. https://doi.org/10.1128/JVI.76.20.10320-10331.2002.

(139) Hellert, J.; Weidner-Glunde, M.; Krausze, J.; Lünsdorf, H.; Ritter, C.; Schulz, T. F.; Lührs, T. The 3D Structure of Kaposi Sarcoma Herpesvirus LANA C-Terminal Domain Bound to DNA. *Proc. Natl. Acad. Sci. U. S. A.* **2015**, *112* (21), 6694–6699. https://doi.org/10.1073/pnas.1421804112.

(140) Lagunoff, M.; Ganem, D. The Structure and Coding Organization of the Genomic Termini of Kaposi's Sarcoma-Associated Herpesvirus. *Virology* **1997**, *236* (1), 147–154. https://doi.org/10.1006/viro.1997.8713.

(141) Cotter, M. A.; Robertson, E. S. The Latency-Associated Nuclear Antigen Tethers the Kaposi's Sarcoma-Associated Herpesvirus Genome to Host Chromosomes in Body Cavity-Based Lymphoma Cells. *Virology* **1999**, *264* (2), 254–264. https://doi.org/10.1006/viro.1999.9999.

(142) Hu, J.; Garber, A. C.; Renne, R. The Latency-Associated Nuclear Antigen of Kaposi's Sarcoma-Associated Herpesvirus Supports Latent DNA Replication in Dividing Cells. *J. Virol.* **2002**, *76* (22), 11677–11687. https://doi.org/10.1128/JVI.76.22.11677-11687.2002.

(143) Yates, J. L.; Camiolo, S. M.; Bashaw, J. M. The Minimal Replicator of Epstein-Barr Virus OriP. *J. Virol.* **2000**, *74* (10), 4512–4522.

(144) Hu, J.; Renne, R. Characterization of the Minimal Replicator of Kaposi's Sarcoma-Associated Herpesvirus Latent Origin. *J. Virol.* **2005**, *79* (4), 2637–2642. https://doi.org/10.1128/JVI.79.4.2637-2642.2005.

(145) Shrestha, P.; Sugden, B. Identification of Properties of the Kaposi's Sarcoma-Associated Herpesvirus Latent Origin of Replication That Are Essential for the Efficient Establishment and Maintenance of Intact Plasmids. *J. Virol.* **2014**, *88* (15), 8490–8503. https://doi.org/10.1128/JVI.00742-14.

(146) Stedman, W.; Deng, Z.; Lu, F.; Lieberman, P. M. ORC, MCM, and Histone Hyperacetylation at the Kaposi's Sarcoma-Associated Herpesvirus Latent Replication Origin. *J. Virol.* **2004**, *78* (22), 12566–12575. https://doi.org/10.1128/JVI.78.22.12566-12575.2004.

(147) Haan, K. M.; Aiyar, A.; Longnecker, R. Establishment of Latent Epstein-Barr Virus Infection and Stable Episomal Maintenance in Murine B-Cell Lines. *J. Virol.* **2001**, *75* (6), 3016–3020. https://doi.org/10.1128/JVI.75.6.3016-3020.2001.

(148) Blaskovic, D.; Stanceková, M.; Svobodová, J.; Mistríková, J. Isolation of Five Strains of Herpesviruses from Two Species of Free Living Small Rodents. *Acta Virol.* **1980**, *24* (6), 468.

(149) Nash, A. A.; Dutia, B. M.; Stewart, J. P.; Davison, A. J. Natural History of Murine γ-Herpesvirus Infection. *Philos. Trans. R. Soc. Lond. B. Biol. Sci.* **2001**, *356* (1408), 569–579. https://doi.org/10.1098/rstb.2000.0779.

(150) Barton, E.; Mandal, P.; Speck, S. H. Pathogenesis and Host Control of Gammaherpesviruses: Lessons from the Mouse. *Annu. Rev. Immunol.* **2011**, *29*, 351–397. https://doi.org/10.1146/annurev-immunol-072710-081639.

(151) Pedro Simas, J.; Efstathiou, S. Murine Gammaherpesvirus 68: A Model for the Study of Gammaherpesvirus Pathogenesis. *Trends Microbiol.* **1998**, *6* (7), 276–282. https://doi.org/10.1016/S0966-842X(98)01306-7.

(152) Habison, A. C.; Beauchemin, C.; Simas, J. P.; Usherwood, E. J.; Kaye, K. M. Murine Gammaherpesvirus 68 LANA Acts on Terminal Repeat DNA To Mediate Episome Persistence. *J. Virol.* **2012**, *86* (21), 11863–11876. https://doi.org/10.1128/JVI.01656-12.

(153) Virgin, H. W.; Latreille, P.; Wamsley, P.; Hallsworth, K.; Weck, K. E.; Canto, A. J. D.; Speck, S. H. Complete Sequence and Genomic Analysis of Murine Gammaherpesvirus 68. *J. Virol.* **1997**, *71* (8), 5894–5904.

(154) Rajčáni, J.; Kúdelová, M. Murid Herpesvirus 4 (MuHV-4): An Animal Model for Human Gammaherpesvirus Research. In *Latency Strategies of Herpesviruses*; Minarovits, J., Gonczol, E., Valyi-Nagy, T., Eds.; Springer US: Boston, MA, 2007; pp 102–136. https://doi.org/10.1007/978-0-387-34127-9_5.

(155) Fowler, P. ORF73 of Murine Herpesvirus-68 Is Critical for the Establishment and Maintenance of Latency. *J. Gen. Virol.* **2003**, *84* (12), 3405–3416. https://doi.org/10.1099/vir.0.19594-0.
(156) Moorman, N. J.; Willer, D. O.; Speck, S. H. The Gammaherpesvirus 68 Latency-Associated Nuclear Antigen Homolog Is Critical for the Establishment of Splenic Latency. *J. Virol.* **2003**, *77* (19), 10295–10303. https://doi.org/10.1128/JVI.77.19.10295-10303.2003.
(157) Paden, C. R.; Forrest, J. C.; Moorman, N. J.; Speck, S. H. Murine Gammaherpesvirus 68 LANA Is Essential for Virus Reactivation from Splenocytes but Not Long-Term Carriage of Viral Genome. *J. Virol.* **2010**, *84* (14), 7214–7224. https://doi.org/10.1128/JVI.00133-10.
(158) Hellert, J.; Weidner-Glunde, M.; Krausze, J.; Richter, U.; Adler, H.; Fedorov, R.; Pietrek, M.; Rückert, J.; Ritter, C.; Schulz, T. F.; Lührs, T. A Structural Basis for BRD2/4-Mediated Host Chromatin Interaction and Oligomer Assembly of Kaposi Sarcoma-Associated Herpesvirus and Murine Gammaherpesvirus LANA Proteins. *PLoS Pathog.* **2013**, *9* (10). https://doi.org/10.1371/journal.ppat.1003640.
(159) Correia, B.; Cerqueira, S. A.; Beauchemin, C.; Miranda, M. P. de; Li, S.; Ponnusamy, R.; Rodrigues, L.; Schneider, T. R.; Carrondo, M. A.; Kaye, K. M.; Simas, J. P.; McVey, C. E. Crystal Structure of the Gamma-2 Herpesvirus LANA DNA Binding Domain Identifies Charged Surface Residues Which Impact Viral Latency. *PLOS Pathog.* **2013**, *9* (10), e1003673. https://doi.org/10.1371/journal.ppat.1003673.
(160) Ponnusamy, R.; Petoukhov, M. V.; Correia, B.; Custodio, T. F.; Juillard, F.; Tan, M.; Pires de Miranda, M.; Carrondo, M. A.; Simas, J. P.; Kaye, K. M.; Svergun, D. I.; McVey, C. E. KSHV but Not MHV-68 LANA Induces a Strong Bend upon Binding to Terminal Repeat Viral DNA. *Nucleic Acids Res.* **2015**, *43* (20), 10039–10054. https://doi.org/10.1093/nar/gkv987.
(161) Paden, C. R.; Forrest, J. C.; Tibbetts, S. A.; Speck, S. H. Unbiased Mutagenesis of MHV68 LANA Reveals a DNA-Binding Domain Required for LANA Function in Vitro and in Vivo. *PLoS Pathog.* **2012**, *8* (9), e1002906. https://doi.org/10.1371/journal.ppat.1002906.
(162) Backliwal, G.; Hildinger, M.; Hasija, V.; Wurm, F. M. High-Density Transfection with HEK-293 Cells Allows Doubling of Transient Titers and Removes Need for a Priori DNA Complex Formation with PEI. *Biotechnol. Bioeng.* **2008**, *99* (3), 721–727. https://doi.org/10.1002/bit.21596.
(163) Bollin, F.; Dechavanne, V.; Chevalet, L. Design of Experiment in CHO and HEK Transient Transfection Condition Optimization. *Protein Expr. Purif.* **2011**, *78* (1), 61–68. https://doi.org/10.1016/j.pep.2011.02.008.
(164) Rajendra, Y. PEI-Mediated Transient Gene Expression in CHO Cells. In *Recombinant Protein Expression in Mammalian Cells*; Hacker, D. L., Ed.; Springer New York: New York, NY, 2018; Vol. 1850, pp 33–42. https://doi.org/10.1007/978-1-4939-8730-6_3.
(165) Thompson, B. C.; Segarra, C. R. J.; Mozley, O. L.; Daramola, O.; Field, R.; Levison, P. R.; James, D. C. Cell Line Specific Control of Polyethylenimine-Mediated Transient Transfection Optimized with "Design of Experiments" Methodology. *Biotechnol. Prog.* **2012**, *28* (1), 179–187. https://doi.org/10.1002/btpr.715.
(166) Kuwae, S.; Miyakawa, I.; Doi, T. Development of a Chemically Defined Platform Fed-Batch Culture Media for Monoclonal Antibody-Producing CHO Cell Lines with Optimized Choline Content. *Cytotechnology* **2018**, *70* (3), 939–948. https://doi.org/10.1007/s10616-017-0185-1.
(167) Rajendra, Y.; Hougland, M. D.; Alam, R.; Morehead, T. A.; Barnard, G. C. A High Cell Density Transient Transfection System for Therapeutic Protein Expression Based on a CHO GS-Knockout Cell Line: Process Development and Product Quality Assessment. *Biotechnol. Bioeng.* **2015**, *112* (5), 977–986. https://doi.org/10.1002/bit.25514.
(168) Lee, J. S.; Park, J. H.; Ha, T. K.; Samoudi, M.; Lewis, N. E.; Palsson, B. O.; Kildegaard, H. F.; Lee, G. M. Revealing Key Determinants of Clonal Variation in Transgene Expression in

Recombinant CHO Cells Using Targeted Genome Editing. *ACS Synth. Biol.* **2018**, *7* (12), 2867–2878. https://doi.org/10.1021/acssynbio.8b00290.

(169) W, P.; Tp, M.; P, G. Intraclonal Protein Expression Heterogeneity in Recombinant CHO Cells. *Plos One* **2009**, *4* (12), e8432–e8432. https://doi.org/10.1371/journal.pone.0008432.

(170) Tharmalingam, T.; Barkhordarian, H.; Tejeda, N.; Daris, K.; Yaghmour, S.; Yam, P.; Lu, F.; Goudar, C.; Munro, T.; Stevens, J. Characterization of Phenotypic and Genotypic Diversity in Subclones Derived from a Clonal Cell Line. *Biotechnol. Prog.* **2018**, *34* (3), 613–623. https://doi.org/10.1002/btpr.2666.

(171) Yates, J. L.; Warren, N.; Sugden, B. Stable Replication of Plasmids Derived from Epstein–Barr Virus in Various Mammalian Cells. *Nature* **1985**, *313* (6005), 812–815. https://doi.org/10.1038/313812a0.

(172) Wang, X.; Le, N.; Denoth-Lippuner, A.; Barral, Y.; Kroschewski, R. Asymmetric Partitioning of Transfected DNA during Mammalian Cell Division. *Proc. Natl. Acad. Sci.* **2016**, *113* (26), 7177–7182. https://doi.org/10.1073/pnas.1606091113.

(173) Lee, J.-H.; Park, J.-H.; Park, S.-H.; Kim, S.-H.; Kim, J. Y.; Min, J.-K.; Lee, G. M.; Kim, Y.-G. Co-Amplification of EBNA-1 and PyLT through Dhfr-Mediated Gene Amplification for Improving Foreign Protein Production in Transient Gene Expression in CHO Cells. *Appl. Microbiol. Biotechnol.* **2018**, *102* (11), 4729–4739. https://doi.org/10.1007/s00253-018-8977-6.

(174) Middleton, T.; Sugden, B. Retention of Plasmid DNA in Mammalian Cells Is Enhanced by Binding of the Epstein-Barr Virus Replication Protein EBNA1. *J. Virol.* **1994**, *68* (6), 4067–4071.

(175) Coleman, H. M.; Efstathiou, S.; Stevenson, P. G. Transcription of the Murine Gammaherpesvirus 68 ORF73 from Promoters in the Viral Terminal Repeats. *J. Gen. Virol.* **2005**, *86* (Pt 3), 561–574. https://doi.org/10.1099/vir.0.80565-0.

(176) Habison, A. C.; de Miranda, M. P.; Beauchemin, C.; Tan, M.; Cerqueira, S. A.; Correia, B.; Ponnusamy, R.; Usherwood, E. J.; McVey, C. E.; Simas, J. P.; Kaye, K. M. Cross-Species Conservation of Episome Maintenance Provides a Basis for in Vivo Investigation of Kaposi's Sarcoma Herpesvirus LANA. *PLoS Pathog.* **2017**, *13* (9), e1006555. https://doi.org/10.1371/journal.ppat.1006555.

(177) Emery, D. W. The Use of Chromatin Insulators to Improve the Expression and Safety of Integrating Gene Transfer Vectors. *Hum. Gene Ther.* **2011**, *22* (6), 761–774. https://doi.org/10.1089/hum.2010.233.

(178) Kennedy, G.; Sugden, B. EBNA-1, a Bifunctional Transcriptional Activator. *Mol. Cell. Biol.* **2003**, *23* (19), 6901–6908. https://doi.org/10.1128/MCB.23.19.6901-6908.2003.